

POLITECNICO DI TORINO

**Master's Degree
in Mechatronic Engineering**

Master's Thesis

Wheels on Water



Supervisors

Prof. Costantino Manes
Prof. Enrico Galvagno
Prof. Federico Colombo

Candidate

Seyedreza Hamedmousaviyan

Signature

.....

Signature

.....

Academic year 2019-2020

Acknowledgement

I would like to express my special thanks to, Prof. Costantino Manes, Prof. Enrico Galvagno and Prof. Federico Colombo, for their continued support and for giving me the opportunity of working on my own idea.

In the beginning, the idea of the project was to create a wearable robot to walk on water. The feasibility of such a concept was really hard to imagine. Luckily, professor Manes did not disappoint me and encouraged me to continue my research and to find an appropriate way of implementing it. After a period of one-to-two months working on the concept, I came up with a new solution to use the same method as a water-craft. To make a long story short, what I want to say is that giving a chance to people's ideas matters and I was really lucky to find people who believed in my idea and never ceased their assistance.

I received a lot of advice and assistance and I am deeply honored to be assisted by them.

Abstract

Water-crafts are not efficient in terms of traveling at high velocities, due to the drastic growth of the drag force against their movement through the water. To cope with this problem various solutions have been proposed which are mainly focused on the design of the wetted surface area, as it can affect the force applying to the body. Yet these solutions cannot perform great differences in the overall performance of the system, especially at high velocities.

The project analyzes how the performance and limitations of water-crafts can be improved using a novel technique inspired by species so-called water runners and a phenomenon called rushing. This phenomenon is mainly based on hydrodynamic forces generated by these species in which they can resist sinking and run on the water surface. Knowing this phenomenon led to a question if it is convenient to use this method for a propulsion system of a water-craft. To answer this question the performance of a conceptual design using a novel propulsion system which is aimed to use the same technique is compared with modern water-crafts, using computational fluid dynamics (CFD) simulations. However, any solution should be able to ensure stability and capable of handling potential issues. Thus, the responses of the system to various inputs and conditions are analyzed using Matlab and Simulink simulations.

The results show a remarkable improvement in the performance of this kind of system. Contrary to other technologies, the wasted energy is not due to the drag force acting directly to the action, thus the water-craft can move faster without encountering noticeable problems. However, the performance may be varied depending on the environmental conditions. Several records are found confirming the plausibility of implementing this system in a real-world situation. Though they are experimental proofs and not investigated scientifically, moreover limited data is found about their performance. Therefore, to ensure the feasibility of the operation, creating a prototype based on current data obtained from similar problems and the results of the simulations is recommended for later studies.

Contents

1. Introduction	1
1.1. Context	1
1.2. Relevance	2
1.2.1. Hydrofoils	3
1.2.2. The surface effect craft or Wing-in-Ground effect (WIG)	4
1.2.3. Walking on water	4
1.2.4. prototype of a water-runner	5
1.2.5. water skippers	10
1.3. Objectives	11
2. Conceptual Design	14
2.1. Geometry	14
2.1.1. Body	14
2.1.2. Propulsion System	15
2.1.3. Maneuvering at low velocity	17
2.1.4. Suspension	19
2.2 Mechanism	20
2.2.1 Hydrodynamics	20
2.2.3 Statics	24
2.3. Forces at plate	26
3. Numerical simulations	34
3.1. Modelling strategy and approximations	34
3.2. Meshing	43
3.3. Conditions	46
3.4. CFD results	49
3.4.1. Computing Lift and tractive in COMSOL	49
3.4.2. Angle of attack	50
3.4.3. Lift and Tractive	50

3.4.4. Coefficients.....	51
3.4.5. Reattachment length (RL)	53
3.4.6. Number of plates	54
3.4.4. Single vs Double row of plates.....	61
3.4.5. Pressure analysis	64
4. Dynamic Analysis.....	66
4.1. Approximations and methods	66
4.2. Results	70
4.2.1. Characteristics of the system	70
4.2.2. Simulink model.....	71
5. Conclusions	90
6. References	91

List of figures

Figure 1 Picture of two kinds of commercial water-crafts operating at high velocity	2
Figure 2 hydrofoil boat, foils create a lift force that can emerge the boat from the water at high velocities	4
Figure 3 WIG-craft, the air-craft designed to fly close to the water surface	4
Figure 4 water runners, Western and Clark's grebes (left), Basilisk Lizard (right), the pictures represent two species capable of running on the water, by splashing the water surface	5
Figure 5 The simulation of a foot during splash stage and the pressure analysis [9].	6
Figure 6 Simulated torque throughout a single revolution for 2, 4, and 8 legs [8].	8
Figure 7 Boundary conditions of different simulations, concerning the lift force, Boundary I is set to estimate the average lift force, Boundary II is set to determine the convergence of the position above the water [11].	8
Figure 8 the scheme of the robot and the forces applied to it [8].	9
Figure 9 four-legged robot, the prototype used for running on the water [11].	10
Figure 10 The pictures of a modified motorbike and a snowmobile operating on the water	11
Figure 11 The flowchart diagram of the project.	13
Figure 12 a simple scheme of the water-craft proposed by the project	15
Figure 13 A sample of the propulsion system, designed in SOLIDWORKS	16
Figure 14 The scheme of a rudder [15].	17
Figure 15 Side view of a rudder and its specifications [15].	19
Figure 16 Running on water, the demonstration of rushing through various stages by a Basilisk lizard [15].	22
Figure 17 The forces applied to a floating object, where F_B is the buoyancy and W is the body weight. The points in which each force is applied are represented as B and G which are corresponding to F_B and W [17].	25
Figure 18 normal force applied to a plate inclined with respect to the vertical axis	26
Figure 19 The effect of the shape on the drag coefficient [17].	29
Figure 20 Some of the possible shapes for the disks used by the robot [10].	30
Figure 21 The transition of the flow from laminar to turbulent in the case of the flow over a flat plate [17].	32
Figure 22 The variation of the friction coefficient over a flat plate parallel to the flow [17].	33
Figure 23 Reynolds averaged Navier Stroke (RANS) averaging the fluctuations within the flow [26]. ..	37

Figure 24 Two different multiphase models, the disperse method (left), the separated flow (right) [27], [28].	38
Figure 25 The sublayers dedicated to the near-wall region [26].	39
Figure 26 The scheme of a plate	41
Figure 27 The comparison of the results provided by three different models, SST, k- ϵ (RNG), k- ω . The results concern the lift, tractive, and reattachment length of a plate.	42
Figure 28 The change of the shape of a mesh element in different directions [29].	43
Figure 29 The boundaries of the COMSOL models are defined as following, (a) input, (b) output, (c) no-slip wall, (d) symmetry, (e) side view of the model.	48
Figure 30 Results of CFD simulations regarding Lift and Tractive forces vs velocity of the flow (which is assumed to be equal to the relative velocity of a plate with respect to the water).	51
Figure 31 The estimated coefficients provided by the simulation to examine the correctness of the results, concerning two different conditions, changing the angle of attack and the velocity of the input flow. C_x and C_L are the tractive and lift coefficients, respectively.	52
Figure 32 measuring the reattachment length concerning a plate perpendicular to the flow, the velocity of the water in inlet boundary is 3[m/s].	54
Figure 33 Total Tractive and Lift forces considering different distances between the plates which corresponds to various number of plates in a specific length.	55
Figure 34 Lift force applying to each plate, concerning different number of plates	58
Figure 35 Tractive force applying to each plate, concerning different number of plates	60
Figure 36 The pictures represent the variation of the flow velocity within the plates, in the case of using one or two rows. The input boundary is set on the right side and the output is on the left. The velocity of the flow in the input is equal to 3 [m/s] and the pressure at the output is zero for both cases.	62
Figure 37 Analyzing the pressure around the plates. In this case, the input velocity is set to 7 [m/s] which is relatively high. Even in this situation, the results do not show any chance of forming cavitation.	64
Figure 38 Free body diagram	66
Figure 39 Comparison of the generalized coefficients concerning the averaged force generated by plates at different velocities and angles.	69
Figure 40 The coefficient corresponding to various angles, the generalized equations of the lift C_L and tractive C_x coefficients are represented above each line	70
Figure 41 The overall scheme of the plant	72
Figure 42 subsystem regarding z-axis (vertical) analysis.	73
Figure 43 subsystem regarding x-axis (horizontal) analysis	73
Figure 44 Speed analysis of the wheels, the relative velocity represents the velocity of the plates through the water and the translational velocity is the same as the velocity of the body.	74

Figure 45 Results of z-axis analysis in static conditions, the body is dropped into the water, the initial position of the body is on the water surface, the time needed for the system to stop bouncing and remains steady, the vertical position of the body at $t \rightarrow \infty$ will be equal to Z_{static}	75
Figure 46 A closer point of view of the previous plot regarding the vertical movement, to measure the frequency.	76
Figure 47 the switch of between active contact areas of the plate, fully or partially submerged	77
Figure 48 The subsystem regarding the efficiency.....	79
Figure 49 The input of the system which is the angular velocity of the motor	79
Figure 50 The output of the system when the entire system relies on the force generated by the plates. The first plot represents the translational velocity of the system along the x-axis, the second plot is the vertical displacement of the system and the last one is the forces applied to the system regarding the z-axis	81
Figure 51 The lift coefficient of the track measured in CFD simulation.....	82
Figure 52 The plot in the top-left represents the relative velocity of the plates through the water and along the x-axis, the top-right plot is the torque of the motor, the plot on the bottom-left is the power required by the system, and the plot on the bottom-right is the efficiency during the energy conversion from mechanical to fluid.....	84
Figure 53 z-axis analysis, The plot in the top-left represents the vertical displacement, the top-right plot is the velocity along the z-axis, the plot on the bottom-left is the acceleration along the z-axis, and the plot on the bottom-right indicates the vertical forces applying to the system.	85
Figure 54 x-axis analysis, The plot in the top-left represents the displacement along the x-axis, the top-right plot is the velocity along the x-axis which is the same as the translational velocity of the entire system, the plot on the bottom-left is the acceleration along the x-axis, and the plot on the bottom-right indicates the forces along the x-axis.	86
Figure 55 The plot on the top is the input velocity and the plot on the bottom is the translational velocity corresponding to the input, the delay in which the output can follow the input is well evident.	88

List of tables

Table 1 The specifications of some speed-boats [2].....	3
Table 2 specifications of the simulation.....	41
Table 3 The equations used for computing different forces in COMSOL Multiphysics, considering two classifications, with or without wall function [31].....	50
Table 4 number of plates corresponding to different distances between them.....	54
Table 5 The comparison between Total Tractive and Lift forces concerning one and two rows of the plates, each chart indicates a specific angle of attack for single and double rows, the distance among each plate is placed in the x-axis and the total lift and tractive forces in the y-axis.....	63
Table 6 the parameters used in Simulink	71

1. Introduction

1.1. Context

More than 70% of the earth is covered by water, thus, it plays a critical role in terms of transportations. For this reason, sailing is known as one of the greatest achievements of human beings.

Though the water is known as an efficient way of transporting heavy objects over long distances, yet it is a time-consuming way of traveling. Due to the limitations caused by the water at high velocities, it is quite challenging for high-speed water-crafts to work efficiently. One of their biggest problems is the drag force due to the contact area between the water and body, that is opposing to the movement and is a function of velocity squared. Since the drag force is strongly related to the velocity, even a small variation of the velocity can increase it significantly and consequently the power requirement can become large, that is the reason why the top speed of commercial water-crafts, such as jet-skis and boats is limited.

Many solutions have been suggested to overcome this problem. These techniques are mainly focused on the reduction of the contact area and the drag coefficient, which can be achieved by implementing particular shapes on the body. Although these ways provide higher efficiency, yet they are not capable of making a big difference on the top speed limit. The benefits and drawbacks of each technique will be discussed later.

The project will go through the analysis of a novel idea implemented on a conceptual water-craft that is mainly focused on the limits of high-speed water-crafts. The technique is inspired by species capable of running on the water by generating a hydrodynamic force formed during a phenomenon called rushing. In comparison to other water skippers, these species have a relatively large body and too dense to use surface tension to resist sinking, so they tackle the problem by generating hydrodynamic forces.

As no similar studies and applications have been recognized regarding this specific case, the works done are generally based on approximations and CFD simulations. The approaches used in this project will represent the functionality of the system in certain

1. Introduction

conditions and give an idea about the efficiency and other characteristics of the concept, while, it also represents all the possible obstacles of the system.

The first studies of the system are based on ideal conditions. Afterward, different approaches are performed to make the analysis more realistic. In the end, the stability and responses of the propulsion system are examined by using Matlab and Simulink simulations, through various inputs.

1.2. Relevance

Several water-crafts have been designed to travel at high velocities, such as boats, jet-skis, etc. However, at high velocities, the drag force opposing the movement becomes so big and to overcome it, great power is required, which leads to having a craft with a huge body and large engines which is not reasonable for ordinary usage. Therefore, commercial boats can be found with the capability of running at a velocity of the range 68-108 [km/h] which corresponds to a power of 60-310 [hp] [1].

Nevertheless, some boats have been designed to break the limits and propel as fast as possible. These speed boats have a remarkably large body and can provide a huge power, which makes them move at very high velocity. Despite the price, they are not insured and difficult to be handled and steering at high velocities is one of their biggest concerns. The table below represents the specifications of the fastest boats.



Figure 1 Picture of two kinds of commercial water-crafts operating at high velocity

1. Introduction

Boat models	Engine	Power	Passengers	Max speed
Spirit of Australia	Westinghouse J34, Turbojet	3000 [hp]	1	510 [km/h]
Bluebird	Jet engine	3500 [hp]	1	444 [km/h]
Problem child	Hemi V8	8000 [hp]	1	421 [km/h]
Mystic powerboat	T53-703	2 × 1850 [hp]	6	402 [km/h]
Skater 46 pleasure	Teague custom	2 × 1500 [hp]	5	281 [km/h]
Nor-tech 5200	Mercury racing	2 × 5200 [hp]	10	241 [km/h]
Cigarette racing team 50 AMG GTS	AMG electric engine	2200 [hp]	5	217 [km/h]
Fountain 47 lightning	Mercury racing	2 × 1075 [hp]	6	185 [km/h]
South bay 925CR	Mercury 1075	1500 [hp]	6	183 [km/h]

Table 1 The specifications of some speed-boats [2].

As said before, at high velocities the drag force becomes so large and to overcome this force, great power is required. Many designs have been done to minimize the effect of the drag force, such as using different body shapes that can reduce the drag coefficient or placing the propulsion system in a position that can reduce the contact area between the water and the body during the acceleration. Even these solutions can not make a significant change in the performance of this kind of application. In the following sections, some of the other water-crafts which are designed to provide higher efficiency will be introduced.

1.2.1. Hydrofoils

One of the latest designs of water-crafts is hydrofoils. The idea is to create a lift force by using hydrofoils attached to the main body, once the speed increases the lift force increases and the body emerges from the water, however, the hydrofoils create a drag force too. The foils represent a poor performance at low velocities, as the boat is in contact with the water and so are the foils, consequently, provide an extra drag force [3].

Because of the presence of a phenomenon termed cavitation, the top-speed of this concept is limited, as it disturbs the lift generated by the foils. The cavitation happens at

1. Introduction

speed above 110 km/h. Another problem is due to the design of the foils that limits the actions of the boat in some specific conditions [4].



Figure 2 hydrofoil boat, foils create a lift force that can emerge the boat from the water at high velocities

1.2.2. The surface effect craft or Wing-in-Ground effect (WIG)

The surface effect is a phenomenon that provides high efficiencies when an aircraft flies near to the surface, which is due to the trapped air between the wing and the runway. The idea has been used to create a new aircraft able to fly close to the water surface and takes advantage of this phenomenon. However, they do not provide good performance for speed below 50-60 [mph], moreover, they require large engines and long wings that lead to having a large frame, which limits the maneuver above the water. Due to the low height of the flight, they are not known as a safe mode of travel [5].

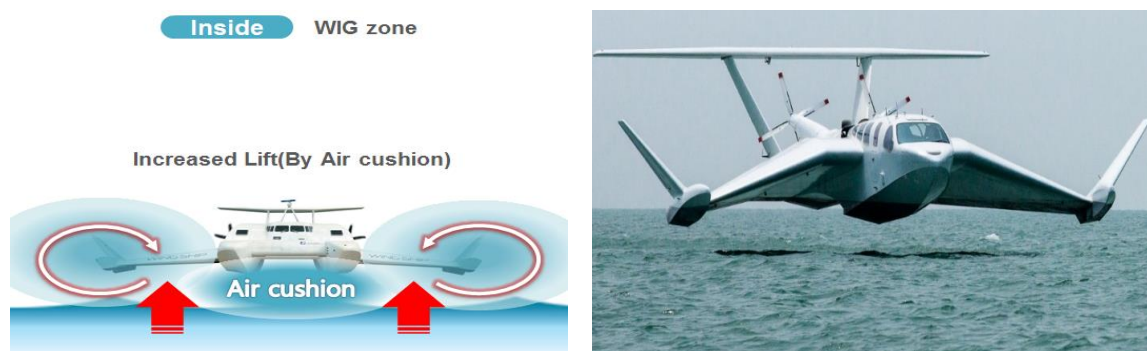


Figure 3 WIG-craft, the air-craft designed to fly close to the water surface

1.2.3. Walking on water

The idea of this project is inspired by species capable of running on the water. Some studies have been done regarding the behavior of these animals. In this chapter, the technique used

1. Introduction

by two species named “*Basilisk Lizards*” and “*Western and Clark’s grebes*” for running on the water will be explained briefly. “*Western and Clark’s grebes*” are the largest animals being able to run on water. These species are not able to use surface tension to support their body weight, so to maintain their body above the water and moving forward, they use a different technique, called rushing. This action consists of three different stages: slap, stroke, and retraction.

Rushing starts with the slapping phase, while in this stage, they start hitting the water surface and by producing an impact they can support up to 30-55% of their body weight. The supporting force produced in this stage is mainly affected by the foot size and body weight while this phase loses its importance for adults with larger bodies. The rest of the force produces in the second stage by pushing the water backward and creating a drag force to accomplish the rest of the support requirement. In the end, they retract their feet laterally and by collapsing them, they can minimize the downward force. Thus, one of the key points of this process is to flatten the foot at the beginning to maximize the drag force and to collapse in the retraction stage. [6], [7].



Figure 4 water runners, Western and Clark's grebes (left), Basilisk Lizard (right), the pictures represent two species capable of running on the water, by splashing the water surface

1.2.4. prototype of a water-runner

To mimic the behavior of the water walkers and rushing, some robots are created. To do so, they go through the same procedures, slap, stroke, and retraction. For this purpose, the behavior of these species is analyzed step by step. Stepping rate is one of the most important factors of the whole process. As studies show Basilisk Lizards can run across the water at a velocity of 1.5 [m/s], which corresponds to a stride rate of 5-10 [Hz] per leg. To achieve the

1. Introduction

goal four factors should be taken into account, such as the mass of the body, characteristic length, running speed and shape of the foot [6].

The first trials are done by using a two-legged robot. This model is able to generate a lift to power ratio equal to 12-15 [g/W], however, it has many difficulties and extremely hard to stabilize. To tackle this problem a four-legged robot is introduced with higher performance and a lift to power ratio of 50 [g/W]. As mentioned earlier, the stride rate plays an important role; in this case, a frequency of the range 7-12 [Hz] is found as an appropriate running frequency to accomplish the process.

These robots have a relatively small body, including several legs with a circular disk connected to the end of each leg, able to splash water surface and create a supporting force for maintaining the body above the water and propelling it forward. The disks are foldable, and in this way, they can expand to maximize the force created in the first two stages (slap and stroke) and be collapsed to minimize the downward force due to the retraction phase. As the robots have a light body, they can take advantage of the force created during a slap phase. The maximum slap impulse created by each leg can be found as,

$$I_{max} = \frac{4}{3} \rho r_{effective}^3 u_{peak} \quad (1)$$

where $r_{effective}$ is the effective radius of the disk and u_{peak} is the velocity of the disk in the moment of hitting the water [8].

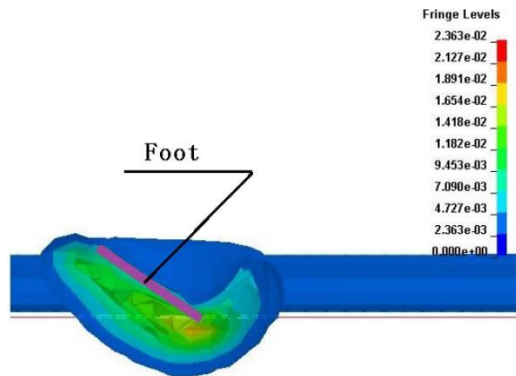


Figure 5 The simulation of a foot during splash stage and the pressure analysis [9].

During the first two phases, an air cavity forms under the disk which facilitates the supporting force needed and also helps the disk to emerge from the water in the retraction

1. Introduction

phase. Nevertheless, the air under the disk can collapse at a certain moment, so to prevent it the robot should provide a velocity which leads to a period, less than the time in which the air cavity would collapse. For a circular disk this the following relation holds.

$$T_{seal} = 2.285(r_{effective}/g)^{0.5} \quad (2)$$

Although each leg can produce a remarkable force during the slap phase, it is still not large enough to accomplish the progress. The rest of the force required can be created during the stroke phase, which is a combination of hydrodynamic drag due to the increase of depth and inertial drag from momentum. The net force created in this stage can be found as follow.

$$D_{(t)} = C_D [0.5S\rho u^2 + S\rho g h_{(t)}] \quad (3)$$
$$(C_D \cong 0.703, S = \pi r_{effective}^2)$$

where C_D is the coefficient dedicated to a circular disk used for this case, S is the contact area, $h_{(t)}$ is the depth through the water, u is the velocity of the disk, ρ is the density.

Some forces such as the surface tension and shear forces are neglected, as they do not have a remarkable influence on the results at high Reynolds numbers. In this case, the foot has a frequency of 7 [Hz] which corresponds to a Reynolds number of 10^4 [8].

- **Characteristics of the robot**

The robot has a mass of 100 [g], containing four miniature DC motors connected to four legs. Each length of each leg is equal to 300 [mm]. To analyze the performance of the robot the ratio of the mass to power is considered and is equal to the following term.

$$Performance = \frac{M_{(g)}}{P_{(W)}} \quad (4)$$

As stated in the literature, an increase in the number of legs can increase the lift and provide higher efficiency. The following figure indicates the difference in using the various number of legs [8].

1. Introduction

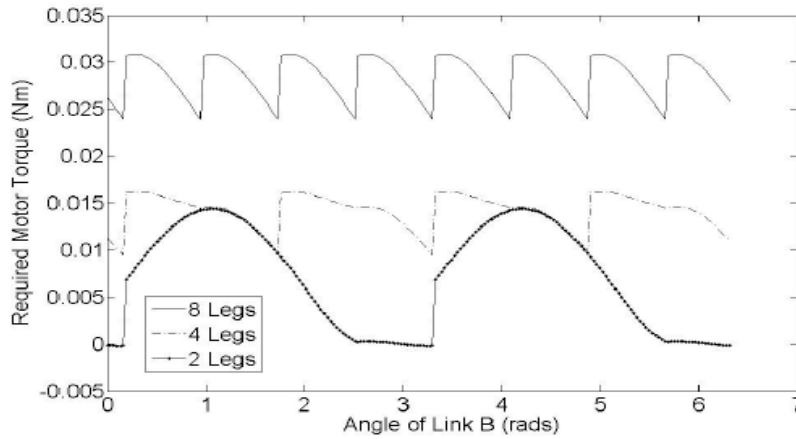


Figure 6 Simulated torque throughout a single revolution for 2, 4, and 8 legs [8].

• Modelling and simulation

The simulation of the robot is done through two conditions, fixed base and vertical prismatic joint. The first analysis is to estimate the average force created corresponding to different vertical positions, while the second analysis concerns the convergence of the body position above the water.

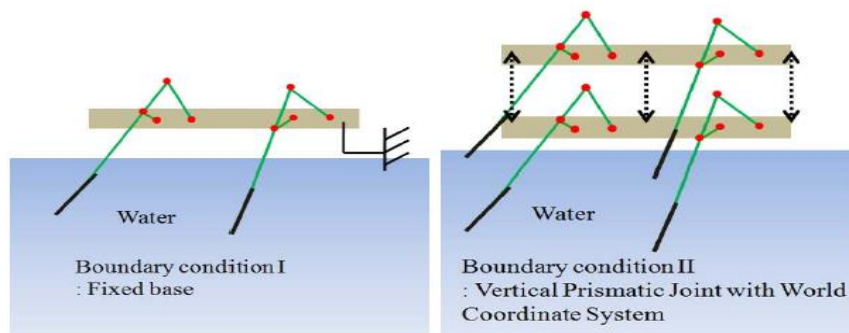


Figure 7 Boundary conditions of different simulations, concerning the lift force, Boundary I is set to estimate the average lift force, Boundary II is set to determine the convergence of the position above the water [11].

The results of the robot indicate that the lift force increases as the foot employs a longer time in the water and reaches the maximum value when it is submerged. However, to have such a situation the body should be closer to the water surface which is not relevant concerning the retraction phase and increasing the downward force in this stage.

To have a balanced behavior of the robot a minimum frequency of 7 [Hz] is suggested which is almost the same rate of Basilisk Lizards action. The steady-state level is highly

1. Introduction

affected by the frequency, as an increase of the frequency increases the level of the body in which the robot reaches a steady state. Though, it should be taken into account that increasing the frequency can also lead to an unstable state.

- **Stability**

The stability studies are done through the motion of the body about each axis. The first analysis is done concerning the pitch motion. Each leg provides a significant force to the body that can lead to a pitch moment and sink the system. Due to the geometry of the robot, the pitch moment causes the robot to flip backward, as shown in the following figure. To counteract the motion, a tail is placed behind the body. The force created by the tail can balance the pitch moment and stabilize the movement.

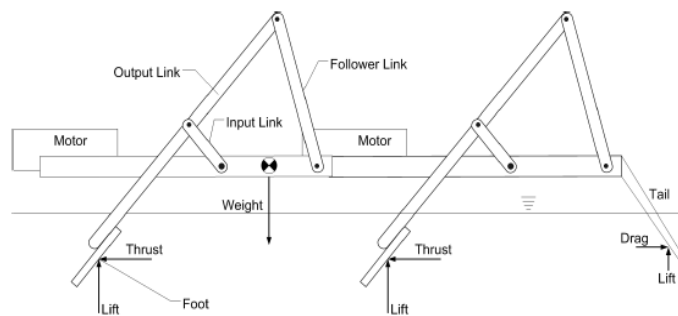


Figure 8 the scheme of the robot and the forces applied to it [8].

To minimize the effect of the tail on the center of mass, light material is preferred for the tail. However, the tail itself can cause some issues, such as applying a drag force that opposes the motion of the body. It is also observed that using a passive tail cannot guarantee the stability of the system in the case of having disturbances due to the variations of the velocity or average pitch moment. To overcome this problem an active tail is suggested. The motion of this tail is slow, so no air cavity will be created during the action.

The other analysis is done regarding the roll motion of the body. As the robot is small, it is so likely to lose control of the roll motion during the action. This problem becomes even worse when the robot uses a pacing gate. To analyze this motion, the following factors should be taken into account: running frequency, roll angle, foot depth, footpad configuration, and the average lift source [8]-[12].

1. Introduction

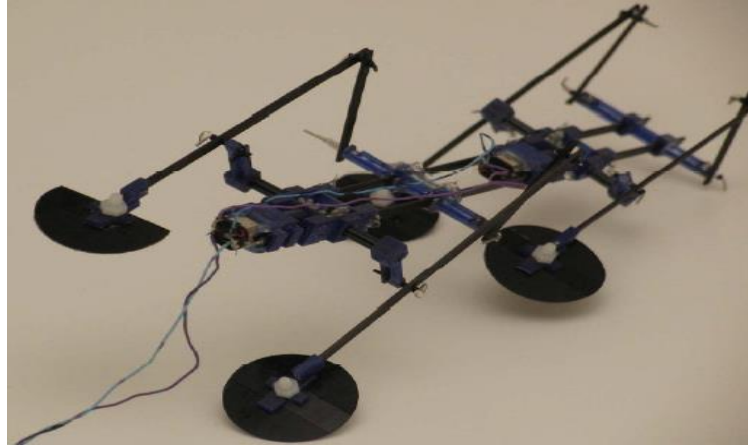


Figure 9 four-legged robot, the prototype used for running on the water [11].

1.2.5. water skippers

The work done in this project is quite new and no particular studies have been found based on this concept. Fortunately, there is some evidence that proves the possibility of using the idea proposed by the project in a real-world situation. Some people have been able to use this method experimentally and skip the water surface by using vehicles that are not designed for such a mission. The first case is a motorbike that is modified in a certain way that can resist sinking and persist above the water while propelling itself forward.

The rear wheel of the motorbike works as a propeller and can generate hydrodynamic force by splashing the water. For this aim, the rear wheel has a specific form to improve the force created by the wheel. Once the wheel starts moving, it creates a force that pushes the body forward, however, to ensure its position above the water, two flat plates are connected to the sides of the wheels that create an upward force.

A Suzuki with a dry weight of 100 [kg] and a maximum power of 58 [hp], was able to skip the water at a speed of 75 [km/h]. This is an unexpected result of a vehicle that is not built for operating in the water.

The most similar case to the project is a snowmobile, that is designed to move in a snowy condition. To have a better grip in these situations, several plates are connected to a continuous track of this vehicle. The role of these plates is to increase the grip of the snowmobile. But it turned out that the plates are useful to create a supporting force in the water too. Then in this way, by splashing the water it can create enough force to ensure the body position above the water and propel it forward.

1. Introduction

These samples show the feasibility of the project in a real-world condition. Although they have been able to use snowmobiles and motorbikes to drive on the water surface, no scientific study has been regarding these cases, and as the news says, at least one person died while trying to use a snowmobile to skip the water. Although it is possible to drive on the water using these vehicles, it does not guarantee the safety of the passengers. Thus, before using this technique, specific investigations and studies should be done, to design a proper system that ensures both safety and high efficiency [13], [14].

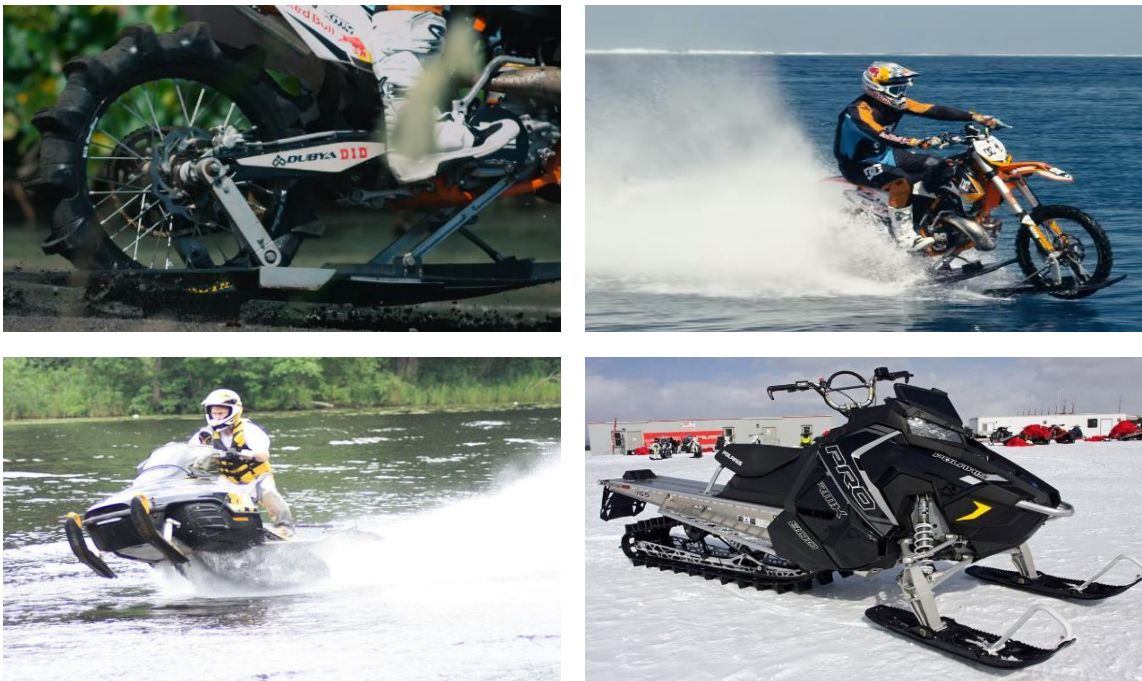


Figure 10 The pictures of a modified motorbike and a snowmobile operating on the water

1.3. Objectives

The project claims a more efficient way for high-speed water-crafts and is mainly focused on the performance of this kind of transport especially at high velocities. The proposed solution considers two important factors, efficiency, and safety.

As the idea is quite new, the plan should be started from scratch. Though, helpful information can be collected by investigating similar phenomena such as the robot designed for running on the water. As introduced earlier, the supporting force created during rushing is mainly formed by hydrodynamic forces.

1. Introduction

This information led to a primary design of the propulsion system employing the same technique.

Like many other concepts, to optimize the cost of the whole process, the idea can be analyzed through several simulations. The most commonly used way of modeling the interaction of fluid over an object, which in this case is a propulsion system is Computational Fluid Dynamics (CFD) simulation. The program used in this project is called COMSOL Multiphysics. These kinds of programs are designed to estimate some important values that can help a designer to predict potential issues. The flow passing through the system is turbulent, and due to the complexity of the flow in this condition, it is quite challenging to provide correct calculations. To optimize the error of the simulations, the structure of the model should be as simple as possible, moreover unnecessary details should be eliminated. Another way of providing high-grade computations is to choose an approach that is relevant to that specific problem, as each approach can be used regarding various situations.

Thus, it is vital to know the working conditions and to choose the best possible strategy for simulations. After validating the correctness of calculations, the results can be used to revise the primary design.

Although CFD results can provide several approximated values such as forces applied to the system, it cannot guarantee the stability of the system, which is essential to ensure safety.

Thus, the results taken from CFD simulations can be further applied in dynamic analysis of the system which is done through Simulink and Matlab simulations. The output of this step represents the responses to various inputs and examines the stability of the system in specific working conditions.

The entire work aims to answer some important questions, is it reasonable to implement this concept rather than using other technologies, and if the answer is positive, how good the performance of such a system would be, to realize the chance of having a market in the future.



Figure 11 The flowchart diagram of the project

2. Conceptual Design

2.1. Geometry

To employ the technique introduced earlier, a concept has been designed capable of generating a supporting force based on this novel method and utilizing the hydrodynamic force for lifting and propelling a watercraft. The lifting force maintains the body above the water and eliminates the contact area between the water and the body, hence, the drag force against the body diminishes. The conceptual design proposed by the project has a body inspired by a jet-ski and a snowmobile and is able to carry up to two passengers. The design contains a propulsion system (that is intended to utilize the method introduced by the project) located under the body, a rudder, a suspension system, etc. The details of each component will be explained separately.

For the sake of simplicity and have more relevant simulations, the CAD model of the concept is done concerning simple structures and shapes that lead to having easier equations in the CFD simulation.

2.1.1. Body

The main advantage of the concept is to eliminate the drag force of the body, that is the greatest issue of a water-craft at high velocities, therefore, the first idea was to design a high-speed water-craft, with a limited number of passengers and of a size comparable to other high-speed crafts such as Jet-skis or boats. As the aim of the project is to represent a new propulsion method, the project is mainly focused on describing the propulsion system and to study its behavior in different situations. However, the effects of the body shape are not negligible; since it can create aerodynamical forces, that can be helpful for the system, as the proper design of the body can generate an additional lift and facilitate the progress.

2. Conceptual Design

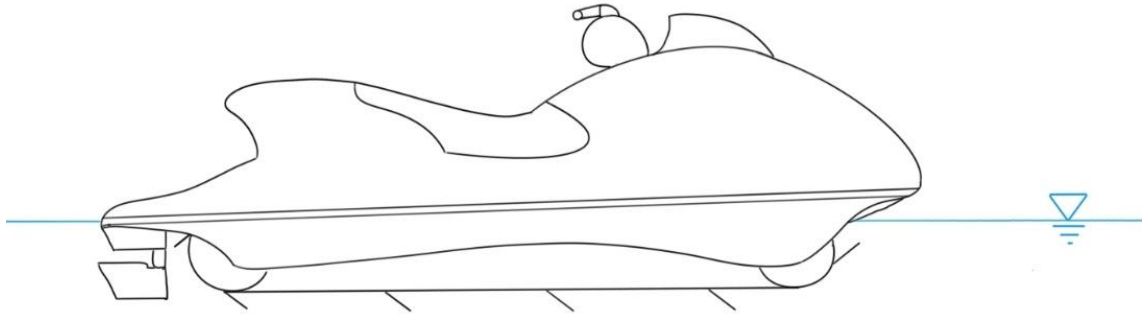


Figure 12 a simple scheme of the water-craft proposed by the project

2.1.2. Propulsion System

The propulsion system is composed of a continuous track, several plates attached to the track, two wheels located in the front and back of the system that represent the position of the direct-drive electric motors and provide the torque required by the system, several rods, and bearings to tighten the tension of the track and facilitate its movement along the path, and at the end, the entire system must be well sealed to avoid any leakage and increasing the weight of the body. An increase in weight makes it more difficult to elevate from the rest position in the water to the water surface.

Modern water-crafts are tending to be environmentally friendly and produce fewer greenhouse gases, for this reason, electric motors have started to replace combustion engines. Using electric motors holds other gains such as the possibility of implementing a more compact design and a lower center of gravity (COG). By lowering COG, the dynamic of the system will be more stable in terms of the roll and pitch moments.

The craft initiates the operation by delivering torque from motors to the track and subsequently the plates, which makes them move through the water. Once the plates start moving, a drag force against their movement occurs. Due to the drag force created by plates, a reaction force appears that pushes the body forward (as the drag force of the plates acts as a supporting force, it will be called “tractive force”). As the main force produced by the system is created by the plates, it is important to design them properly. Plates can affect the behavior of the system in several ways, whether by changing the tractive coefficient which is a function of shape and angle or by affecting the flow passing from one plate to another, which is a matter of the distance between each plate.

2. Conceptual Design

Different shapes provide various tractive and lift coefficients. As mentioned earlier, to simplify the equations solved by simulations, it is more relevant to choose simple shapes concerning parts interacting with the flow. Accordingly, plates selected by the project have a simple rectangular shape.

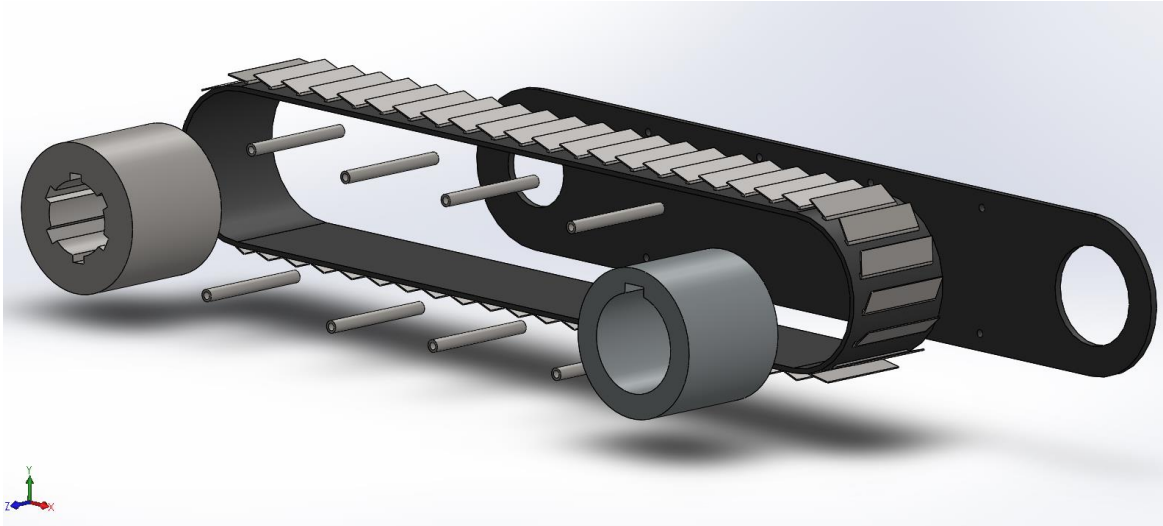


Figure 13 A sample of the propulsion system, designed in SOLIDWORKS

The number of plates is determined by evaluating their effect on the resultant force and the magnitude of the force applied to each plate; while less number of plates generates a larger force on each plate that raises the risk of having issues such as vibration and instability caused by the uneven division of forces along the track.

The force generated by the plates must be manipulated into two directions, to lift and propel the body simultaneously. For this purpose, the plates must be oriented concerning the flow field direction. Hence, two kinds of plates can be used, plates with a fixed angle or plates with a variable angle, that requires an active device for manipulating the angle of plates when required. Plates with a predefined angle, are simpler and can be simply linked to the track, but they have some drawbacks too, as their angle is not adjustable, they cannot provide good performance under all circumstances, e.g. when the lift or propel generated by the system is greater than an expected value, to balance the forces in either direction, the angle of plates should be manipulated, which in this case it is not practicable. Although it is possible to balance forces through the usage of plates with adjustable angles, such plates represent some drawbacks too. These plates require an active device such as an actuator that

2. Conceptual Design

can change the angle, and consequently, the complexity of the system raises which is not relevant.

2.1.3. Maneuvering at low velocity

- **Rudder**

The system possesses different dynamics regarding different ranges of velocities (corresponding to various Reynolds numbers), thus, techniques used for maneuvering the watercraft might vary at each range of velocities.

The low-velocity range can be assigned as the moment when the body is still immersed and is not reached to its relaxing position where the body is assumed to be out of the water and only the propulsion system is in contact with water. Therefore, to maneuver the craft in this situation, a rudder can be used, which is the most typical way used for ships and boat applications.

Maneuvering in this situation can be done through a rudder placed behind the body. Choose a proper rudder is important in terms of safety, efficiency, and cost of maintenance. To do so, some factors should be taken into account, such as the Reynolds number, the angle of attack, the shape of the rudder, the position of the rudder concerning the propulsion system, etc.

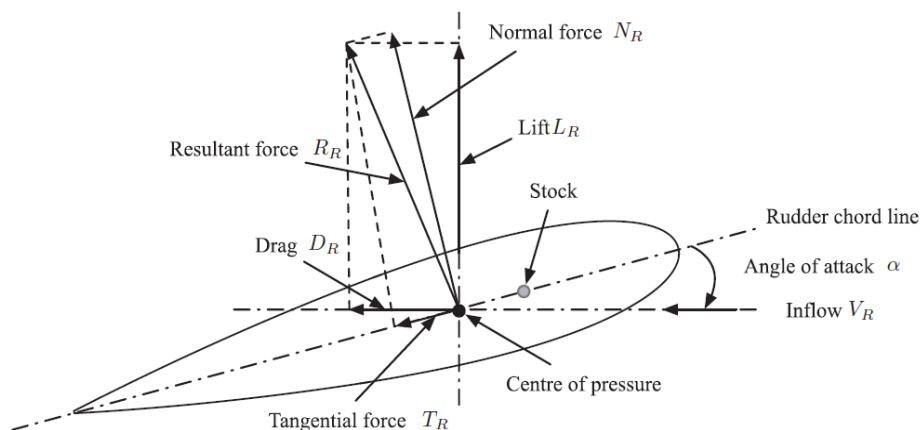


Figure 14 The scheme of a rudder [15].

To compare the performance of rudders, some non-dimensional parameters are defined, which can be useful for choosing a proper rudder concerning a particular problem. These parameters are the coefficients corresponding to the lift C_L and drag C_D , the maximum lift

2. Conceptual Design

C_{Lmax} , the normal force C_N , the tangential force C_T , and the ratio among the lift and drag coefficients C_L/C_D . The coefficient can be evaluated through the following equations,

$$C_L = L_R / (0.5\rho V_R^2 A_R) \quad (5)$$

$$C_D = D_R / (0.5\rho V_R^2 A_R) \quad (6)$$

$$C_N = C_L \cos\alpha + C_D \sin\alpha \quad (7)$$

$$C_T = C_D \cos\alpha - C_L \sin\alpha \quad (8)$$

where α is the angle of attack, V_R is the velocity of the inflow, A_R is the area of rudder.

To study the orientation of the body, some angles such as the angle of attack α , the rudder angle δ , and the body drift angle β should be taken into account. Then, the effective rudder angle can be written as

$$\alpha_R = \delta - \beta \quad (9)$$

Other important factors affecting the performance of rudders are the shape and the contact area of the rudder, which can affect the maneuverability of a rudder and the cavitation. The force generated by a rudder is directly related to the area, therefore, to guarantee the force required for maneuvering sufficient contact area is needed. As the concept is assumed to elevate the body at high velocities, the rudder starts losing the contact area as well. At high velocity the force created by rudder can become so great, therefore, one way to compensate it is to reduce the contact area. As the figure shows the rudder has a narrow section at the lower part, that allows the rudder to have smaller contact area during the elevation and emerging from the water. To analyze a relevant response of a rudder the following ratio is defined. This limit can be assigned as follow

$$\frac{A_R}{L_{pp}T} = 0.01 \left[1 + 50C_B^2 \left(\frac{B}{L_{pp}} \right)^2 \right] \quad (10)$$

2. Conceptual Design

where C_B is the block coefficient and B is the beam of the body. The suggested value of the ratio $\frac{A_R}{L_{pp}T}$ is to be greater than the right term, for the rudders placed behind propellers [15].

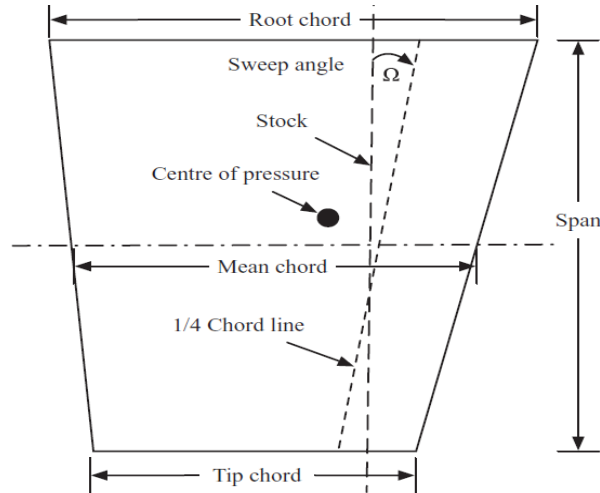


Figure 15 Side view of a rudder and its specifications [15].

- **Leaning**

Because of the comparable size of a driver to the size of the entire system, turning at higher velocities can be employed through leaning and the inertial force generated by the leaning. In the case of following a perfect circle during turning, the angle of leaning can be found as

$$\theta = \arctan\left(\frac{v^2}{g r}\right) \quad (11)$$

where v is the forward velocity and r is the radius of the turn. As the study is based on a craft working in water the lateral forces applied during turning are quite complex to analyze and model, and as the main goal of the project is to study the behavior of the propeller, the study will not go into details of such analysis.

2.1.4. Suspension

To have a more comfortable and safer water-craft, a suspension system can be located between the connection of the body and the propulsion system, in this way, it can absorb shocks and sudden changes of vertical displacements that can be created by waves of the

2. Conceptual Design

water. Because of the similarity of the propeller to a snowmobile, the suspension and shock absorber can be used similarly.

The project is not going into details of this part of the system and will mainly focus on the behavior of the propulsion system and the power required.

2.2 Mechanism

Most of the high-speed water-crafts use a propeller fixed at the back of the body and floated through the water. The movement starts with the thrust force generated by a propeller that pushes the body forward through the water. Because of the continuous contact between the body and the water, a hydrodynamic force creates that is known as a combination of two forces lift and tractive. The presence of such forces limits the operation of the system, as at high velocities the force applying to the body becomes so large and creates severe shocks to the body, which makes it inappropriate in terms of safety and power required.

On the contrary, the technique presented in this project follows a totally different way to generate a supporting force for transporting the entire body. As explained earlier, the body and propulsion systems are separated, and the body will not be directly in contact with the water after a certain velocity. The idea is to eliminate the drag force applying to the body that is floating through the water. To do so, the propulsion system must be able to ensure a lift equal to or greater than the bodyweight of the system. To obtain this goal, the track that conveys several plates must start moving across the water, this movement creates a tractive force against the plates that yields to a propel and lift delivering to the system. Once the force created by the plates is large enough and the body totally emerges from the water, the contact area would be among the bottom of the propulsion system and the water. At this moment, it is straightforward to realize the difference between the concept and other watercrafts such as boats. In this case, at high velocities, the lower side of the propulsion system will be in contact with the water, while the bottom of the propulsion system that includes the plates has a relative velocity with respect to the water and the force generated by them acts as a supporting force and not against the move.

2.2.1 Hydrodynamics

As mentioned earlier, the phenomenon of walking on the water is called rushing. Rushing is studied in three different stages, slap, stroke and retraction. The same stages can be

2. Conceptual Design

considered for studying the forces created by the plates. The technique used by the concept mainly relies on the hydrodynamic force created by the plates in the stroke phase. As a matter of fact, the estimation of the hydrodynamic force is quite complex and requires accurate information such as the velocity of the fluid, pressure gradients and stresses along with the plates. Due to the complexity of such analysis, such problems usually solve numerically.

To analyze the mechanism, the change of fluid momentum must be additionally taken into account. For the sake of simplicity, hydrodynamic analysis of a craft can be characterized by some dimensionless numbers. In this way, some forces with less importance and lower magnitude can be neglected and the overall equation of the system can be simplified. Water runners are mostly defined by high Reynolds number. To analyze the forces applied to the system Bernoulli equation can be considered,

$$\frac{\partial \Phi}{\partial t} + \frac{1}{2}|u|^2 + \frac{p}{\rho} - g \cdot x = c \quad (12)$$

Where u is the velocity of fluid, Φ the velocity potential, x the position of the body, and c a constant.

The equation can be also written as the following, by replacing the pressure with stress tensor T and the curvature force.

$$F = \int_S \left[\left(\rho \frac{\partial \Phi}{\partial t} + \frac{1}{2} \rho |u|^2 - \rho g \cdot x + \sigma(\nabla \cdot n) \right) \right] n - \nabla \sigma dA \quad (13)$$

The equation above gives the possibility of addressing all the possible forces applied to the system.

$$|F| \sim \rho U^2 A + \rho g h A + \rho V \frac{dU}{dt} + \mu U A + \sigma \frac{1}{w} A - \nabla \sigma A \quad (14)$$

tractive buoyancy added mass viscosity curvature Marangoni

2. Conceptual Design

Depending on the characteristics of the problem and its working conditions, terms with lower importance can be neglected. As mentioned earlier, the major part of the supporting force required can be generated during the stroke phase. The most effective forces produced in this stage are the tractive force, the added mass and the buoyancy. Though, the effect of the slap and retraction phases cannot be eliminated as they might affect the stability of the system and cause vibrations.

In the following sections, the effect and importance of each stage on the overall behavior of the system will be explained [15].

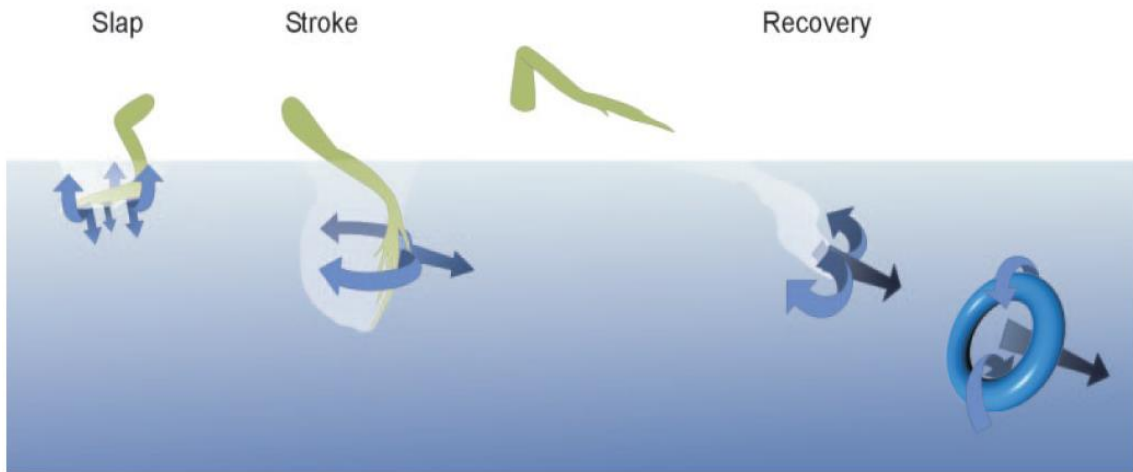


Figure 16 Running on water, the demonstration of rushing through various stages by a Basilisk lizard [15].

- **Slap**

By looking at the works of literature, and studies done based on the behavior of water-walkers with a large body, useful information regarding the slapping phase can be extracted. Two species capable of running on the water are Basilisk lizards and Clark's grebes, which are the largest water runners ever known. Several studies have been done base on their behavior, and as experiments show Basilisk lizards are able to generate up to 30% of their body weight in the slapping phase alone, whereas, the force created at this phase loses its importance for adults with larger bodies. Comparing to Basilisk lizards, grebes are able to provide higher slap forces which are due to the complex shape of their foot.

As a result, the hydrodynamic forces generated in the slapping phase are related to size, shape, and velocity. As the literature shows, several experiments have been done regarding the forces generated at this phase and the factors that can affect it. For this purpose, the

2. Conceptual Design

forces generated by a circular disk dropped into water are measured. The impulse created by the disk is related to the water accelerated by the disk, which has a sphere shape and a radius similar to the radius of the disk. The results also show that 25% increasing the area of the disk can lead to having an increase of 40% in the slap phase. It is also important to note that, as hydrodynamic force is a function of velocity squared, even a small change of the velocity can increase the force extremely.

In conclusion, the size, shape, and velocity can be specified as the main factors of the extent of an impact. The impulse created by an object falling into water can be estimated:

$$Impulse_{slap} = M_{object} \Delta u_{slap} \quad (15)$$

$$\Delta u_{slap} = u_{impact} - u_{end} \quad (16)$$

where M_{object} is the mass of the object, u_{impact} is the velocity at the beginning of the action when the object hits the water, and u_{end} is the velocity in which the slap phase finishes [6].

To analyze the behavior of a plate concerning a multiphase flow, dynamics of free surface are needed. The dynamic force applied to a plate can be written as

$$F = \int_S T \cdot n \, dS + \int_C \sigma t \, dl \quad (17)$$

where S represents the area of the body in contact with the water and C is the line where the free surface exists. Two terms representing in the equation are the hydrodynamic stress and the force produced by the surface tension. Surface tension applies tangentially to the surface [16].

- **Stroke**

The stroke phase starts soon after slapping, while it plays an important role in terms of supporting the movement of large water-walkers, as they are not able to produce enough force in the slap phase and to resist sinking the rest of the force required can be created in the second phase. The forces applying to the plates at this stage will be completely explained

2. Conceptual Design

in the following section "forces at plate" that are dedicated to the hydrodynamic forces applied to a plate during the stroke phase [16].

- **Retraction**

To accomplish rushing and prevent sinking, a water-walker must be able to minimize downward forces that can appear in the recovery phase, when a foot starts emerging from the water and prepares for the next stride. The drag force created in this stage can be minimized by collapsing the foot and reduce the contact area. Accordingly, one of the most important factors of this stage is the shape of the foot. Although the downward force generated by the plates in the concept might not be so large with respect to the supporting force created by other active plates, it can play an important role in starting conditions when the body is partially immersed and wants to emerge from the water. Downward forces created during the retraction phase are also important in terms of the stability of the system, while they can affect the overall behavior of the system and must be taken into account as disturbances of the system. Such forces can be minimized by using foldable plates capable of collapsing during the recovery phase [16].

2.2.3 Statics

Generally speaking, water-crafts have a dense body with a density greater than the water, therefore, it is also important to ensure the position of the watercraft and to avoid sinking in static conditions. Depending on the size of an object different methods can be used to keep it above the water. As an example, small objects can be floated across the water using a combination of forces such as buoyancy and curvature. In this case, the curvature and buoyancy forces act as supporting force and are equal to the body weight. To analyze whether an object is able to overcome its body weight by using such forces, a term called capillary length has been defined. By comparing the length of the object and capillary length, one can have an idea about the possibility of supporting the bodyweight of an object above the water. However, these forces concern small bodies and can be neglected in this case.

In static conditions, large bodies are mostly supported by buoyancy, and cannot rely on forces such as surface tension, curvature, etc.

2. Conceptual Design

Considering the body is initially on the water surface and dropped into the water. At this moment, the forces applying to the body are mainly the body weight, the buoyancy, and the drag force, that will act against the movement of the body and after several bouncing and losing energy, the motion will be damped, and the forces will be balanced. In the stationary condition when the body stops bouncing the bodyweight is almost equal to the buoyancy force [16].

- **Buoyancy**

When a large body is immersed in an incompressible fluid, it displaces the same volume of the fluid as the immersed part of the object. This principle gives the possibility of estimating the forces acting to a body submerged in a liquid and whether it would sink in the liquid or remains floating. The gravitational force of the body is

$$F_G = \int_V \rho_{body} g dV \quad (18)$$

And the buoyancy force is

$$F_B = \oint_S p dS \quad (19)$$

In the case of a floating object, the two forces must be equal and cancel each other.

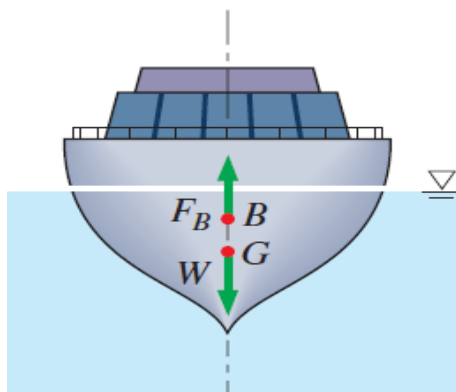


Figure 17 The forces applied to a floating object, where F_B is the buoyancy and W is the body weight. The points in which each force is applied are represented as B and G which are corresponding to F_B and W [17].

2. Conceptual Design

The total force can be written

$$F_{Total} = F_G + F_B = \int_V (\rho_{body} - \rho_{fluid}) g dV \quad (20)$$

Knowing the buoyancy force applying to an object is important in terms of the balance of the body in static conditions and having an idea about the depth of the immersed part of the body. Knowing the volume occupied by the body at static conditions is also important in the starting state. The position of the body in static conditions is also vital to estimate the time needed for the system to reach a steady-state condition. The depth of the body will be used in later simulations and dynamic analysis, as the initial condition of the system [17].

2.3. Forces at plate

To simplify the analysis of plates, hydrodynamic forces applied to each plate can be studied in different stages. The supporting force generated by the propulsion is mainly performed by active plates submerged in the water. The forces applied to the active plates can be divided into two components, tractive and lift, which are mainly due to the resultant pressure and shear force acting on the plate.

To simulate the lower part of the track, where the plates are totally submerged in the water, it is assumed that the plates are fixed, and the fluid is flowing over the plates. Thus, due to the interaction between the plates and the flow, a tractive and lift forces form [18].

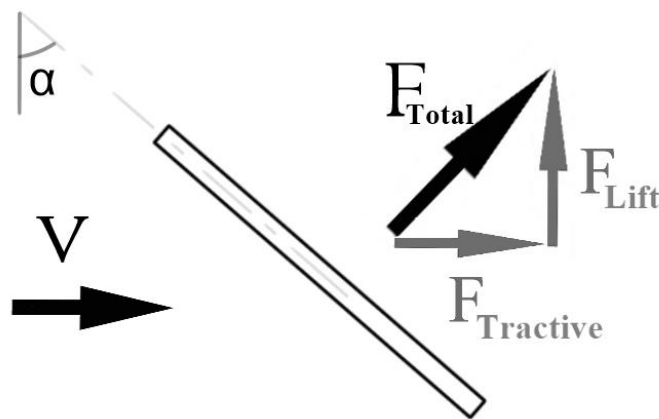


Figure 18 normal force applied to a plate inclined with respect to the vertical axis

2. Conceptual Design

The forces acting on the plates are the summation of the pressure and shear forces, which are divided into two directions. The overall lift and tractive forces can be estimated by integrating the following equations

$$F_{Lift} = \int_A dF_{Lift} = - \int_A (P \sin\alpha + \tau_w \cos\alpha) dA \quad (21)$$

$$F_{Tractive} = \int_A dF_{Drag} = \int_A (-P \cos\alpha + \tau_w \sin\alpha) dA \quad (22)$$

where PdA and $\tau_w dA$ are the pressure and shear forces on a differential section area respectively.

These forces are highly related to the angle of plates, which is called the angle of attack. Due to the presence of such an angle, a pressure difference between the top and bottom of the plate appears that leads to generating a lift force and pushes the body upward. It is not relevant to compute the forces applying to a plate directly, instead a typical way is to use dimensionless numbers. Two dimensionless numbers, tractive and lift coefficients can be defined as

$$C_D = \frac{F_{Tractive}}{\frac{1}{2} \rho V^2 A} \quad (23)$$

$$C_L = \frac{F_{Lift}}{\frac{1}{2} \rho V^2 A} \quad (24)$$

where V is the upstream velocity, ρ is the density, A is the frontal area, and the term $\frac{1}{2} \rho V^2$ is referred to dynamic pressure. These coefficients are also a function of the shape, the orientation of plates, the Reynolds number and the roughness.

The coefficients introduced earlier can vary along the surface, as the velocity of the flow changes locally, but usually, coefficients corresponding to the entire area consider, which can be found by averaging the local coefficients and can be estimated as

2. Conceptual Design

$$C_D = \frac{1}{L} \int_0^L C_{D,x} dx \quad (25)$$

$$C_L = \frac{1}{L} \int_0^L C_{L,x} dx \quad (26)$$

where L is the length.

The tractive force is a combination of wall shear and pressure forces. Wall shear stress is due to the frictional forces close to wall boundaries, while pressure drag is directly related to pressure and depends on the shape of the object. The coefficients regarding to these forces can be found as

$$C_{D,friction} = \frac{F_{friction}}{\frac{1}{2} \rho V^2 A} \quad (27)$$

$$C_{D,pressure} = \frac{F_{pressure}}{\frac{1}{2} \rho V^2 A} \quad (28)$$

The summation of these coefficient is equal to the net drag coefficient found in equation (23) [17].

The friction drag greatly depends on the position of the object with respect to the flow direction, as it is assumed to be zero for a flat surface oriented vertically with respect to the flow direction and oppositely, it is maximum if the flow is parallel to the surface. It is also a function of viscosity which means, depending on the type of fluid, the friction force can be different.

The importance of the friction force can be analyzed by knowing the Reynolds number referring to the case of study, as the Reynolds number and the viscosity are inversely proportional. In other words, increasing Reynolds number reduces the effect of the friction force. Therefore, for problems with great Reynolds number, the effect of the friction force on the net drag force is negligible and it can be concluded that the drag is mainly generated by pressure drag. The same assumption holds for cases with low Reynolds number, but in these cases, the drag is mostly due to friction drag. Moreover, as explained earlier, the supporting force generated by the propulsion system is mainly due to the drag force created by the motion of plates.

2. Conceptual Design

- **Flow separation and Reattachment length**

Flow separation usually occurs to flow at high velocities and resulting in a sudden change in the direction of the flow. For the propulsion system, the flow separation can be expected to happen after facing a plate and recirculating behind the plate. The separation point varies, depending on various conditions, such as the Reynolds number, the changes of free stream, the shape of the surface.

The region in which separation happens is called separated region. In this case, the region can be assumed to appear behind the plate. The pressure in this region is lower than the frontal part of the plate, furthermore, bigger regions provide greater drag.

Estimating the region of separation flow is important in terms of designing the propulsion system and choosing the proper distance among the plates. To optimize the force produced by each plate, it is vital to know the point in which recirculation of the flow ends, this distance is called Reattachment length. The number of plates and their distance from each other can be chosen considering the reattachment length [19].

- **Geometry**

One of the most important factors affecting the drag and lift is the shape of the plate. Hence, an object with various shapes represents different drag coefficients. The value of the drag coefficient is usually obtained experimentally, while, numerous coefficients have already been given in the literature, concerning objects with different shapes and characteristics.

The drag coefficient is related to the Re number, for flows with a Re number below 10^4 , while for higher Re number, corresponding to fully turbulent flows, the value of the coefficient does not change and the effect of the Re number is negligible. This assumption is true for most of the geometries.



Figure 19 The effect of the shape on the drag coefficient [17].

2. Conceptual Design

A proper design of the plate can help to optimize the performance of the system. In this section, some disks with different designs used for water skipping robots are introduced. However, in this case, the robot is small compared to the watercraft designed in this project, which gives it the possibility of using the trapped air below each leg and cannot be considered the same as the current project, but it can provide some information regarding the design of the propeller.

Compliant feet: these feet have a circular shape and can be folded in one direction, which makes the foot rigid during the creation of supporting force, and folded in the last stage when a downward force can be created during the recovery phase of plates.

Elastic feet: they use a piece of elastic material that is connected to the folding joints and can increase the effect of spring stiffness.

Elliptical: as its name represents, they have an elliptic shape. They were designed to see whether they can affect the air trapped under feet since as it is mentioned earlier, the trapped air has an important role for these robots while they have a light body and the air can affect their move along the water.

Holed foot: this foot has a circular shape and contains several holes at the center. The holes are designed to let the air pass in the retraction phase, besides, they have to be so tiny to pass the air only and do not let the water pass through.

Hydrophobic: these feet take advantage of a circular shape hydrophobic coating of WX2100.

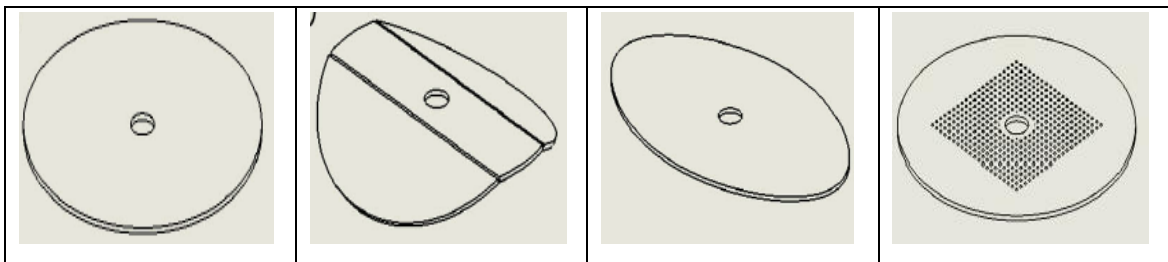


Figure 20 Some of the possible shapes for the disks used by the robot [10].

2. Conceptual Design

The time response of the flat, hydrophobic and holed feet are quite similar, at the same time, the hydrophobic feet represent slightly better results and the holed feet worse. For the sake of simplicity, the track designed for the project has a simple rectangular shape. The reason for choosing such shape at this level is to simplify the simulations and compare their results with the experimental data [10].

- **Flow over continuous track**

Plates are attached to the propulsion system by means of a continuous track, that moves at the same velocity of the plates. Since the track is in contact with water, it is accountable to some forces delivered to the system. Although, it is quite difficult to estimate and analyze the flow over the track, as the flow becomes chaotic after hitting a plate, consequently, the flow facing the track is irregular.

The region in which a track is in contact with water can be considered as the distance separating two plates. For the preliminary studies, the track can be considered as a flat plate.

As the wall boundaries of the entire system are assumed to be in no-slip condition, the velocity of the first layer near the wall is considered to be zero, that slows down other layers close to this layer, while, the velocity of the upper layers increase until the effect of this layer becomes negligible and can be neglected.

For the sake of simplicity, some parameters are defined to scale the thickness of the layers in a no-slip condition. Considering the problem in the x and y axes, while the plate is located along the x -axis and the flow is parallel to the plate. The velocity of flow u varies along the y -axis, as it is zero at $y = 0$ and is nearly equal to V at $y = \delta$, where u is the velocity of the fluid along the x -axis and V is the free stream velocity. The distance in which the flow velocity remains constant and not affected by turbulent layers is assigned as δ . This thickness can be allocated at the region in which velocity u is equal to $0.99 V$. Once the thickness is located and the boundary layer is estimated, the flow can be studied concerning two different regions, as in the boundary layer, the effect of viscosity is unavoidable, while, on the contrary, beyond the thickness, that is also called irrotational flow region, the effect of viscosity is negligible and the velocity does not change significantly [17].

2. Conceptual Design

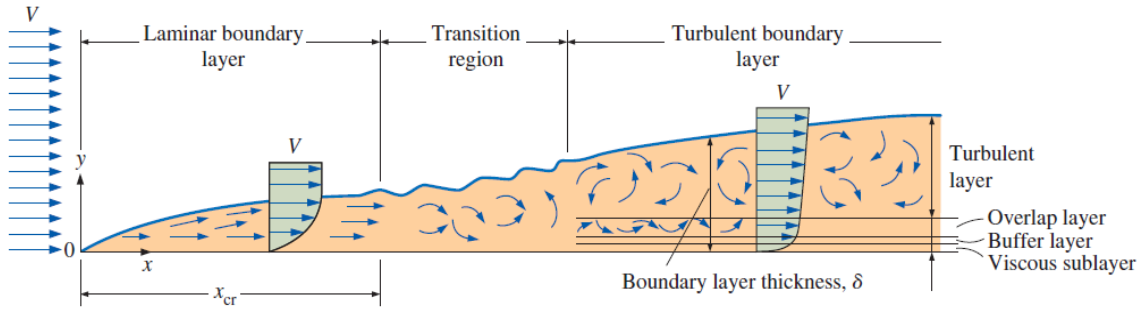


Figure 21 The transition of the flow from laminar to turbulent in the case of the flow over a flat plate [17].

In the case of having flow parallel to a plate, the drag coefficient is mainly due to the presence of the friction drag coefficient and the pressure drag can be neglected. The friction drag can be estimated from

$$F_{Drag} = F_{friction} = \frac{1}{2} C_f A \rho V^2 \quad (29)$$

where C_f is the average of friction coefficient (the pressure drag effect is neglected so $C_D = C_f$), A is the total surface area, V is the relative velocity of fluid.

The boundary layer itself is divided into several sublayers with different characteristics. The sublayers are defined by the vertical distance from the plate. Starting from the sublayer close to the wall, called the viscous layer, where the flow is highly affected by the viscous effect. After that, the buffer layer appears, where the effect of turbulent is considerable but the viscous effect is still playing an important role, while, by going further, the turbulent effects become more and more dominant and the viscous effect becomes negligible. The layer in which the viscosity loses its influence and the flow is mainly characterized by turbulent effects is called outer layer. Knowing sublayers, help a designer to assign a proper mesh size to simulate a turbulent flow in a CFD simulation.

The transition of a flow from laminar to turbulent over a flat plate depends on several factors such as the roughness, the velocity of the flow, the extent of a plate and the characteristics of the fluid itself. To estimate the behavior of the flow, one can take advantage of the Reynolds number. Therefore, to analyze the flow over the surface, the Reynolds number of that specific point can be calculated. The Reynolds number associated to a point at a distance from the starting edge can be found as

2. Conceptual Design

$$Re_x = \frac{\rho V x}{\mu} \quad (30)$$

where μ is the viscosity of the fluid, V is the upstream velocity. In order to realize the position in which the flow has the potential to transit from laminar to turbulent, the Reynolds number can be found, as it is already defined by literature, in the case of flat plates a flow is likely to become turbulent at $Re \cong 1 \times 10^5$ and fully turbulent for Reynolds numbers greater than 3×10^6 .

Knowing these regions is important in the sense that each region represents various friction coefficient. The following figure represents how this coefficient changes according to different conditions [17].

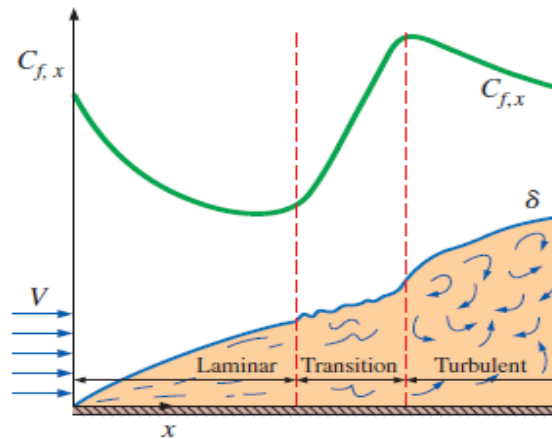


Figure 22 The variation of the friction coefficient over a flat plate parallel to the flow [17].

3. Numerical simulations

3.1. Modelling strategy and approximations

Computational fluid dynamics (CFD) simulations give the possibility of predicting the behavior of a fluid flow before actually employing it in a real-world condition, and as a matter of fact, the cost of the project will be reduced significantly. The software used in the project is COMSOL Multiphysics. It has been used for predicting the responses of the system in different working conditions.

To render high-grade results, the turbulent model used for the simulation must guarantee a good estimation concerning the near-wall layer, otherwise, a wall function must be defined beside that. However, some approaches do not require a wall function, but the grid size concerning near-wall regions must be selected accurately. To find a reliable approach concerning the problem, various modeling strategies methods are examined, such as RNG k-epsilon, k-omega model, SST model.

Another important factor concerning CFD simulations is the running time, which becomes significant in the case of more complex simulations. So, it is convenient to take into account not only the accuracy of the results but also the time consumption.

First, the flow domain in which the program is going to deal with must be defined. Since the system works at high velocities, corresponding to high Reynold's number, the flow domain utilized for the application is turbulent.

- **Navier-Stokes equations**

One of the most known equations used for fluid simulations and modeling is the Navier-Stokes equation, which can be written as follow, concerning a compressible Newtonian fluid:

$$\rho \left(\frac{\partial u}{\partial t} + u \cdot \nabla u \right) = -\nabla p + \nabla \cdot \left(\mu (\nabla u + (\nabla u)^T) - \frac{2}{3} \mu (\nabla \cdot u) I \right) + F \quad (31)$$

3. Numerical simulations

While $\nabla \cdot \mathbf{u} = 0$ for an incompressible flow and simplifies the equation by neglecting the term from viscous force, $-\frac{2}{3}\mu(\nabla \cdot \mathbf{u})$. \mathbf{u} and p represent the velocity and pressure of the fluid respectively, ρ is the density and μ is the fluid dynamic viscosity. The equation can be divided into four terms, that each describes an individual characteristic of the fluid motion. These terms are the inertial forces, pressure forces, viscous forces, and external forces. Although, beside them, the continuity should be solved,

$$\frac{\partial \rho}{\partial t} + \nabla \cdot (\rho \mathbf{u}) = 0 \quad (32)$$

the conservation of momentum and the continuity can be represented by the Navier-Stokes and the conservation of mass respectively. Nevertheless, these equations are complex especially regarding an asymmetric model with diverse shapes and geometries. To solve the equations of a model, the boundaries (such as inlet, outlet, walls, etc.), must be defined.

To simplify the computations of the model, it is vital to identify the characteristic of the flow, which gives the possibility of neglecting some terms in the equations and consequently makes it more adaptable to be solved. To have an idea about the behavior of the flow, non-dimensional numbers such as Reynolds and Mach number can be used, which express a preliminary outline of the flow, for instance, to realize whether the flow is laminar or turbulent.

The Reynolds number can be simply found as, $Re = \rho UL/\mu$, which can be also considered as a ratio between the inertial and viscous forces. Another nondimensional number utilizing in fluid mechanics is the Mach number, $M = U/c$, where U is the velocity of the fluid and c is the velocity of sound in the same fluid. The resulting number will represent whether a fluid is compressible or not [20]-[25].

- **Turbulent flow (High Reynolds number problem)**

For the problems with high Reynolds number, and when the inertial forces are dominating, small eddies play an important role in terms of modeling a turbulent flow. To overcome such a problem and identify small eddies in the flow, a fine mesh must be dedicated. However, using a fine mesh makes the problem computationally expensive. One way to

3. Numerical simulations

simplify this problem is to use Reynolds-averaged Navier-Stokes (RANS) that can use the average value of the velocity and the pressure of flow in time [26].

- **Limits of the Navier-Stokes equations**

There are some specific cases in which Navier-Stokes (NS) equations cannot be applied. These cases are introduced by a number called Knudsen number, $K_n = \lambda/L$, that is used to figure out whether NS equations can be applied or not. Basically, K_n refers to the physical length scale L of the model with respect to the mean free path λ of the particles of the fluid, and as a result, the NS can be valid for length larger than the free path.

Turbulent flow can be simulated through different formulations providing by COMSOL: The L-VEL, algebraic yplus, splart-Allmaras, k- ϵ , k- ω , low Reynolds number k- ϵ , SST, and v2-f turbulence models. In the following parts, each of them will be explained briefly [20]-[25].

- **Turbulence modeling (single phase)**

The specified fluid used in simulations is assumed to be Newtonian since the body would interact with water and air. The propulsion system works at a high Reynolds number, which corresponds to turbulent flows. Turbulent flows make the problem more complex, due to the unexpected behavior of the flow. Usually, turbulent flows are divided into sub-layers and can be studied separately.

The passage of the flow from laminar to turbulent occurs within three subregions, laminar, transition and turbulent. Eddies start appearing from the transition state until the flow becomes turbulent. The simulation has to be performed taking into account time-dependent Navier-Stokes equations. Therefore, a proper mesh size has to be determined to consider the smallest eddies in the flow. As Reynolds number increases, small eddies become more visible, and it is vital to remark that, eddies make the flow unstable, as the velocity becomes negative spontaneously, and induces oscillations.

To deal with this problem computations can be done using Reynolds-averaged Navier-Stroke (RANS), which provides an average value concerning fluctuations among the flow.

3. Numerical simulations

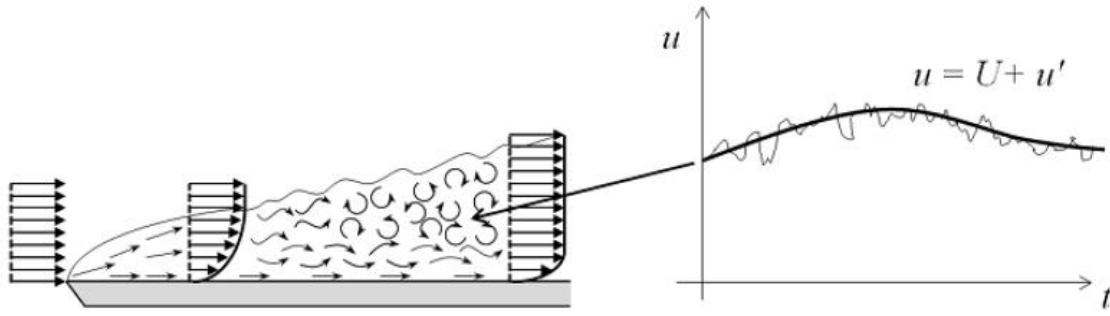


Figure 23 Reynolds averaged Navier Stroke (RANS) averaging the fluctuations within the flow [26].

To make the simulations feasible, the layer close to the wall or as it is also called viscous sublayer can be defined separately. To analyze the behavior of the flow in the near-wall region, some models take advantage of the low Reynolds number model, which refers to the region close to the wall, at y tending to zero. The flow in this region is governed by the viscous effect, moreover, in a non-slip condition, the velocity of the flow reduces for layers closer to the wall and tends to zero for a thin sublayer near the wall [26].

- **Turbulence modeling (multi-phase)**

Although the supporting force is mainly formed by the active plates submerged in the water, it is also important to assess the forces created during the slap and retraction stages. The plate should be modeled in a multiphase condition since it is supposed to interact with the air and water.

Considering the plate possesses a rigid body, its motion can be computed by solving ordinary differential equations. The total stress applied to the boundaries of the object is given by

$$f = n \cdot \left\{ -pI + (\mu(\nabla \mathbf{u}_{\text{fluid}} + (\nabla \mathbf{u}_{\text{fluid}})^T) - \frac{2}{3} \mu (\nabla \cdot \mathbf{u}_{\text{fluid}}) I \right\} \quad (33)$$

where $\mathbf{u}_{\text{fluid}}$ is the velocity of the fluid, μ the dynamic viscosity, p the pressure, n the outward normal to the boundary.

Multiphase models can be analyzed in two groups, the interface tracking (or separated multiphase flow) and the disperse methods. The interface tracking method is usually used in the case of modeling two immiscible fluids with a well-defined interface. It is suitable

3. Numerical simulations

for modeling bubble formation, separated fluid flows, etc. On the contrary disperse methods are typically used for modeling applications such as solid particles in gas or liquid, bubbles in a liquid, while they can be performed through several models, such as the Euler-Euler model, bubbly flow model, mixture model [27], [28].

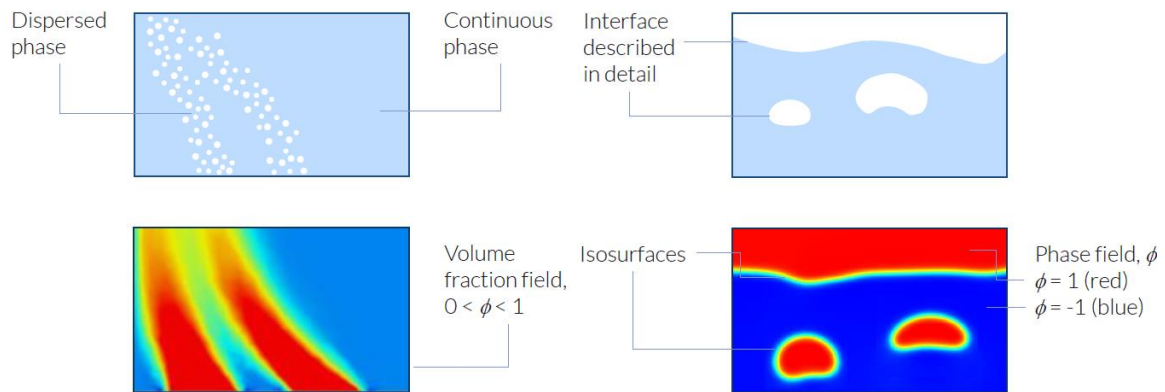


Figure 24 Two different multiphase models, the disperse method (left), the separated flow (right) [27], [28].

- **Wall functions**

As mentioned earlier, due to the complexity of a turbulent flow, it should be classified into different regions, such as viscous sublayer, buffer layer, log-law region, free stream flow region. Considering no-slip condition at the wall, the velocity of the flow can be assumed to be zero. The relation between the flow velocity and the distance from the wall is linear. By increasing the distance from the wall, another layer can be specified as the buffer layer, where the viscous stresses start losing their effect and the stresses of the turbulent flow will take place. The next layer is the log-law region, where the flow becomes fully turbulent and the relation between the velocity and the distance is logarithmic. The distance of the viscous and buffer layers is very small compared to the region concerning the log-law region, in other words, assuming that the distance of the viscous and buffer layers is δ , the distance to the end of the log-law region would be 100δ . The last layer is the free-stream flow region, which is so far from the wall [26].

3. Numerical simulations

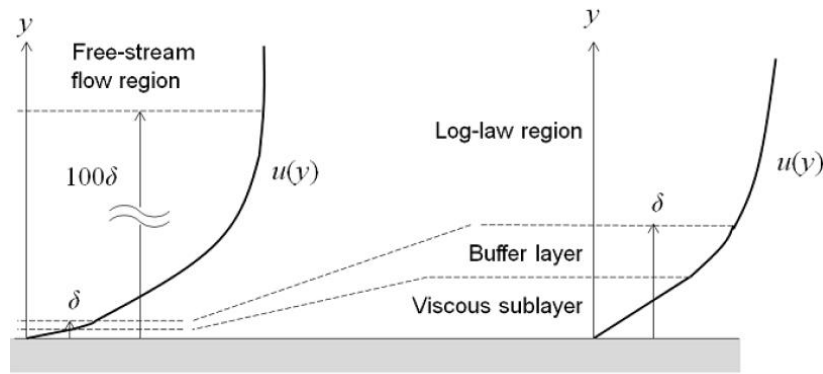


Figure 25 The sublayers dedicated to the near-wall region [26].

From the computational point of view, it is more reasonable to use wall functions in the buffer region, while the software itself will evaluate an analytic solution that eases the simulation for many applications. However, if accurate results are required, then wall functions might not be the best option since better results can be rendered adopting one of the low Reynolds number models. These models are recommended for the cases that lift and drag, or the heat transfer, are involved [26].

The main difference among the RANS models is the way they handle the near-wall region. In the following, each model will be explained briefly.

- **L-VEL and yPlus**

These models estimate the eddy viscosity but without considering additional transport equations, which makes them the simplest models concerning computational aspects and also with the least accuracy among the other models. They are usually used for simulating a cooling system of electronic devices or internal flows [26].

- **Spalart_Allmaras**

This model was created for aerodynamics problems, and it is capable of using a low Reynolds number model for the entire region, by taking advantage of an additional term for undamped kinematic eddy viscosity. It can be concluded that this model has a better resolution than the previous models and provide stable results. However, it has some limits and is not feasible for separated flows [26].

3. Numerical simulations

- **k- ϵ**

The calculations of this model are based on two variables, the turbulence kinetic energy and the rate of dissipation. It uses wall function for the sublayer close to the wall and is known as a popular model for industrial problems, while it does not require so much memory and is suitable for simulating external flow. The weakness of this model is to be unable to provide high-grade results for extreme curvature [26].

- **k- ω**

This model is similar to the previous case, but instead of ϵ , it considers the specific rate of dissipation. In some cases where the k- ϵ model is not feasible, this model can be used to have more accurate results, but as it is more complex and solves nonlinear equations, it is less convergence than a k- ϵ model [26].

- **Low Reynolds number k- ϵ**

On the contrary to the k- ϵ model, this model does not require wall functions, however, for this purpose, a finer mesh should be used, to make it possible for providing accurate results taking advantage of low Reynolds number models. Using a denser mesh will slow simulations down, so to overcome this problem and optimize the time required for each simulation, it is reasonable to start with a coarse mesh size and decrease it gradually. Once the error of results becomes negligible, it can be selected as a proper size for meshing [26].

- **SST**

This model is capable of utilizing two techniques, which means, in the free stream region it solves the problem similar to a k- ϵ model and for near-wall regions, it behaves like a k- ω model. The combination of these two models makes the simulation have the advantages of either model and also not limited by most of their restrictions [26].

The plates used for simulations have a rectangular shape with the following dimensions:

3. Numerical simulations

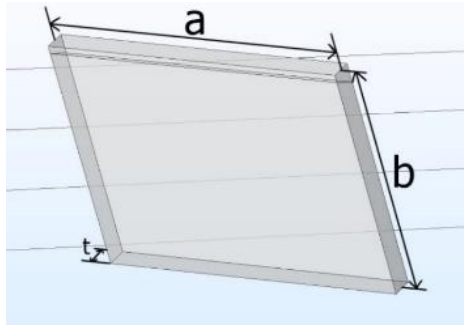


Figure 26 The scheme of a plate

size of the plate				Water domain					
a[m]	b[m]	t[m]	A[m ²]	W[m]	L[m]	H[m]	inlet velocity [m/s]	minimum grid size [m]	ρ [kg/m ³]
0.0762	0.1143	0.00762	0.00871	0.8	2.286	0.6	3	0.0001	997

Table 2 specifications of the simulation

The properties of the fluid and the plates need to be chosen as well. However, most of the materials are already available in COMSOL and it is not necessary to redefine them.

To adopt a proper model for latter analysis, several simulations are performed concerning the following configurations and conditions: a rectangular plate with a fixed constraint on the top side and submerged in the water domain, the top side of the water domain is set as a wall boundary with no-slip condition (the same for the walls of plate), the velocity of the flow in the inlet boundary is perpendicular to the surface and has a magnitude of 3[m/s], the outlet boundary pressure is zero. The results of simulations employing three different models are listed below.

3. Numerical simulations

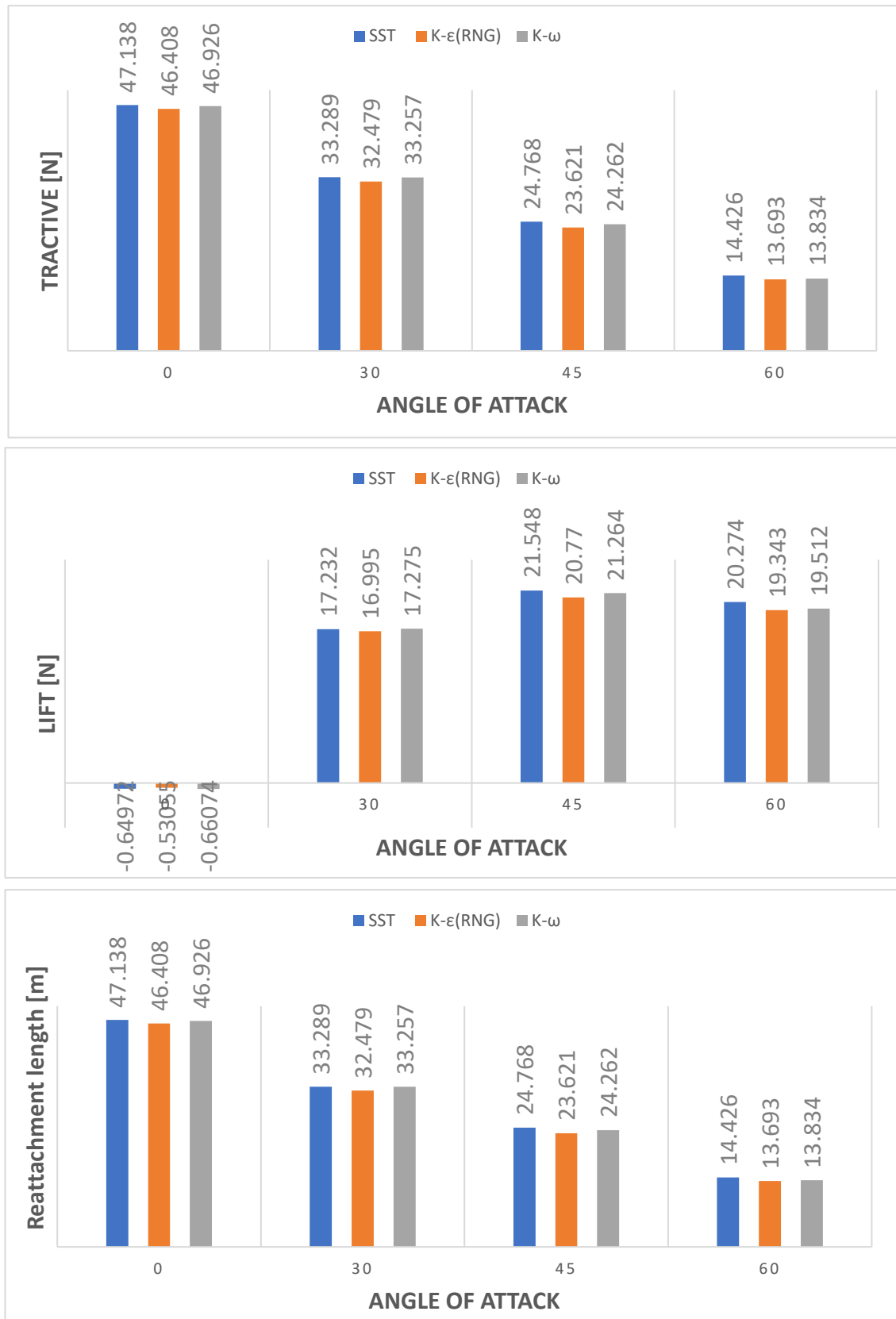


Figure 27 The comparison of the results provided by three different models, SST, $k-\epsilon$ (RNG), $k-\omega$. The results concern the lift, tractive, and reattachment length of a plate.

3. Numerical simulations

As the results show, the error between each model is negligible, moreover, the needed time of each model is almost the same. The SST model is one of the most recommended models among the other, regarding problems including turbulent flows, furthermore, this model is also known for providing accurate results without the need of using wall functions. So, it can be concluded that the simulations can work properly using an SST model with a minimum meshing size of the range 0.1-1 [mm].

3.2. Meshing

Choose a proper mesh size is essential for simulation, as it can affect the accuracy of the outcomes. To provide solid results, using a fine mesh might be required, but it can lead to a computationally expensive simulation and expect a large amount of memory, therefore, it is more relevant to make a trade-off between the time consuming of the simulation and the accuracy of the results. To make a good decision for the shape and size of meshing elements, one needs to understand the problem precisely, as having further information about the problem and its conditions, such as boundary conditions, can help to facilitate the process.

The best mesh element can be expressed as isotropic shape, accordingly, COMSOL Multiphysics has defined some sort of quality factor to analyze the results of meshing of an object and to avoid mesh element with collapsed or inverted structure, while these elements have the least quality and, in some cases, not acceptable [29], [30].

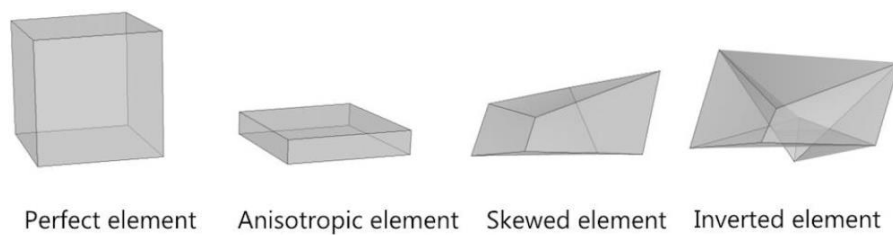


Figure 28 The change of the shape of a mesh element in different directions [29].

Although changing the structure of mesh elements is inevitable, it can be acceptable for the cases, such as compression in one direction. To analyze the quality of each element after deforming, the “aspect ratio” is defined, which is the division of the longest side to the shortest one and elements with higher aspect ratio represent higher quality.

3. Numerical simulations

One of the worst cases of deforming an element is to skew it, which usually happens in curved or sharp geometries. Skewing an element makes equations more difficult and inaccurate. To manage such a situation, another factor called skewness is defined, which blocks elements with lower than a certain tolerance to be employed. Another factor for checking the quality of the elements is the growth rate, that defines the variation of the size of each element with respect to its neighbor [29], [30].

- **Primary steps for meshing a CFD model**

To have a better idea of the model, it is important to define and anticipate all the possible problems that can occur during meshing. Thus, it is important to design and recognize all the boundaries from the very first sketches and CAD models, in this way, it would be easier to realize where mesh should be finer.

It is also important to analyze the interaction between the flow and the object, to neglect some unnecessary details which can affect the time consuming by the simulation. It can be simply done by removing or replacing some sharp edges and parts which potentially possess irrelevant computational efforts.

Partitioning is also an important tool for simplifying a mesh, as it can be used to distinguish parts which can be modeled by a coarse mesh and to use a fine mesh only when it is necessary.

- **Meshing selections in COMSOL based on physics and flow conditions**

It is reasonable to determine the conditions of a model in the program and let the software design a mesh appropriately, according to the selected conditions. For instance, the turbulent flow would have a finer mesh size than laminar flow, while, the software is also capable of monitoring the boundaries and to choose a finer mesh for regions near the wall. If the model still needs more correctness it can be verified manually, by changing the setting of each mesh.

A mesh can have various shapes, nevertheless, an unstructured triangular mesh is common as it provides high quality and can be used for different geometries, but, this form of the mesh should be finer than a structured one to give the same accuracy [29], [30].

3. Numerical simulations

- **Meshing in boundary layers**

Although, meshing in near-wall regions becomes extremely anisotropic but still can represent high quality. There are some features to take into account, such as the height of the first layer, which is normally defined with respect to the scale of the surface. The other two factors are the growth rate (which explained earlier) and the number of layers.

Choosing a proper meshing size for the physical model is crucial, since, using a coarse grid size leads to inaccurate results in near-wall regions and using unnecessary fine grid size leads to a time-consuming simulation. Nevertheless, to have a faster simulation in terms of running time, it is possible to choose a non-uniform grid size, which can be refined for the regions of interest, such as the near-wall layer. To choose a proper model, the dependence of each model to the grid size at different conditions is taken into account.

As said before, the grid size close to the walls plays an important role in terms of accuracy, then it is more convenient to use a finer grid size for these areas. The boundary layer of turbulent flow can be divided into inner and outer regions. These regions have already been characterized, therefore, by knowing some parameters, the near-wall region can be estimated. The variables can be characterized using the following relations. The characteristic velocity and length scales are given by,

$$u_* = \sqrt{\tau_w/\rho} \quad (34)$$

$$l_* = \nu/u_* \quad (35)$$

$$y^+ = y/l_* \quad (36)$$

As the layers are classified by y^+ , it is possible to find the region of interest and consequently, a grid size can be selected. To make sure that the grid size provides reasonable results, and to examine its effect on the results, a comparison among the simulations utilizing different mesh sizes is made. For this purpose, the simulations are done using three meshing sizes in the near-wall region, 1[mm], 0.5[mm], and 0.1[mm] [29], [30].

- **Moving mesh (multiphase)**

There are several ways to model a free liquid surface: level set, moving mesh, phase field, and stationary free surface. Moving mesh method represents better performance, therefore,

3. Numerical simulations

it can be considered as the first choice for modeling a free surface problem. The moving mesh method models the free surface by separating two domains, in this way, surface tension and other forces applied to the surface are considered as boundary conditions. Using this method gives the possibility to neglect to calculate the velocity and pressure fields in the gas phase, which are not needed in this case. It has to be taken into account that, this method is not suitable in case of topology changes [27], [28].

3.3. Conditions

As discussed previously, most of the supporting force generated by the propulsion system forms in the stroke phase, hence, for analyzing this stage in a manageable way, the model is supposed to work at a steady-state condition, with a predefined constant velocity perpendicular to the inlet boundary, and the pressure in the outlet boundary. Instead of moving the plates, the water flows through the plates, therefore, the plates have a fixed constraint on the top side, which prevents them to move freely. The simulations concern the forces applied to the lower part of the propulsion system at a steady-state, where the plates are submerged in the water, and in this way, the effect of plates during splash and retraction phases is neglected.

The pressure in the outlet boundary is often the static pressure at flow outlets, hence, it can give a better result when backflow occurs during iteration. The next step is to choose an approach for the simulation.

The tests have been done in different conditions, such as modifying the angle of the plate with respect to the water flow and changing the mesh grid size. To make a comparison the results of employing various approaches and mesh sizes have been investigated.

- **Boundary conditions**

In the exterior flows such as flow around the plates, the distance of the obstacle from inlet and outlet boundaries should be selected appropriately, to avoid any effect on the solutions. In such cases, constant velocity and pressure are set for inlet and outlet boundaries respectively. The distance can be selected considering pressure variations around the plate and find the region where these variations become negligible.

3. Numerical simulations

The variation of the pressure can be found as $\sim D/R$ in 2D and $\sim A/R^2$ in 3D and 2D axisymmetry, where R is the distance to the center of the plate, D is the length and A is the area of the object perpendicular to the flow. It is also important to note that, the deviation of the velocity should not exceed predefined tolerance from the free stream velocity on pressure boundaries, while, this assumption is different in the wake and pressure on velocity boundaries.

To have more reliable results and expanding the working state of the plate, other sides of the water domain are considered to have geometrical symmetry, which mirrors the behavior of the domain, in a time-effective way.

3. Numerical simulations

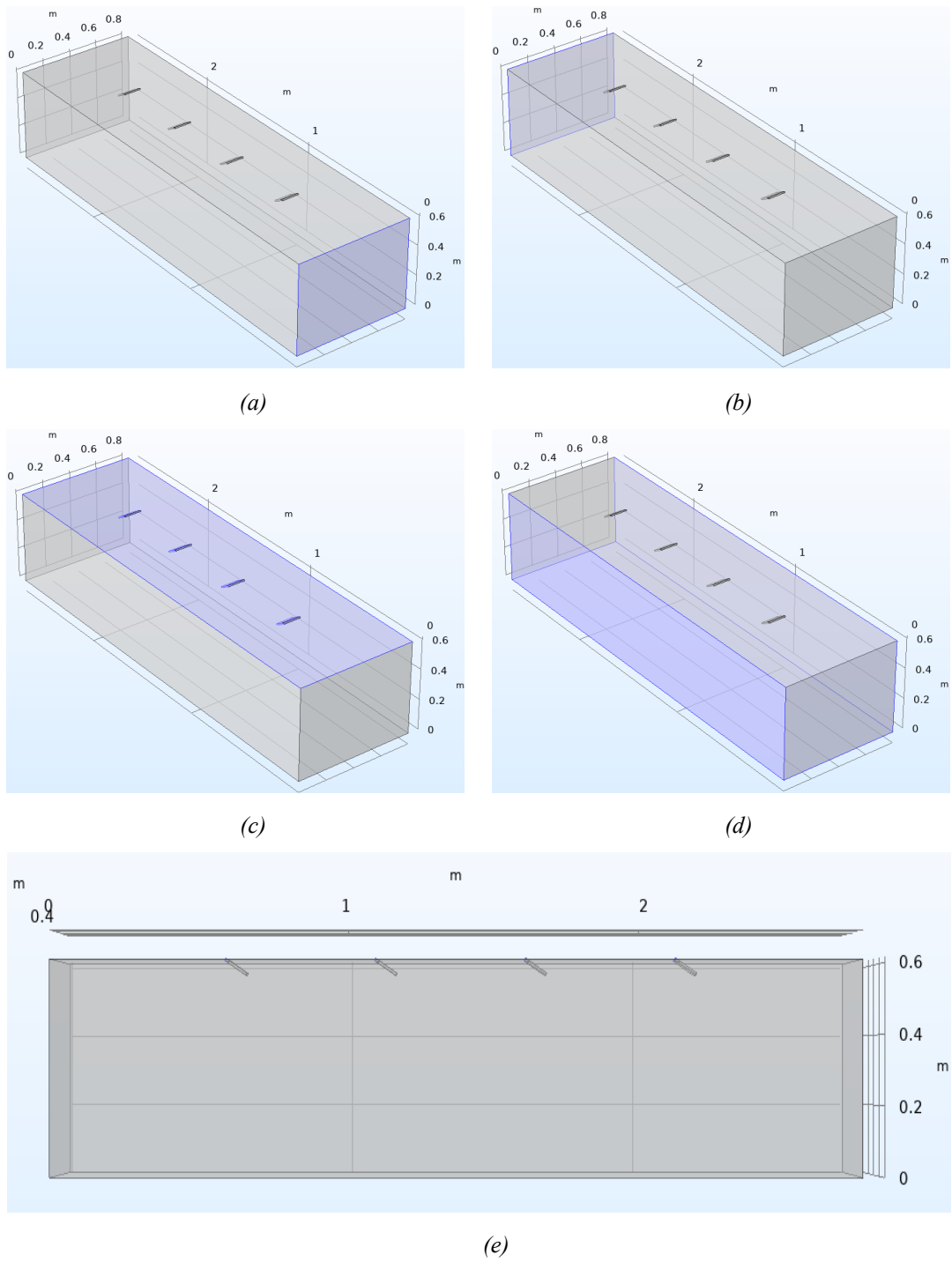


Figure 29 The boundaries of the COMSOL models are defined as following, (a) input, (b) output, (c) no-slip wall, (d) symmetry, (e) side view of the model

3.4. CFD results

3.4.1. Computing Lift and tractive in COMSOL

Once fluid flows over an object, it creates a force that is usually divided into two components on a two-dimensional plane; the force applying in the vertical direction and parallel to the z-axis is “Lift” and the one applying along the x-axis is “Tractive”. The pressure and viscous forces are the main components of the force generated by the plates. The pressure force is due to the pressure difference besides the object, while the viscous force is due to friction force and is charged against the direction of the flow.

Once the simulation is done, the forces applied to the surface of the plates can be found in different ways, such as integrating a boundary. One way is to integrate the total stress in each axis, but it should be remarked that the total stress involves the pressure and the viscous forces.

The viscous and the pressure forces can be obtained separately, which can be done by integrating the viscous stress and multiplying pressure (that is a scalar) by the normal vector respectively. These analyses provide useful information in the cases when the wall function is required (for instance in the case of using k- ϵ and k- ω models for turbulent flows). The local shear stress at the wall can be found as:

$$u_\tau = \sqrt{\frac{\tau_w}{\rho}} \quad (37)$$

$$\tau_{wy} = \rho u_T^2 \frac{u_y^T}{u^T} \quad (38)$$

where u^T is the velocity at the wall. The equation can be rewritten using the dimensionless velocity by replacing u_τ . u^+ instead to u^T [31].

The table below represents the differences of expressions among the models with or without wall function.

3. Numerical simulations

	Without wall function	With wall function
Pressure Force	$\text{spf.nymesh} * p$	$\text{spf.nymesh} * p$
Viscous Force	$-\text{spf.K_stressy}$	$\text{spf.rho} * \text{spf.u_tangy} / \text{spf.uPlus}$
Total Force	$-\text{spf.T_stressy}$	$\text{spf.nymesh} * p + \text{spf.rho} * \text{spf.u_tangy} / \text{spf.uPlus}$

Table 3 The equations used for computing different forces in COMSOL Multiphysics, considering two classifications, with or without wall function [31].

3.4.2. Angle of attack

Because of the orientation of the plates, the net force applying to the plates is not aligned with the flow direction. Assuming that the water flow is parallel to the x-axis and the plate is oriented with respect to the z-axis.

The angle among the total force applying to a plate and the flow direction (which is assumed to be aligned with the x-axis) is called the “angle of attack” (shown by the symbol α). There are two ways of considering the angle of attack, whether by rotating the object concerning the flow direction or by fixing the object and changing the direction of the flow at the inlet boundary [18].

3.4.3. Lift and Tractive

As explained before, the force generated by the plates is a function of velocity squared. To verify this fact, the force applying to a plate at various velocities is measure through COMSOL simulations.

3. Numerical simulations

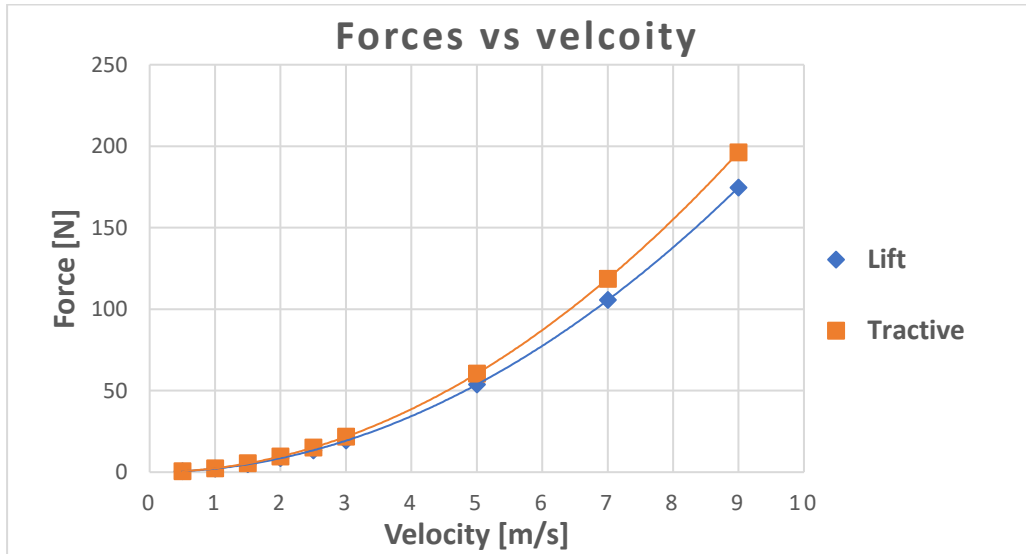


Figure 30 Results of CFD simulations regarding Lift and Tractive forces vs velocity of the flow (which is assumed to be equal to the relative velocity of a plate with respect to the water).

To verify the validity of the data given by simulations, it is more relevant to use nondimensional coefficients than using dimensional forces. The calculation of the dimensionless coefficients can be simply done by knowing the lift and the tractive force given by the simulation and considering all the other parameters are already known.

These coefficients are also useful to represent the relation between the angle of attack and the force produced in each axis, which in this case are the lift and the tractive forces.

The lift force created by the plate has a reduction if the angle of attack increases too much. This reduction is called “stall” in fluid dynamics, which should be considered in the analysis of the force creating by a plate and can be useful to have an optimized choice of the angle of attack.

3.4.4. Coefficients

To confirm the correctness of the results provided by simulation, the coefficients corresponding to different angles and velocity are evaluated. By extracting the forces applied to the plate and using the following relations, the coefficients corresponding to x and z axes can be found.

3. Numerical simulations

$$\begin{cases} F_{tractive} = \frac{1}{2} C_x \rho A v^2 \\ F_{lift} = \frac{1}{2} C_L \rho A v^2 \end{cases} \rightarrow \begin{cases} C_x = \frac{2 F_{tractive}}{\rho A v^2} \\ C_L = \frac{2 F_{lift}}{\rho A v^2} \end{cases} \quad (39)$$

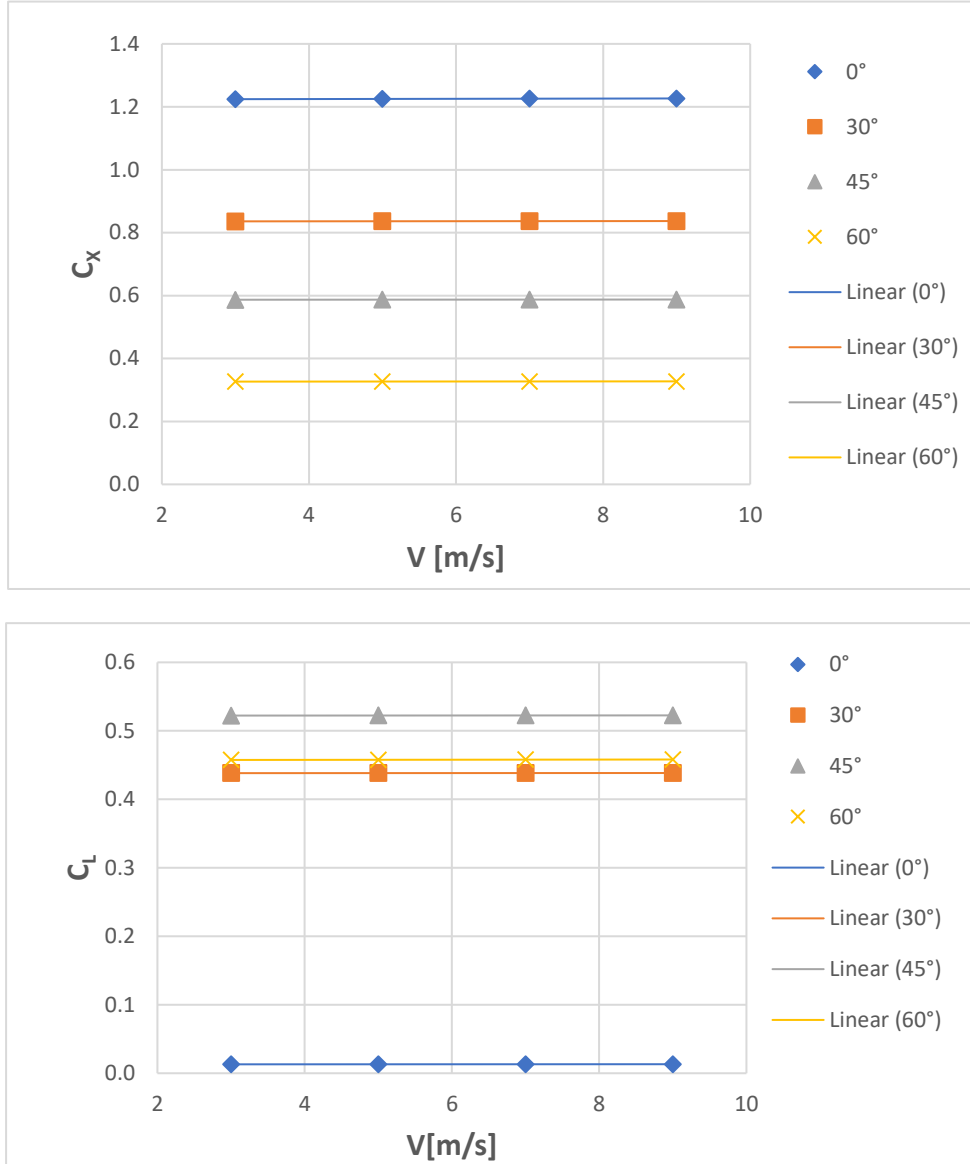


Figure 31 The estimated coefficients provided by the simulation to examine the correctness of the results, concerning two different conditions, changing the angle of attack and the velocity of the input flow. C_x and C_L are the tractive and lift coefficients, respectively.

As the results of each angle represent, the coefficients have similar values and the variation of the velocity does not make a significant change to the results, thus, it can be said that the simulation operates correctly. The water flow deflects after hitting a plate,

3. Numerical simulations

which causes a reduction in the velocity of the water and consequently, the force produced by the following plates will be affected. So, it is important to find an appropriate distance between each plate, to provide a good response from the plates. By knowing the distance between the plates, it is also possible to figure out the number of plates in a specific length.

3.4.5. Reattachment length (RL)

The water flow deflects after hitting a plate, which causes a reduction in the velocity of the water and consequently, the force produced by the following plates will be affected. So, it is important to find an appropriate distance between each plate, to provide a good response from the plates. By knowing the distance between the plates, it is also possible to figure out the number of plates in a specific length.

When the water flow is distracted by a plate, it starts recirculating and separates from the flow, which creates instantaneous negative velocity fields in the flow and makes the flow chaotic in that region. The reattachment length (RL) is the distance when the velocity of the flow becomes positive after distracting and no negative velocity vectors appear. A separated flow involving a reattachment flow increases some issues in the flow such as unsteadiness, vibration, pressure fluctuations, etc.

The estimation of this length in simulations is important for two reasons, first to have an additional term for examining the results of different turbulent models, second, for determining the distance between each plate, therefore, it can be used as a reference length for observing the effect of the distance between plates, and to select a proper number of plates in a certain length.

3. Numerical simulations

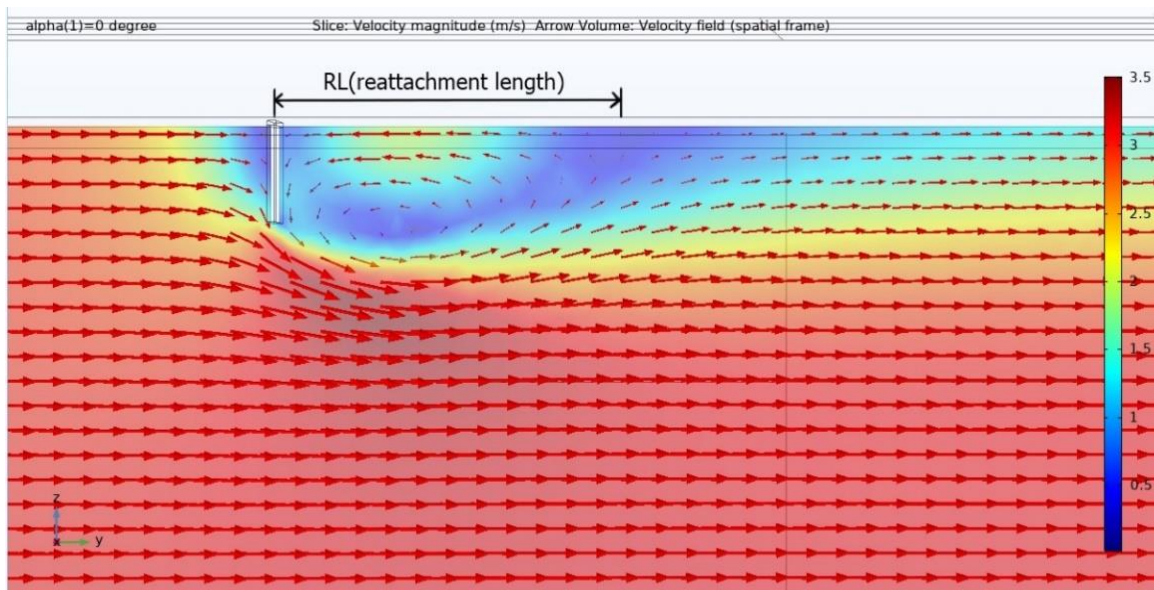


Figure 32 measuring the reattachment length concerning a plate perpendicular to the flow, the velocity of the water in inlet boundary is 3[m/s].

3.4.6. Number of plates

To design the propulsion system and choose a proper number of plates, various simulations are made, considering a different number of plates in a specific length. The length takes into account the area dedicated to the active plates attached to the lower side of the track (where the plates are fully through the water).

To examine the effect of using a different number of plates, considering the same length, various quantity of plates is considered, while the size of the plates is the same. Therefore, the number of plates can be simply found by rounding down the division of the specific length and the gap specified for each trial.

The distances between plates regarding each simulation are: 0.6RL, 0.8RL, RL, 1.25RL, 1.5RL, 1.75RL, 2RL, 2.25RL, 2.5RL (RL stands for the reattachment length and is equal to 0.23[m]). Each of them corresponds to a different number of plates that can be placed in a total length of 2 [m]. The number of plates is shown in the table:

The distance between each plate [m]	0.14	0.18	0.23	0.29	0.35	0.40	0.46	0.52	0.58
The distance between each plate, concerning RL	0.6RL	0.8RL	1RL	1.25RL	1.5RL	1.75RL	2RL	2.25RL	2.5RL
number of plates	13	10	8	6	5	5	4	4	3

Table 4 number of plates corresponding to different distances between them

3. Numerical simulations

For choosing an appropriate number of plates, some aspects should be taken into accounts, such as the overall force and how it is distributed through the plates, which is an important factor in terms of stability.

The following charts show how the total force providing by several plates in a specific length changes, concerning different gaps between the plates. The inlet velocity of the water is constant and equal to 3[m/s].

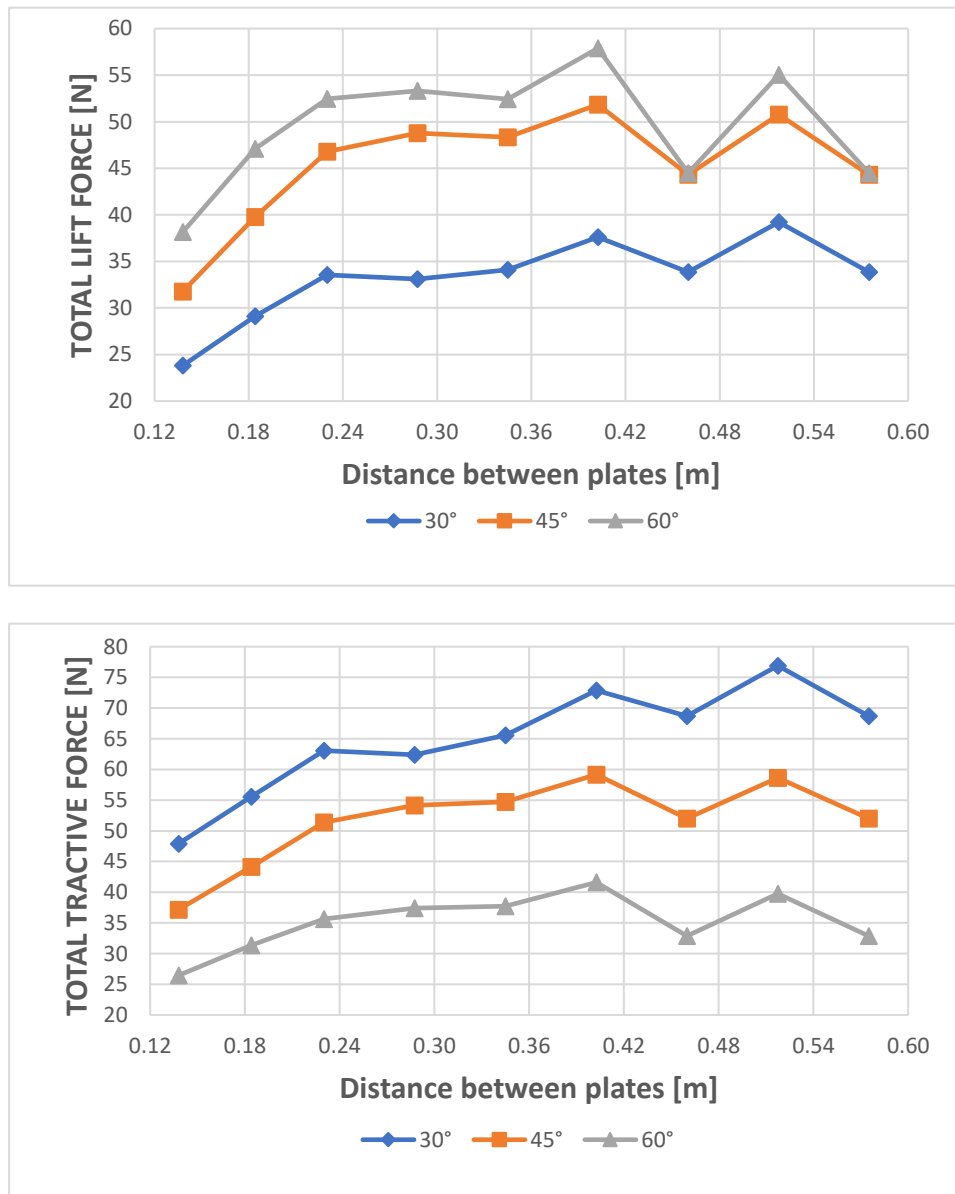


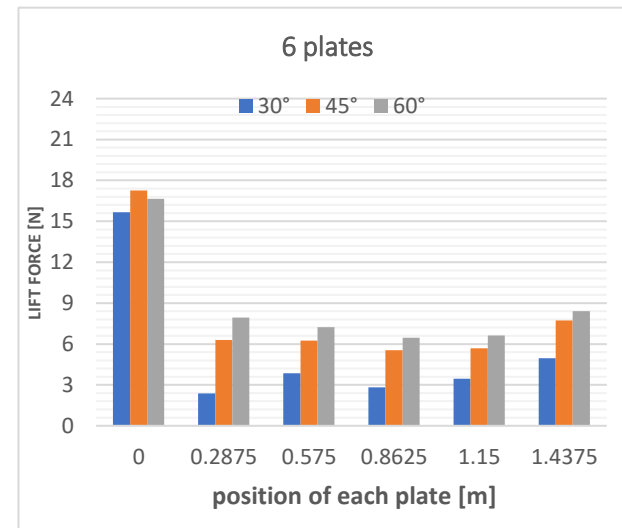
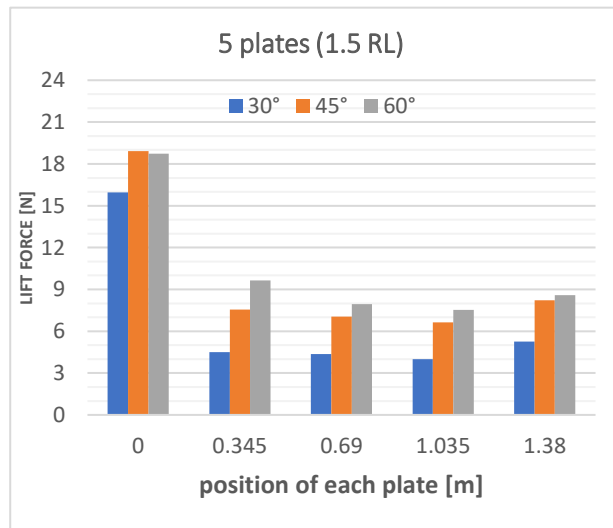
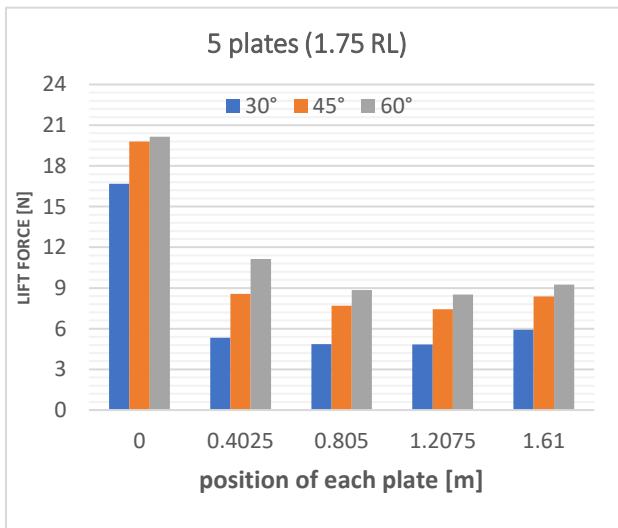
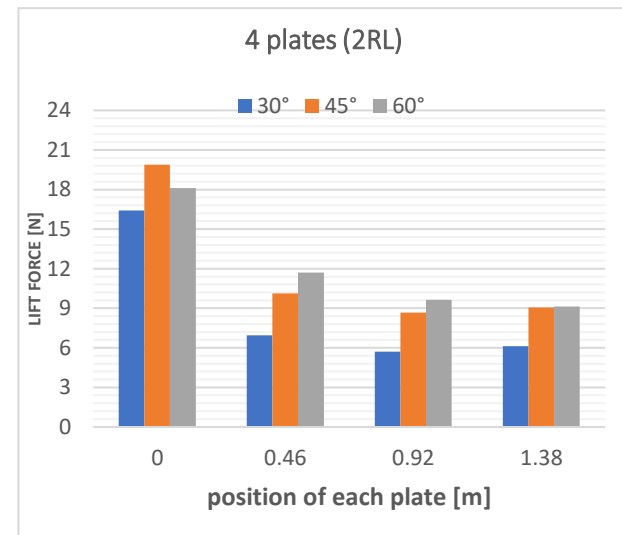
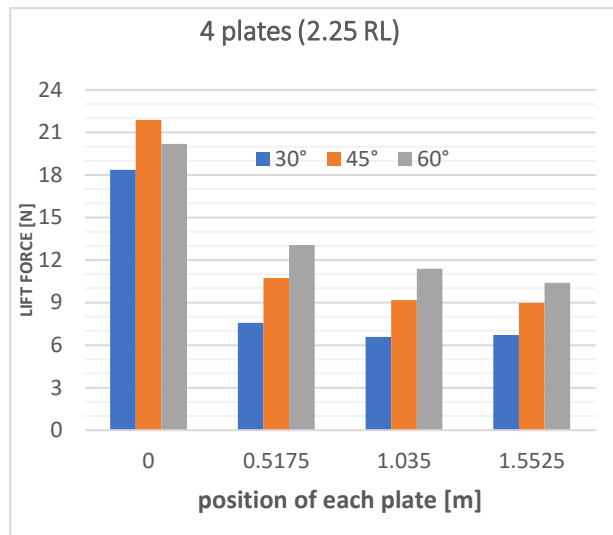
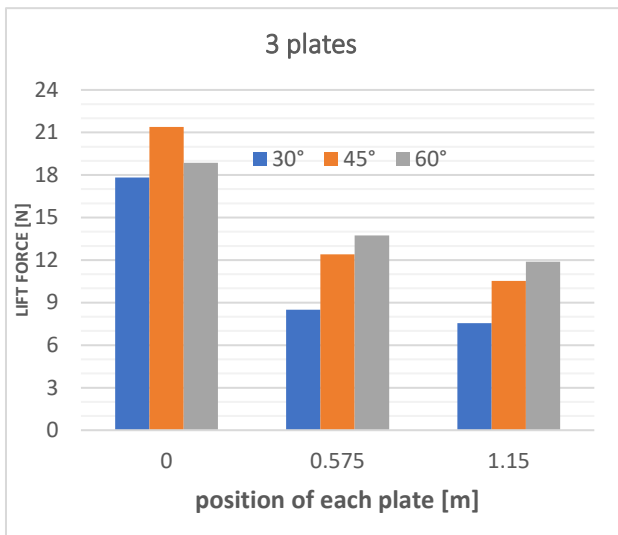
Figure 33 Total Tractive and Lift forces considering different distances between the plates which corresponds to various number of plates in a specific length

3. Numerical simulations

As shown in the charts, the forces corresponding to the shortest distance within the plates that is equal to the highest number of plates (13 plates), possess the least values of forces, which is due to the negative force generated by some plates. The negative force appears due to the recirculation of the flow behind the plates, as in this situation the flow does not have enough time to become positive and creates a force that is not relevant to what is demanded by the system.

The forces increase by extending the gap between the plates and consequently reducing the number of plates. However, the results show two peak values concerning the gaps of 0.4 and 0.52 [m], which results in 5 and 4 plates respectively.

The charts below indicate how the forces are distributed through the track. Knowing the force distributions is important in terms of stability and safety of the system, while a sudden change of the force from one plate to another is not relevant, and can create vibrations due to the unbalanced forces generated by different plates. Therefore, it is more feasible to choose a greater number of plates. However, as stated earlier, by increasing the number of plates the total force of the plates decreases, hence, a trade-off between the total force and the stability of the system should be made. In the following charts, the position of each plate and the forces applied to them are represented. Charts with more plates have a shorter interval among each plate.



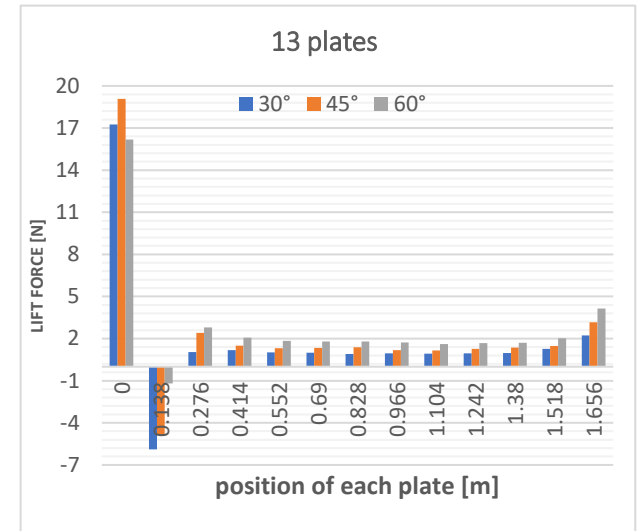
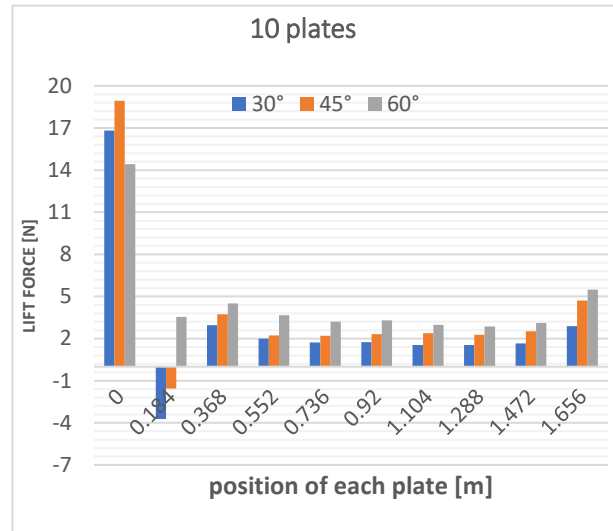
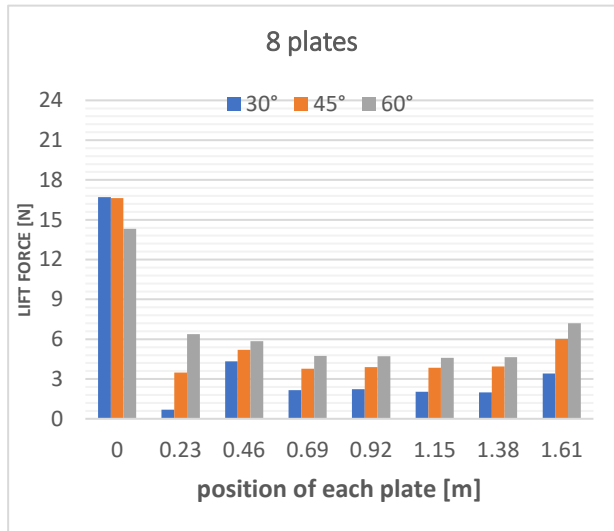
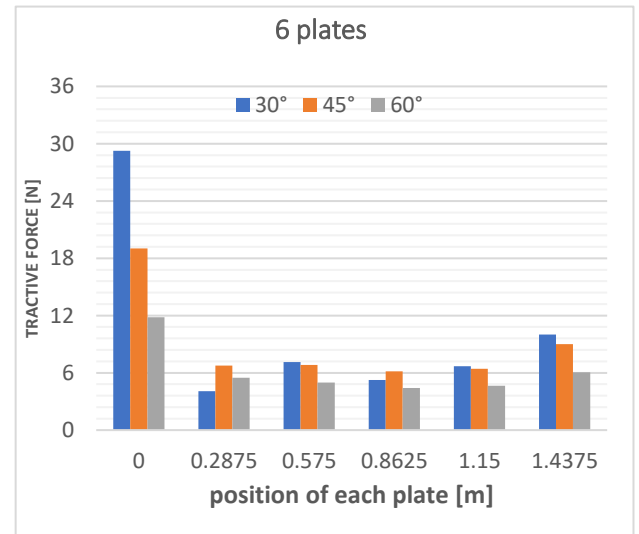
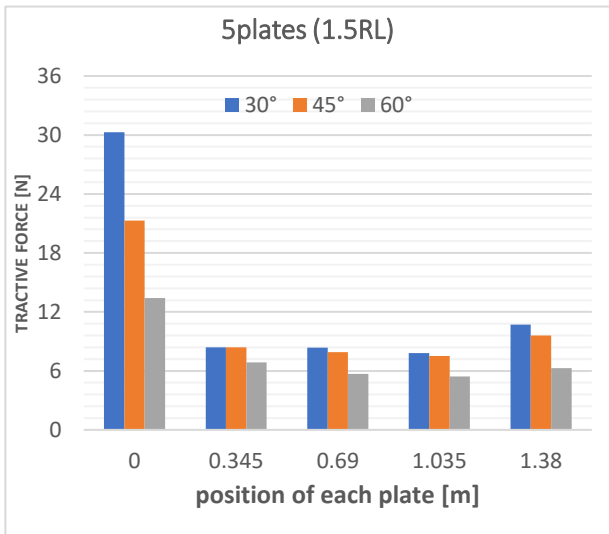
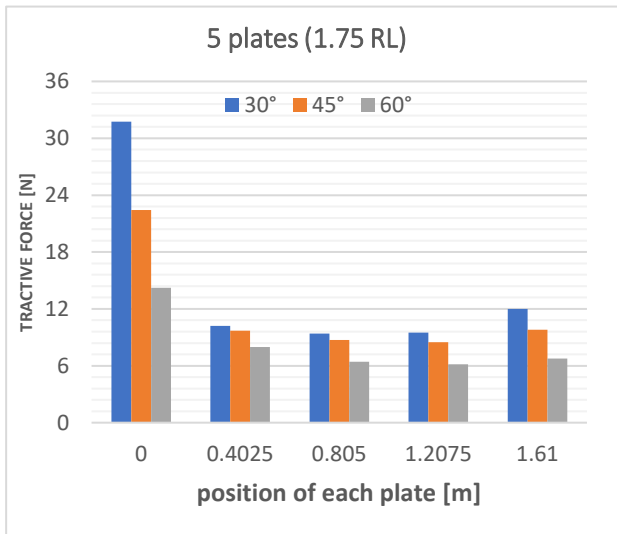
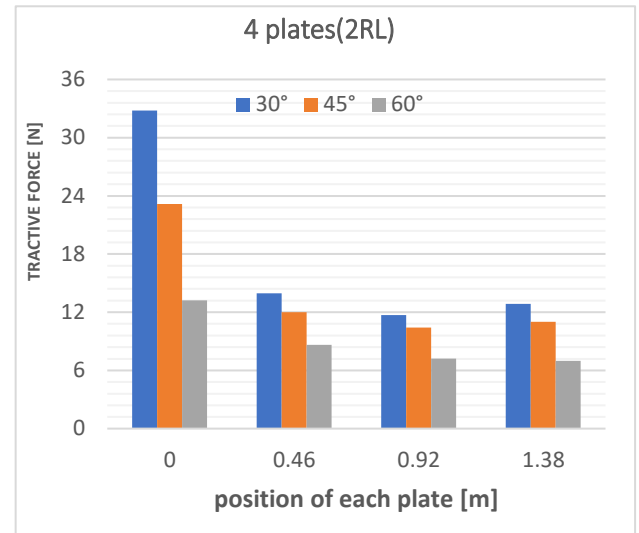
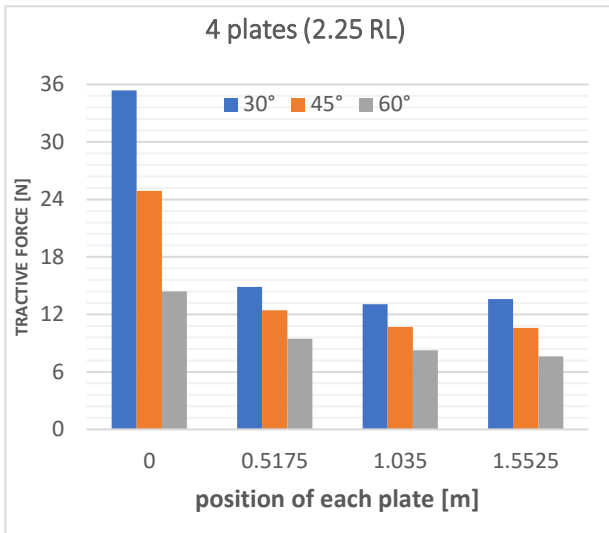
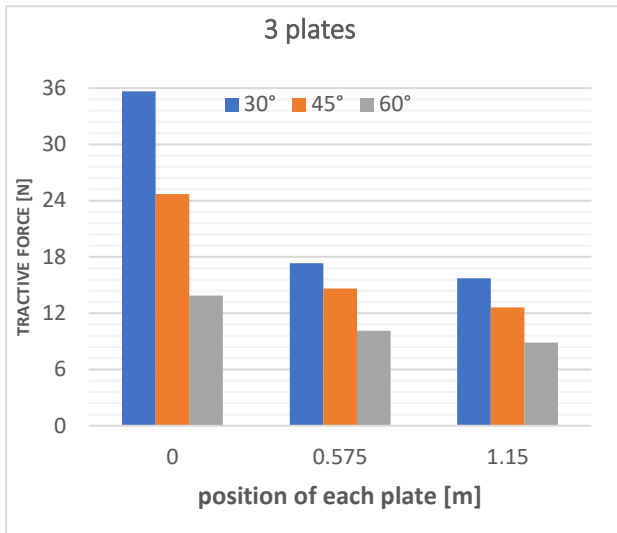


Figure 34 Lift force applying to each plate, concerning different number of plates



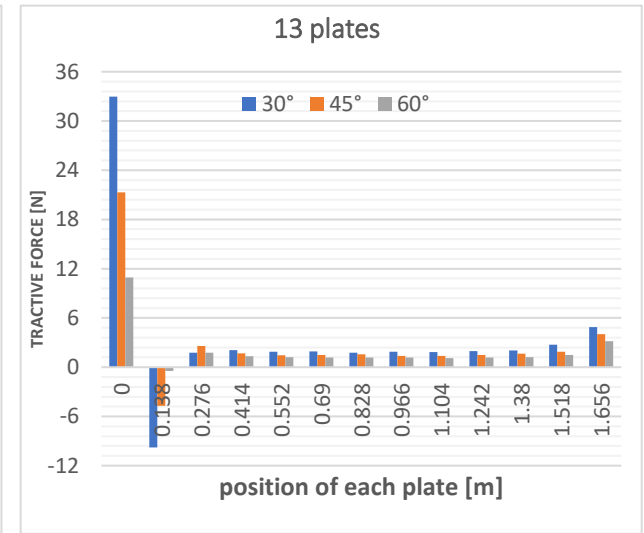
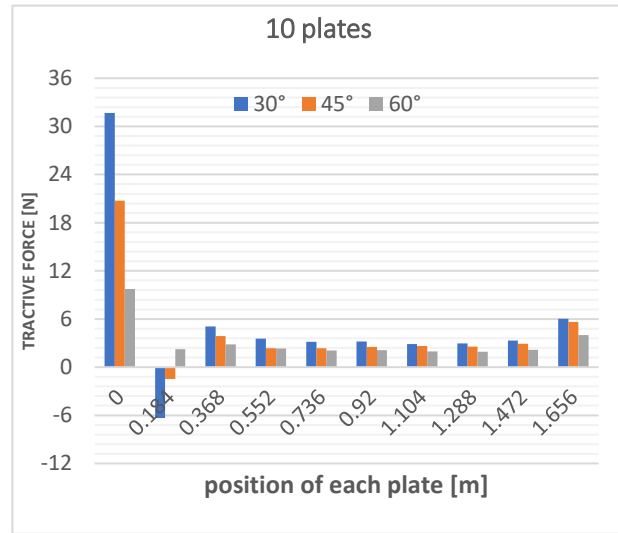
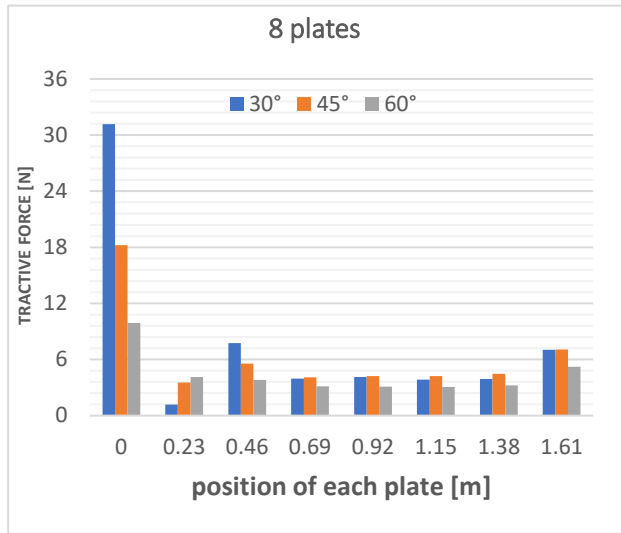


Figure 35 Tractive force applying to each plate, concerning different number of plates

3. Numerical simulations

As a result, holding the total force created by a different number of plates and the force distributions, a proper number of plates can be found. In this case, 5 plates show higher performance, therefore the subsequent simulations will be done considering 5 plates corresponding to a gap of $1.75RL$ (0.4 [m]) between each plate.

Because of the irregular distribution of the force generated by each plate, a pitch moment would appear during the operation of the system and consequently, the nose of the body tends to rise upward.

3.4.4. Single vs Double row of plates

All the previous simulations are made concerning the plates positioned in a single row. The plates designed in this project have a relatively small area and cannot produce enough force to ensure a supporting force for the entire system.

To increase the generated force several methods can be used. The first way is to increase the number of plates which can be done by increasing the number of plates, which leads to a decrease in the performance, due to the shortening of the distance among them. Another way is to specify a longer track path that can hold more plates, however, in this way, the weight of the system will increase as well and can create difficulties during a maneuver.

Another solution is to expand the area of the plates. Though, it also represents numerous issues such as not a well distribution of the force along the track path that increases the risk of having troubles in terms of stability and vibration. It also increases the forces created in the splash and retraction phases, that can be formed by a large plate.

To avoid such problems, the suggested solution is to increase the number of plates by increasing the number of rows and located in parallel to the origin plates. Due to the distraction of the water and to avoid increasing the force in some parts of the system, it is more relevant to consider an offset between each row along x and y directions.

3. Numerical simulations

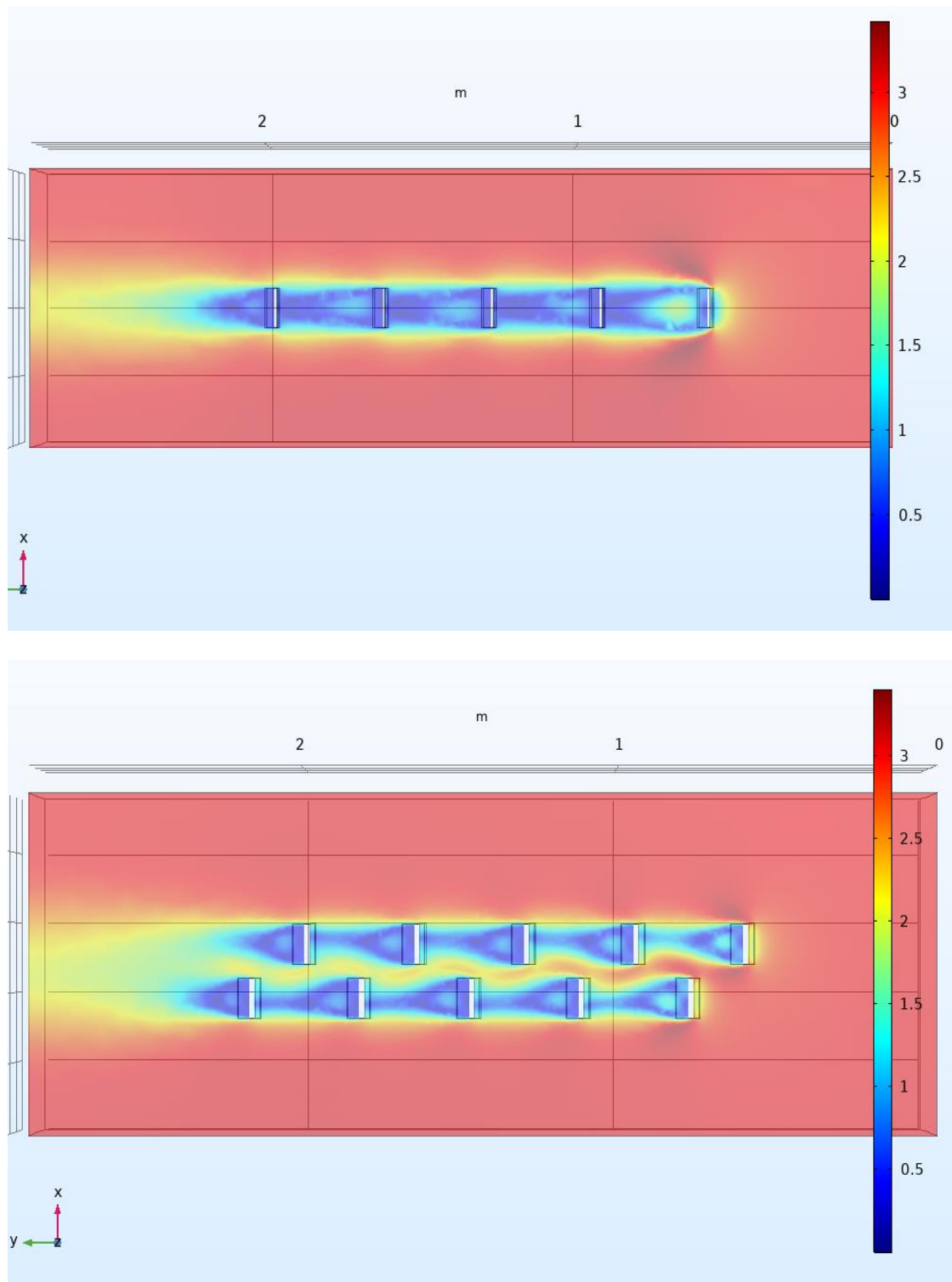


Figure 36 The pictures represent the variation of the flow velocity within the plates, in the case of using one or two rows. The input boundary is set on the right side and the output is on the left. The velocity of the flow in the input is equal to 3 [m/s] and the pressure at the output is zero for both cases.

3. Numerical simulations

The charts below indicate the total forces generated by one and two rows of the plates, with different angles.

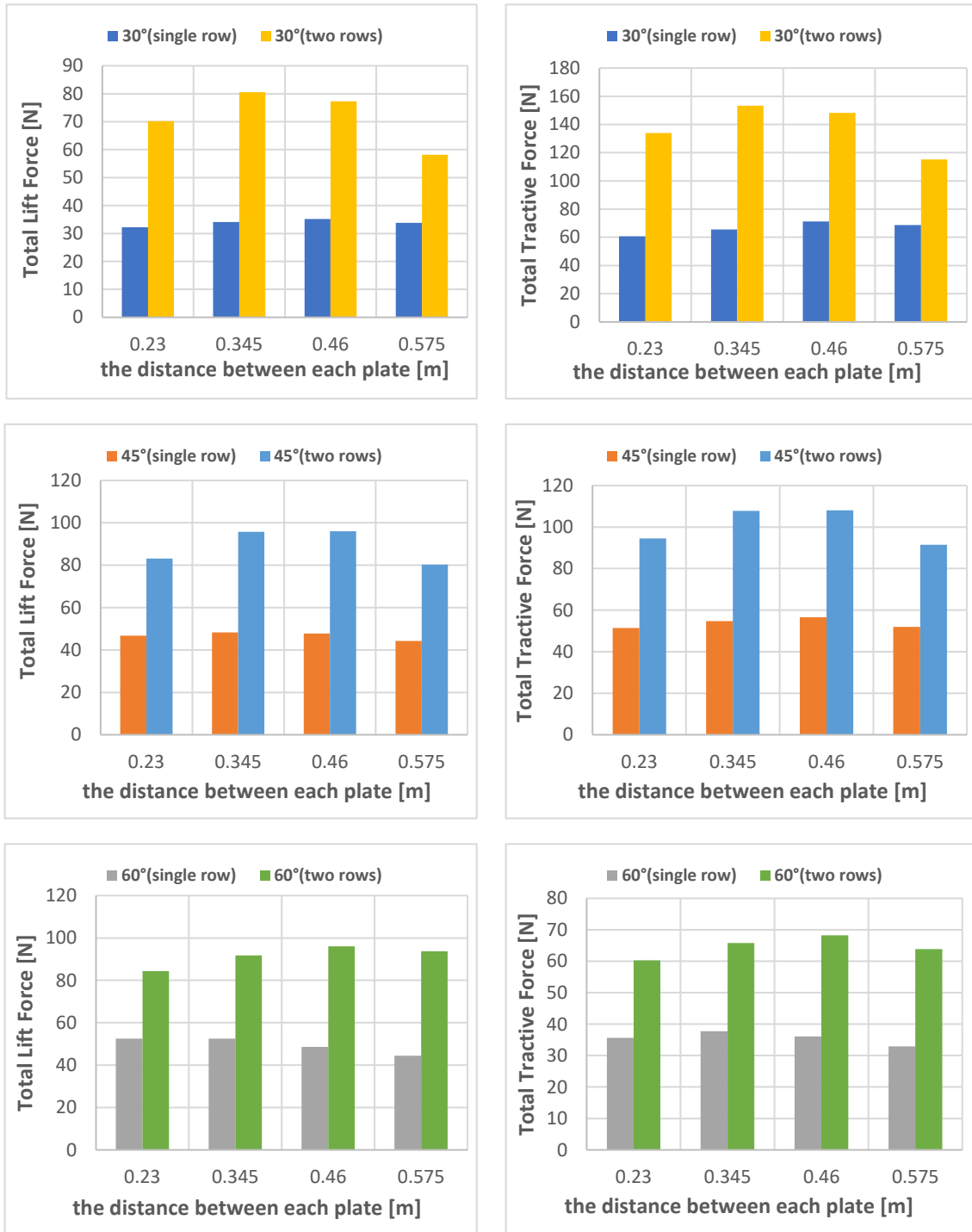


Table 5 The comparison between Total Tractive and Lift forces concerning one and two rows of the plates, each chart indicates a specific angle of attack for single and double rows, the distance among each plate is placed in the x-axis and the total lift and tractive forces in the y-axis

3. Numerical simulations

As the results show, by adding another row, as shown in the figure, for most of the cases, the increase of total force is nearly double. Thus, it can be assigned as a proper way of increasing the supporting force of the propulsion system.

3.4.5. Pressure analysis

A sudden drop in pressure can create vapor bubbles in the liquid at low-pressure regions, which can take place in the regions where the liquid accelerates suddenly. The presence of cavitation should be restricted as much as possible, as it can cause erosion at the plates and other issues such as noise, vibrations, a reduction of efficiency, etc. The cavitation appears when the pressure of a region decreases to the vapor pressure of the liquid, in such a situation vapor bubbles, start to appear and collapse when they approach a region of greater pressure.

In the case of having cavitation, the designer has to take into account the regions in which the pressure has a great reduction and has the capability of creating cavities, once the regions are detected, specific shape and design might be required. In some cases, a new strategy might be needed.

To ensure the absence of cavitation, the pressure of the plates and in the regions where the water accelerates immediately should be analyzed carefully.

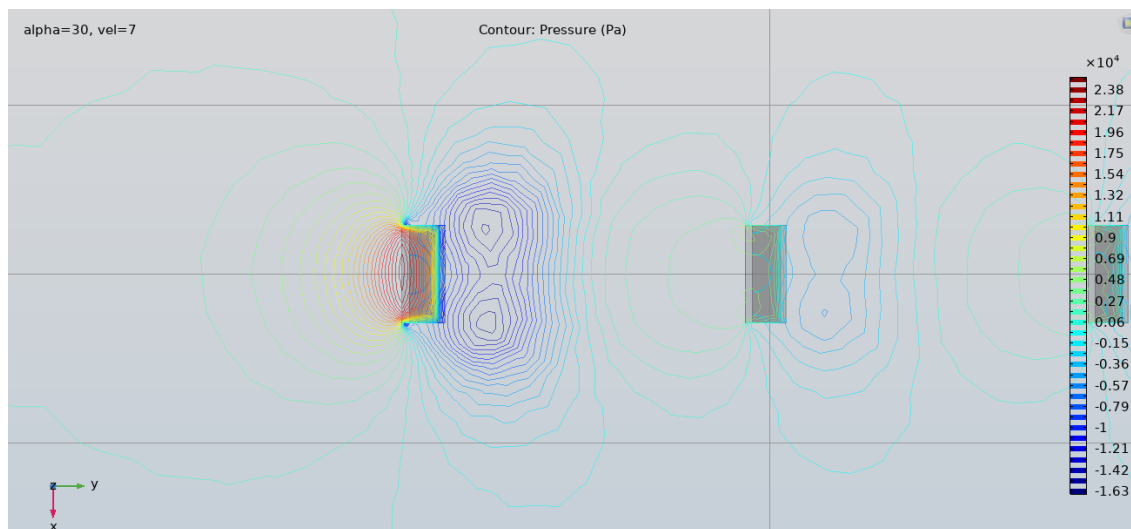


Figure 37 Analyzing the pressure around the plates. In this case, the input velocity is set to 7 [m/s] which is relatively high. Even in this situation, the results do not show any chance of forming cavitation.

To overestimate the results and guarantee reliable performance of the system also in the worst cases, the inlet velocity of the water is set to high values.

3. Numerical simulations

The figure shows a top view of the system, representing the pressure concerning a velocity of water of 7[m/s], which is a quite great velocity, to overestimate the situation and check the results. Fortunately, as the results show, the pressure drop is not significant and it is far from the vapor pressure of the water, which means it is incomparable to the case in which cavitation can exist.

4. Dynamic Analysis

4.1. Approximations and methods

To analyze the dynamic behavior of the system, several simulations are performed in Simulink. For simplifying the problem, the analysis is made along x and z axes. The figure below represents a free body diagram of the propulsion system, considering roll and pitch angles are zero.

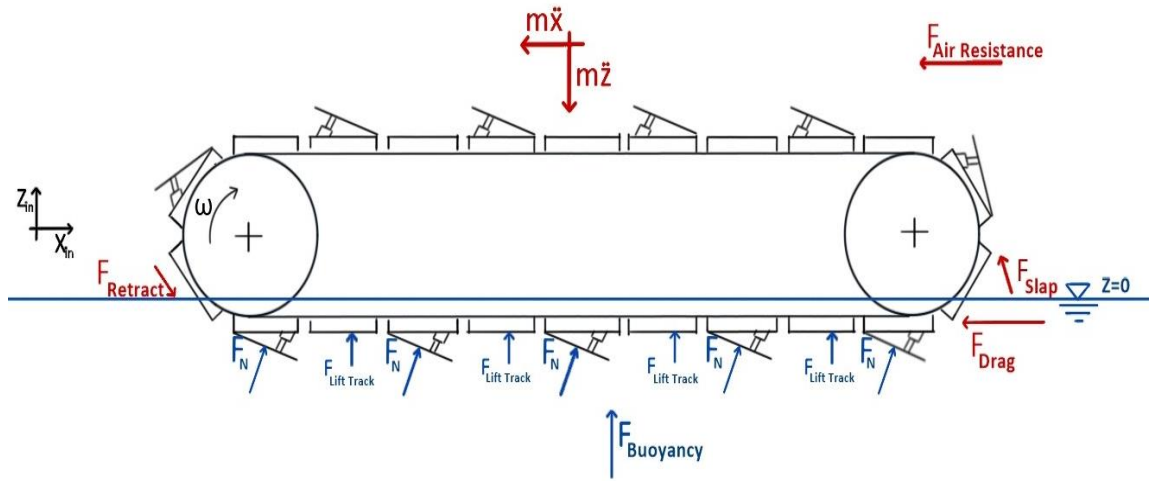


Figure 38 Free body diagram

For the sake of simplicity, the effect of the slap and retraction forces is neglected in the following analysis. The forces along the z-axis can be written as

$$-m\ddot{z}(t) + c\dot{z}(t) + \rho g A_{bb} z(t) - mg + \frac{N}{2} \rho C_{L(\alpha)} A_p |V_{rel}(t)| V_{rel}(t) + \frac{1}{2} \rho D C_{L,Track} A_{bb} |V_{rel}(t)| V_{rel}(t) = 0 \quad (40)$$

$$\ddot{z}(t) = \frac{1}{m} \left(-mg + c\dot{z}(t) + \rho g A_{bb} z(t) + \frac{1}{2} \rho C_{L(\alpha)} A_p |V_{rel}(t)| V_{rel}(t) + \frac{1}{2} \rho D C_{L,Track} A_{bb} |V_{rel}(t)| V_{rel}(t) \right) \quad (41)$$

where m is the mass of the body, A_{bb} is the area of lower part of the body through the water, that is equal to $L \times w$ (Length \times width), C_L the lift coefficient, c the damping coefficient, N is the number of active plates, V_{rel} is the relative velocity of the plates with

4. Dynamic Analysis

respect to the water, D is the factor defined to reduce the effect of the force generated by the track (as the estimated coefficient used for this force concerns an ideal condition when the track is directly in contact with the water, thus, to consider the effect of the plates this factor is used), $C_{L,track}$ is the lift coefficient of the track, A_p is the contact area of a plate through the water and is equal to $a \times b$ when the plate is totally submerged and equal to $b \times (a - \frac{z}{\cos(\alpha)})$ when the body emerges from the water and the plate loses its contact area with the water.

The reference frame of the propulsion system is set at the lower side of the track, thus, the vertical position of the system is equal to zero ($z=0$) when the track is at the water surface and only the plates are immersed through the water.

The forces along x-axis can be written as

$$m\ddot{x}(t) + \frac{1}{2}\rho C_{db}A_{bf(z)}\dot{x}(t)^2 + \frac{1}{2}\rho_{air}C_{air}A_{ba}\dot{x}(t)^2 - \frac{N}{2}\rho C_{x(\alpha)}A_{p(z)}|V_{rel(t)}|V_{rel(t)} = 0 \quad (42)$$

$$\ddot{x}(t) = \frac{1}{m} \left(-\frac{1}{2}\rho_{air}C_{air}A_{af}\dot{x}(t)^2 - \frac{1}{2}\rho C_{db}A_{bf}\dot{x}(t)^2 + \frac{N}{2}\rho C_{x(\alpha)}A_{p(z)}|V_{rel(t)}|V_{rel(t)} \right) \quad (43)$$

where C_{db} is the drag coefficient of the frontal area through the water, A_{bf} the frontal area through the water that is equal to $z \times w$ (depth×width), C_{air} is the air resistance coefficient, A_{ba} the contact area of the body corresponding to air resistance that is equal to $h \times w$ (height×width), C_x the tractive coefficient corresponding to a plate. Assuming that the system moves along x-axis, the drag force created by the track, in the gaps between plates is assumed to be negligible.

In static conditions, the body is mainly supported by the buoyancy force which is a function of the volume occupied by the body through the water. If the body is perfectly horizontal, and assuming that the contact area of the lower part remains constant, the buoyancy force will be a function of the depth. Thus, the buoyancy force can be modeled as a spring.

$$F_{buoyancy(z)} = \rho g A_{bb} z(t) = K_b z(t) \quad (44)$$

4. Dynamic Analysis

Therefore, the buoyancy force acts as a spring and causes the body bouncing in the water. The bouncing decays in time due to the dissipation of energy through the water. The loss of energy can be stated as a damping force which is a function of the velocity. It is also important to mention that, by elevating the body, the buoyancy force decreases as well. The air resistance opposing the body movement is considered to be applied horizontally and directing to the COG. The effect of the splashing and retracting plates positioned in the front and back of the propulsion system is ignored.

In dynamic states, the body is mainly supported by hydrodynamic forces generated by the plates. As mentioned previously, the force created by the plates is not equally distributed among the plates. However, to generalize the equations of the system, the force applied to each plate is assumed to have the same magnitude and equally distributed. For doing so, the coefficients corresponding to the total force generated by plates are considered.

Thus, it is vital to analyze the error of the coefficients in various conditions, such as different angles of attack and the velocity of the water flow. The tractive and lift coefficients of the plates concerning different velocities and angles are listed below,

4. Dynamic Analysis

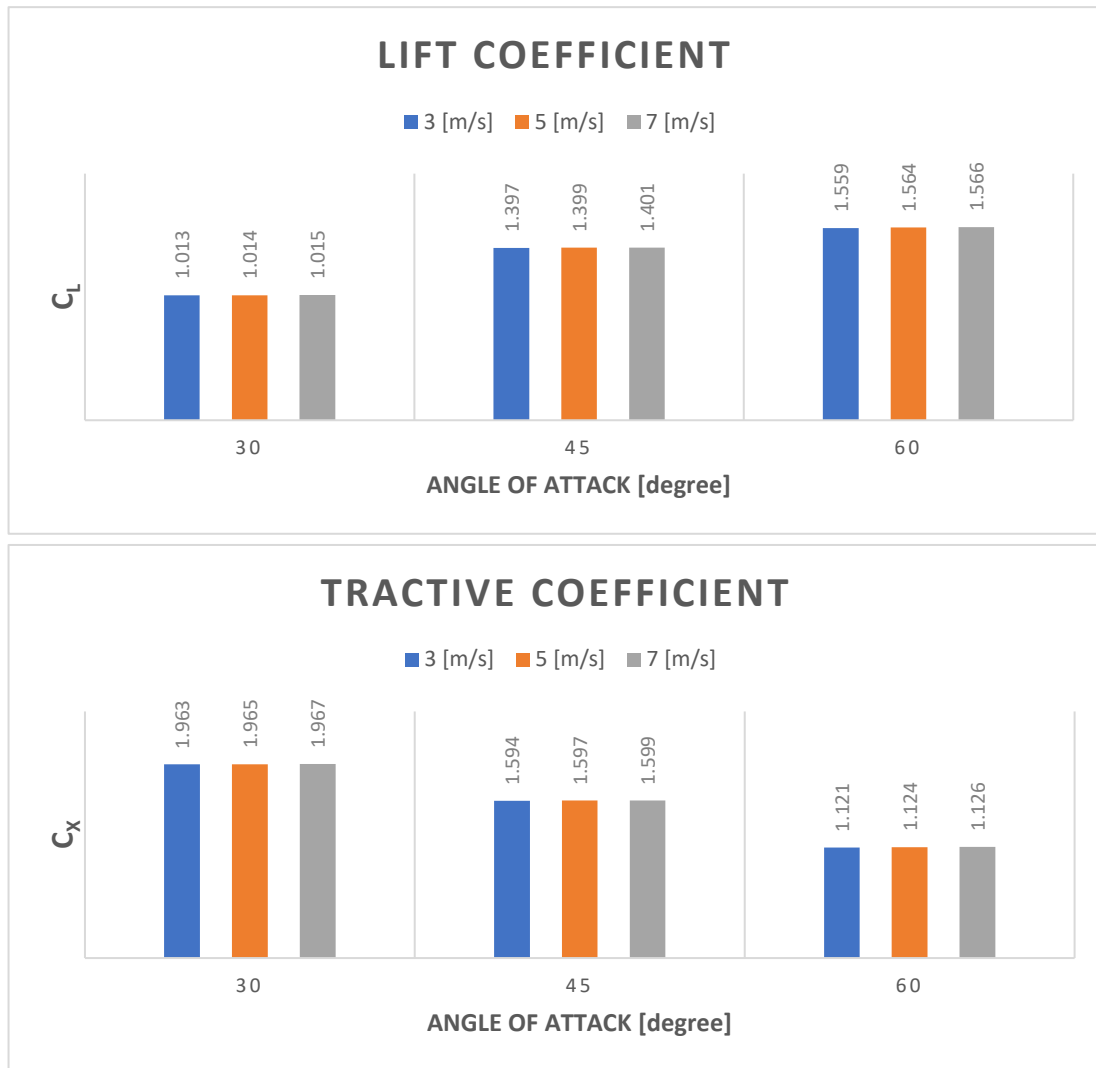


Figure 39 Comparison of the generalized coefficients concerning the averaged force generated by plates at different velocities and angles

The coefficients corresponding to each angle have a small error at different velocities, thus, the values corresponding to each angle can be kept constant and used in later analysis.

The relation of the coefficient with and the angle of plates is estimated as follow

4. Dynamic Analysis

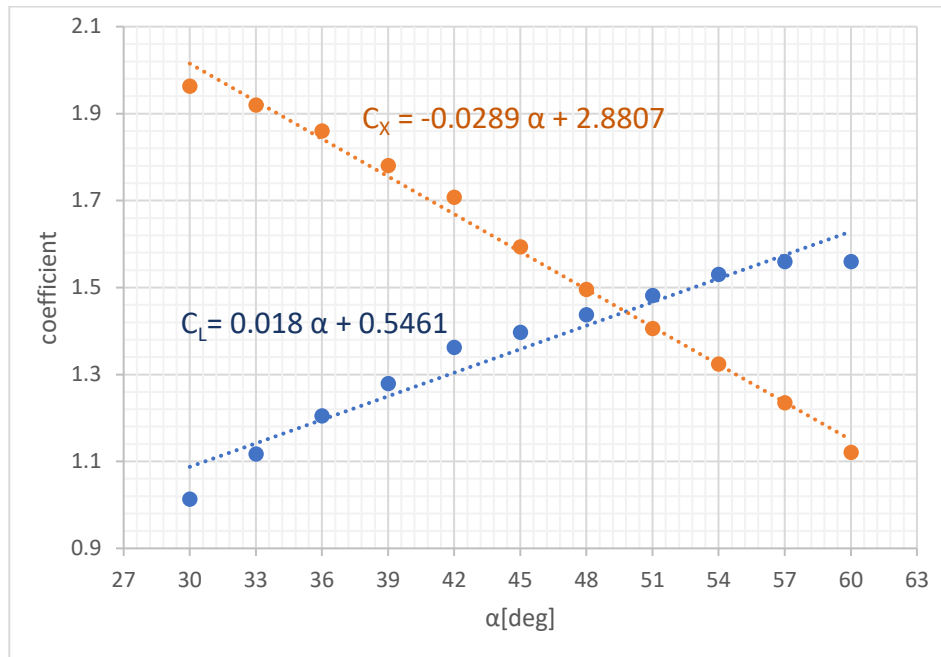


Figure 40 The coefficient corresponding to various angles, the generalized equations of the lift C_L and tractive C_x coefficients are represented above each line

4.2. Results

In the first studies, the body is considered to be horizontal and the force applying to the track in the gap between the plates is neglected, hence, it is expected that the force required by the system is generated by the plates.

4.2.1. Characteristics of the system

The specifications of the entire system are chosen concerning similar applications, such as jet-skis, snowmobiler, etc. For instance, the plates chosen for the simulations have a similar size to lugs of snowmobiles. The air resistance coefficient is the same as the common value used in car applications. The moment of inertia taken for the motor has a remarkably large magnitude, to consider the presence of the frictions between components and the inertia of the track itself. The configurations of the system are listed below

4. Dynamic Analysis

plate						
number of plates/row	number of rows	total number of active plates	a[m]	b[m]	t[m]	α [deg]
5	6	30	0.0762	0.1143	0.00762	45°

body					
m[kg]	H(height)[m]	L(length)[m]	W(width)[m]	diameter of the motor [m]	moment of inertia of the motor[kg.m ²]
400	1	2	0.6858	0.5	0.5

Coefficients				
plate		body		
CL (lift)	C _x (tractive)	CL _b (Lift,track)	C _{db} (Drag,track)	C _{air} (body)
1.4	1.59	2.3	0.27	0.5

Table 6 the parameters used in Simulink

4.2.2. Simulink model

The following figure represents the overall plant of the model used in Simulink simulations.

4. Dynamic Analysis

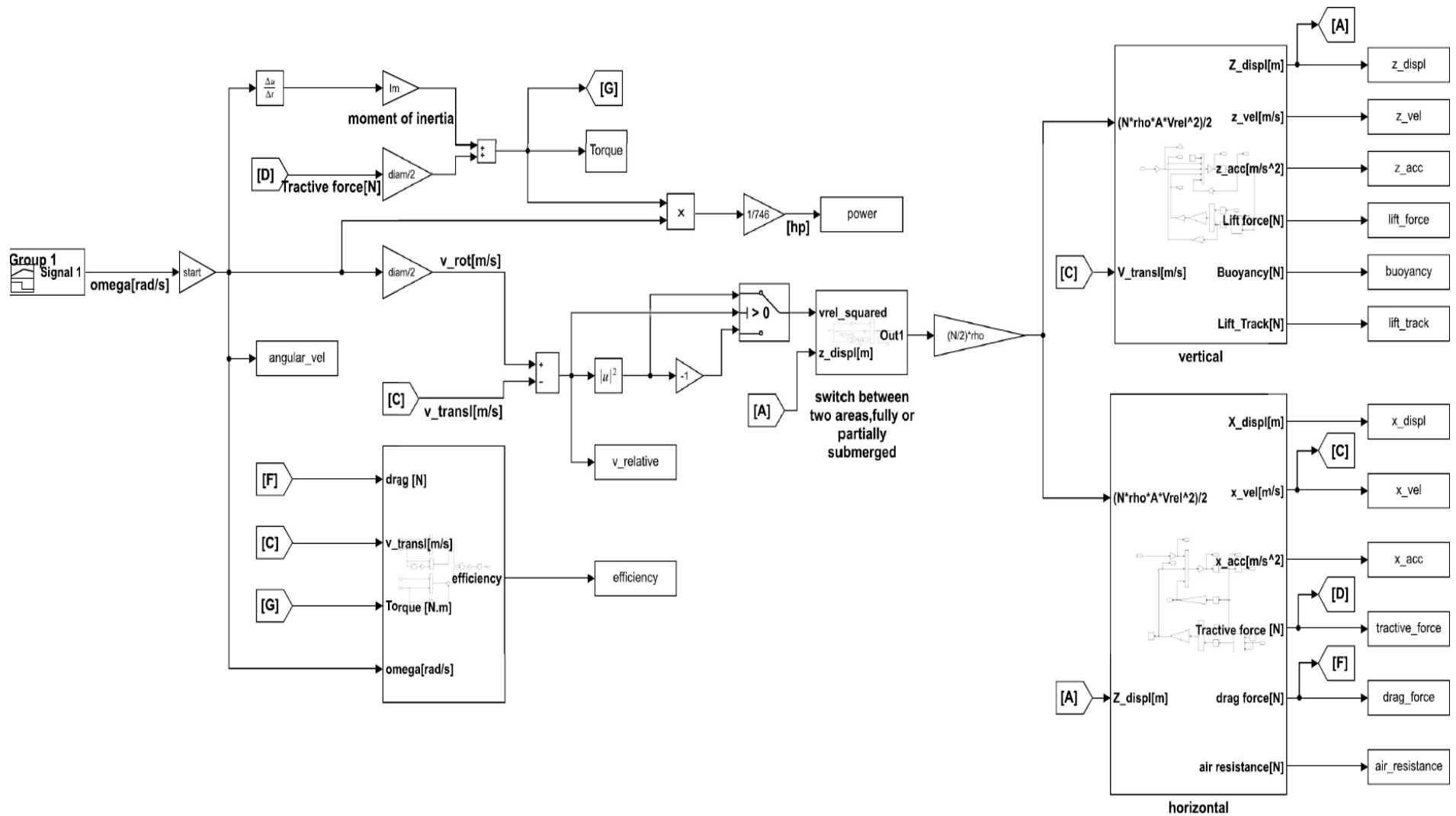


Figure 41 The overall scheme of the plant

4. Dynamic Analysis

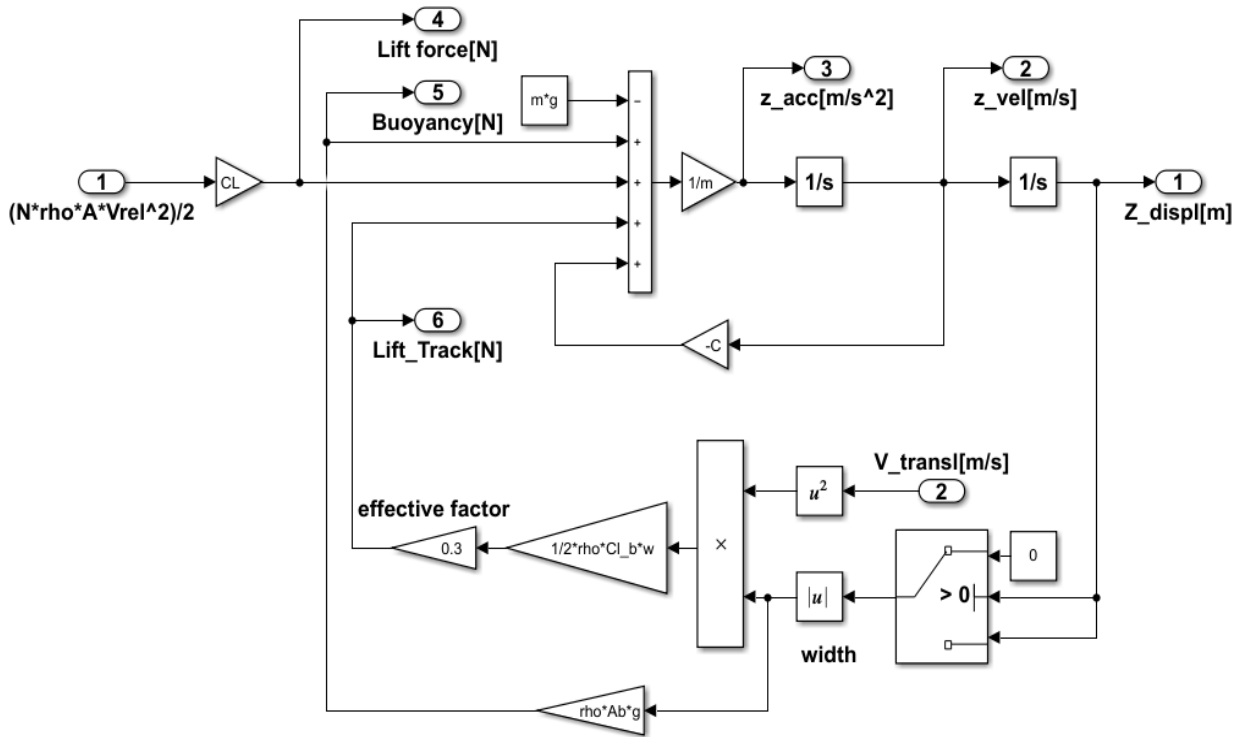


Figure 42 subsystem regarding z-axis (vertical) analysis

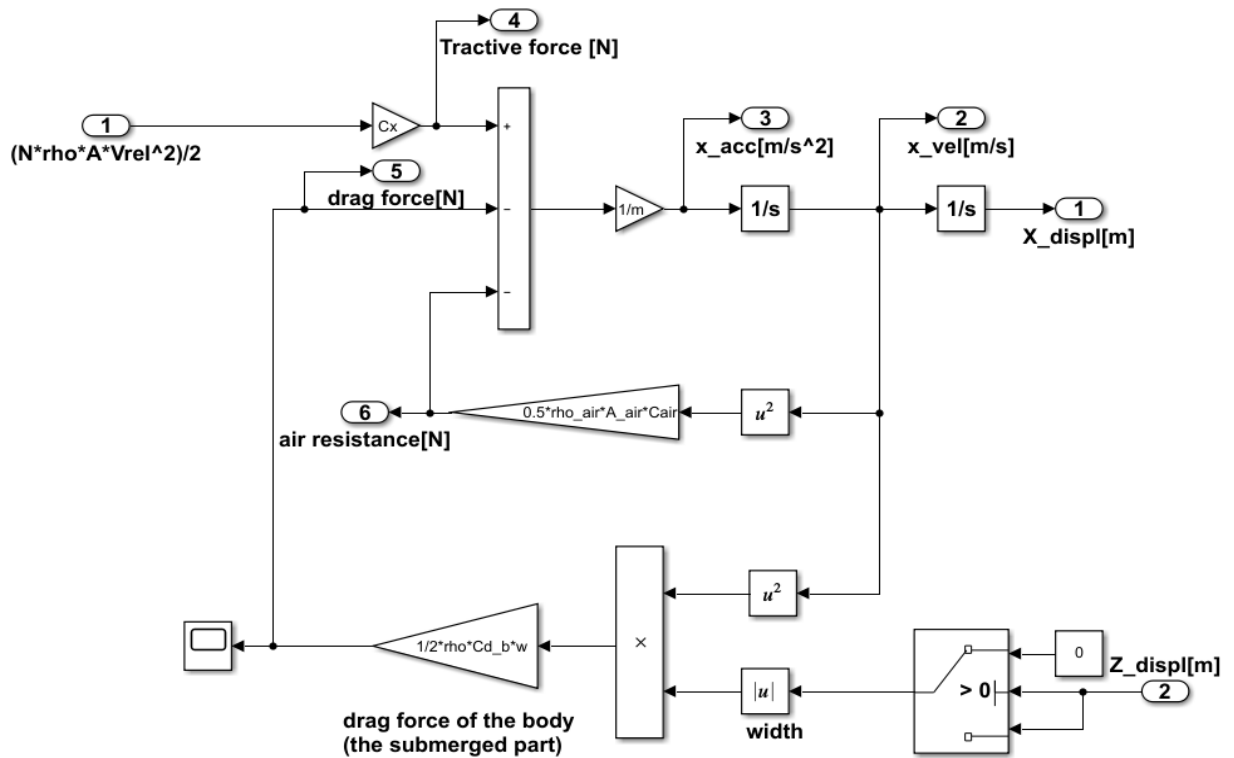


Figure 43 subsystem regarding x-axis (horizontal) analysis

4. Dynamic Analysis

- **Input**

The input of the plant is the angular velocity of the motor. By knowing the rotational velocity of the motor and estimating the translational velocity of the body, it is possible to find the relative velocity of the plates with respect to the water, which is the velocity needed for generating the supporting force.

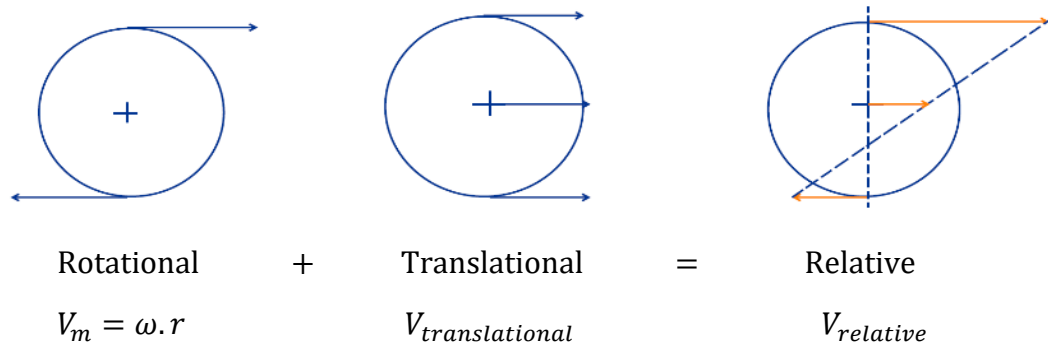


Figure 44 Speed analysis of the wheels, the relative velocity represents the velocity of the plates through the water and the translational velocity is the same as the velocity of the body.

- **Initial conditions**

To define the initial conditions of the system, it is assumed that the lower side of the propulsion system is located on the water surface $z = 0$ and will be dropped through the water at time $t_0 = 0$.

As explained earlier, the buoyancy force acts as a spring, thus, after dropping the body through the water, it starts bouncing until it reaches a steady-state condition when the buoyancy force becomes equal to the body weight. Assuming that the body is perfectly horizontal at static conditions, the depth in which the body remains steady can be found from equation 44 and rewritten as

$$Z_{static} = \frac{m}{\rho A_{bb}} \quad (45)$$

By knowing the initial position of the system through water, the time and the energy required for emerging from the water can be estimated.

4. Dynamic Analysis

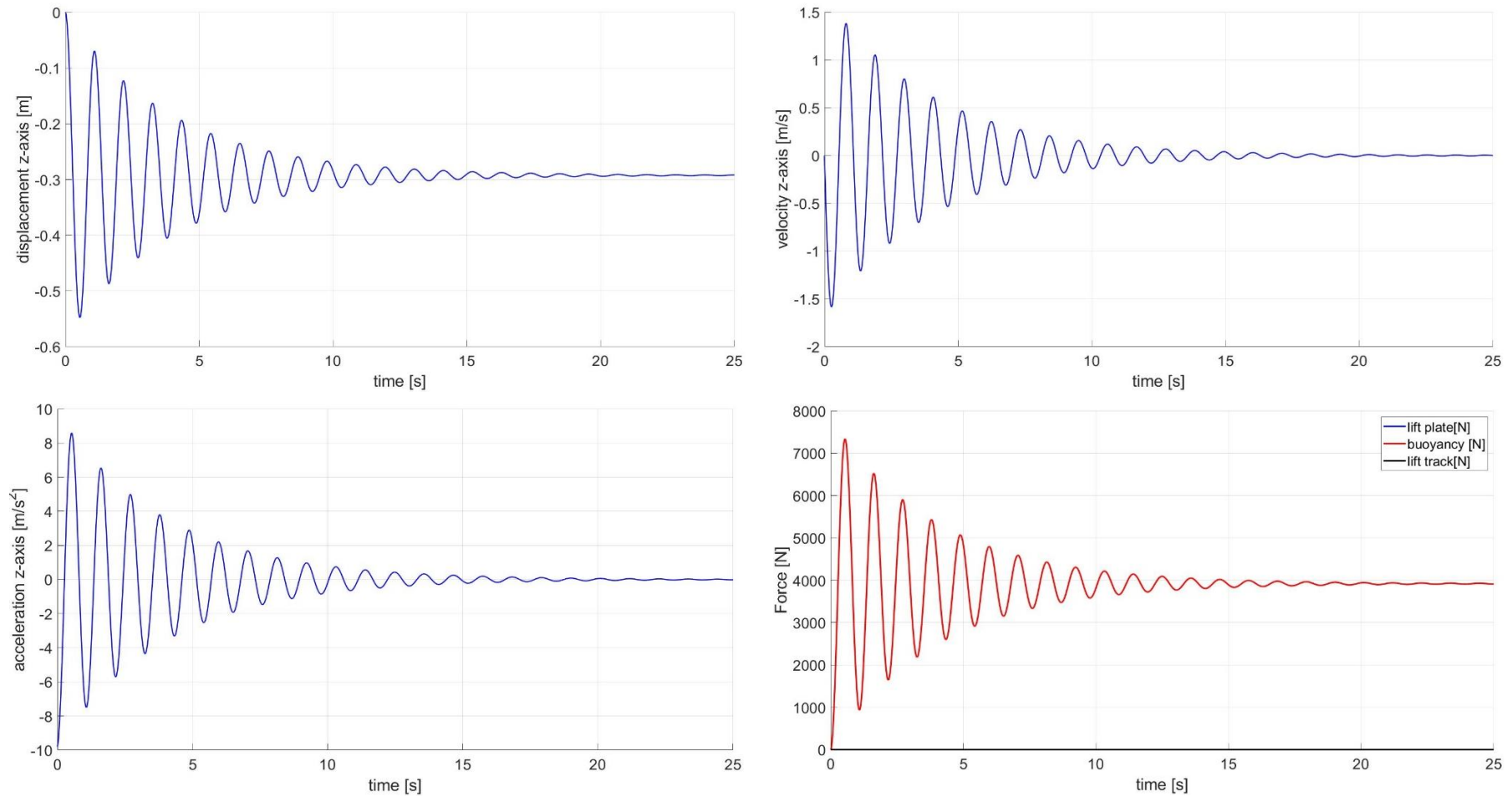


Figure 45 Results of z-axis analysis in static conditions, the body is dropped into the water, the initial position of the body is on the water surface, the time needed for the system to stop bouncing and remains steady, the vertical position of the body at $t \rightarrow \infty$ will be equal to Z_{static} .

4. Dynamic Analysis

As the figure represents, at static states, when the body is originally placed on the water surface and at time $t=0$ dropped through water, it starts oscillating until it loses the energy and remains steady at the position $Z = Z_{static} = -0.2925$ [m].

- **Natural frequency**

The natural frequency of the movement along the z-axis can be found using the following equation.

$$\omega_n = \sqrt{\frac{k}{m}} \quad (46)$$

where ω_n is the natural frequency, k is the stiffness, and m is the mass of the body. To compare the frequency obtained from the previous figure, the natural frequency can be compared to the frequency obtained from the previous figure.

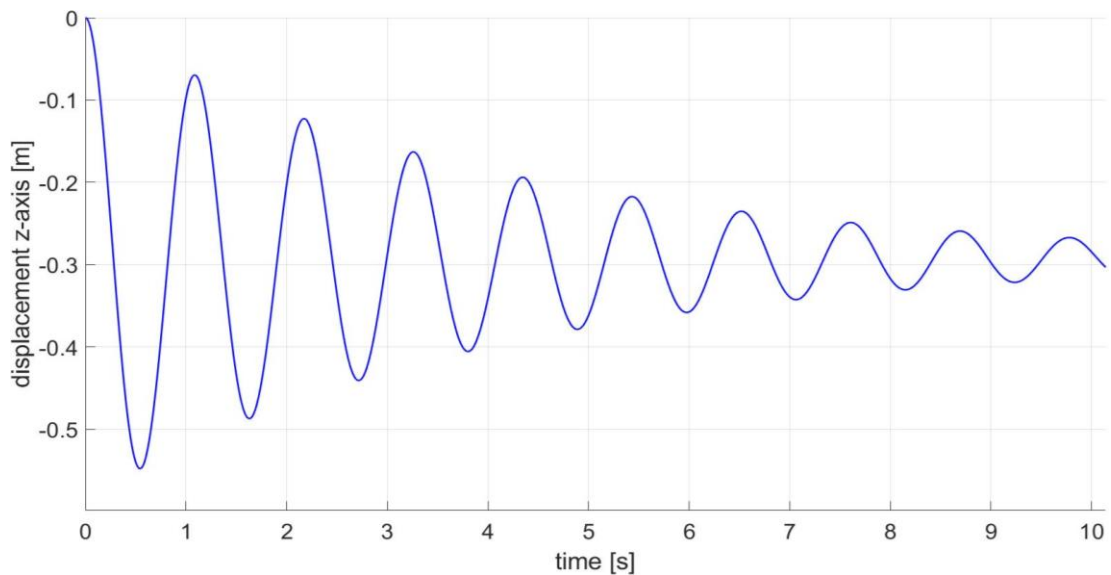


Figure 46 A closer point of view of the previous plot regarding the vertical movement, to measure the frequency.

The natural frequency obtained from equation (46) and the frequency measured from figure 43 are 0.9212 [Hz] and 0.9166 [Hz] respectively.

4. Dynamic Analysis

- **Damping factor**

Regarding figure 45, the damping factor of the vertical movement of the body can be estimated applying logarithmic decrement

$$\delta = \ln\left(\frac{x_i}{x_{i+1}}\right) = 2\pi \frac{\zeta}{\sqrt{1-\zeta^2}} \approx 2\pi\zeta \quad (47)$$

The estimated value of ζ is about 5%.

- **Switch**

For taking into account the reduction of the contact area of the plates during the elevation of the body from water, the switch represented in the figure 42 is designed. The switch considers the position of the body with respect to the water surface, therefore, once the plates start emerging from the water, it switches from totally to partially submerged contact area.

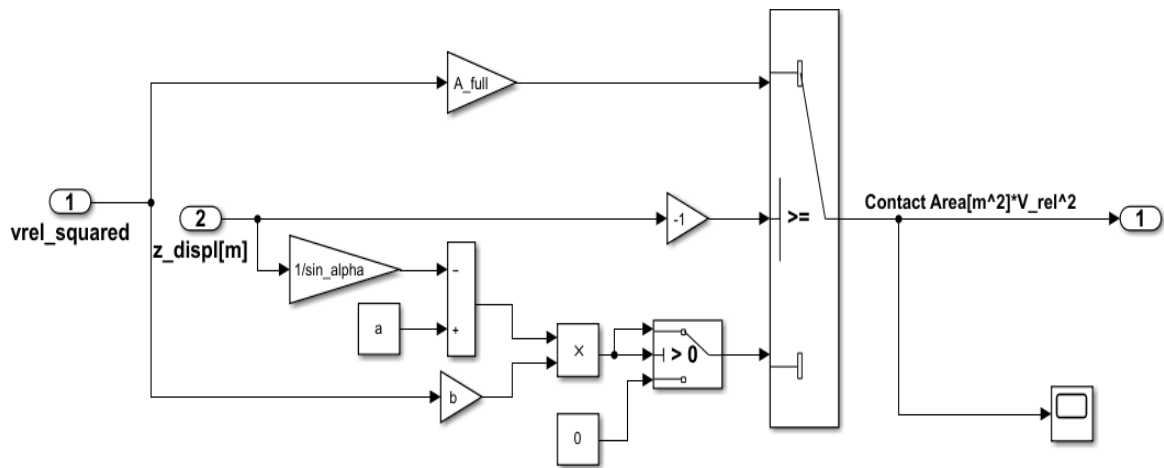


Figure 47 the switch of between active contact areas of the plate, fully or partially submerged

- **Efficiency**

The pitch angle is supposed to be small especially at high velocities and steady states. As represented in figure 37, for small variations of angles such as 1 to 3 degrees, the coefficients do not vary significantly, accordingly, it is assumed that the effect of small pitch angles on the force providing by the plates remains constant.

4. Dynamic Analysis

Considering the plates moving along the x-axis, the relative velocity of the plates with respect to water can be found as follow

$$V_{relative} = V_{rotational} - V_{translational} \quad (48)$$

To estimate the torque, power, and loss of efficiency of the motor, the following equation is used in the Simulink model.

$$T = \sum F_{tractive,plate} r + I\dot{\omega} \quad (49)$$

$$P_{total} = T\omega \quad (50)$$

$$\eta = \frac{F_{drag}V_{body} + m\dot{V}_{body}V_{body}}{P_{total} - I\dot{\omega}\omega} \quad (51)$$

where T is the torque, $F_{tractive,plate}$ represents the tractive force generated by each plate, r is the radius of the motor, I is the moment of inertia, $\dot{\omega}$ is the angular acceleration, P_{total} is the total power generated by the motor, ω is the angular velocity of the motor, η is the efficiency due to the power conversion, V_{body} is the velocity of the system along x-axis which is equal to $V_{translational}$.

4. Dynamic Analysis

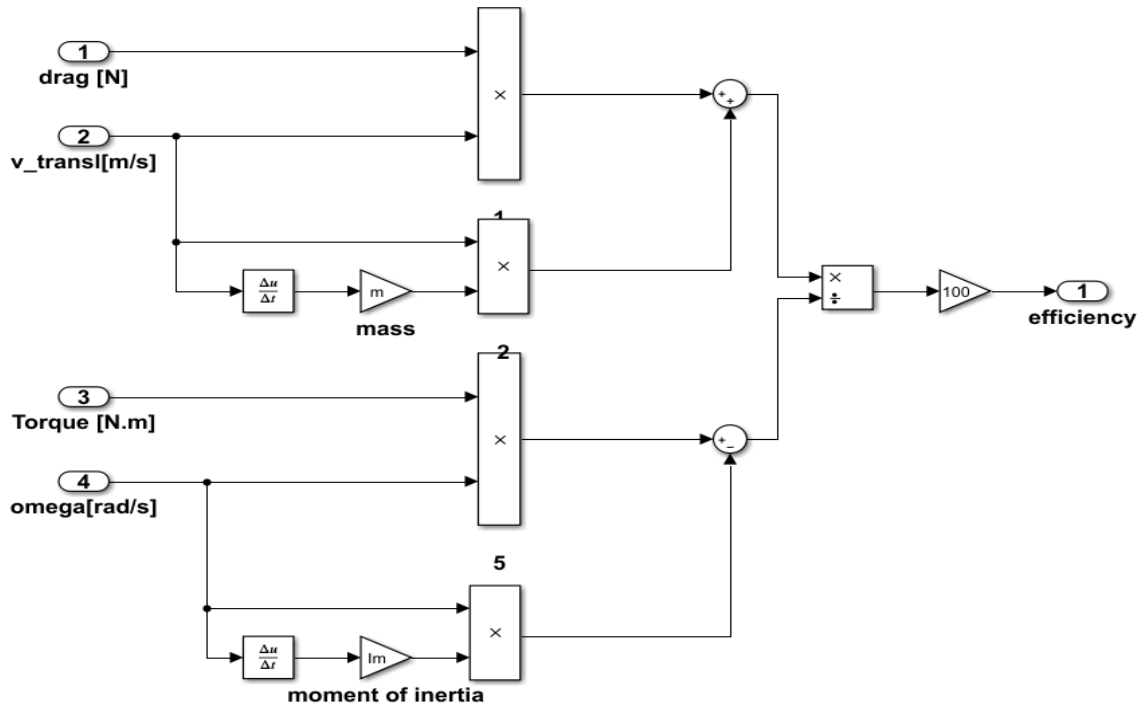


Figure 48 The subsystem regarding the efficiency

• Dynamic simulations

The input of the plant, which is the angular velocity of the motor, is a ramp at the beginning, and becomes a step for a period and in the end, it goes back to zero again. The following figure represents the input of the system.

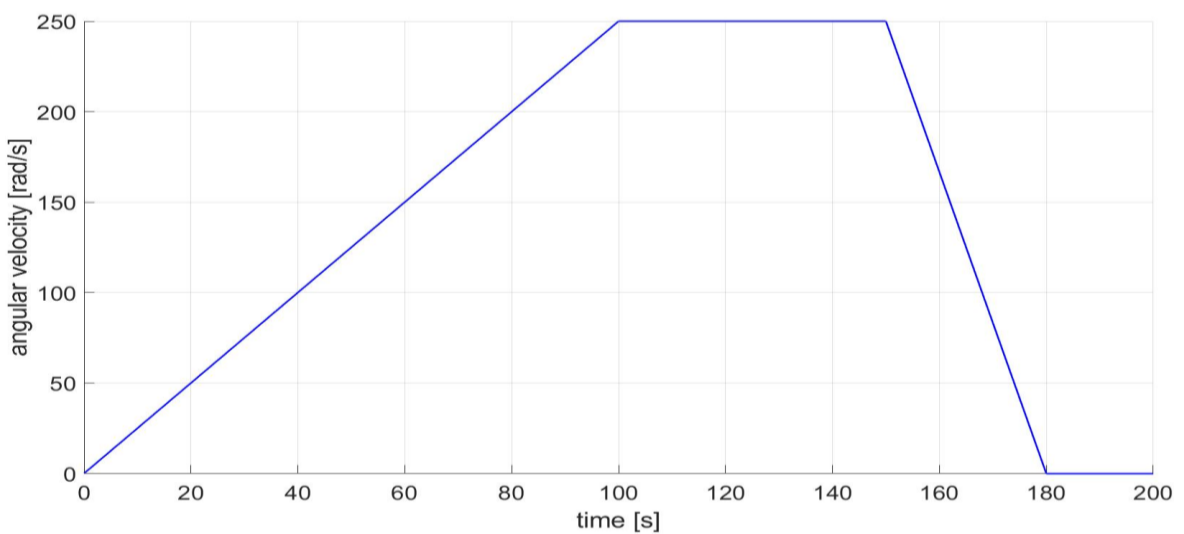


Figure 49 The input of the system which is the angular velocity of the motor

4. Dynamic Analysis

The input of the system is the angular velocity of the motor and it is assumed to be a ramp from $t_0=0$ [s] to $t_1=100$ [s] and remains constant until $t_2=150$ [s]. At the time t_2 , the velocity starts decreasing until it goes to zero at $t_3=180$ [s], which means the motor is decelerating.

- **The results of the plant (without the force applying to the track)**

The following figures indicate the outputs of the system in the case of neglecting the force applied to the track.

4. Dynamic Analysis

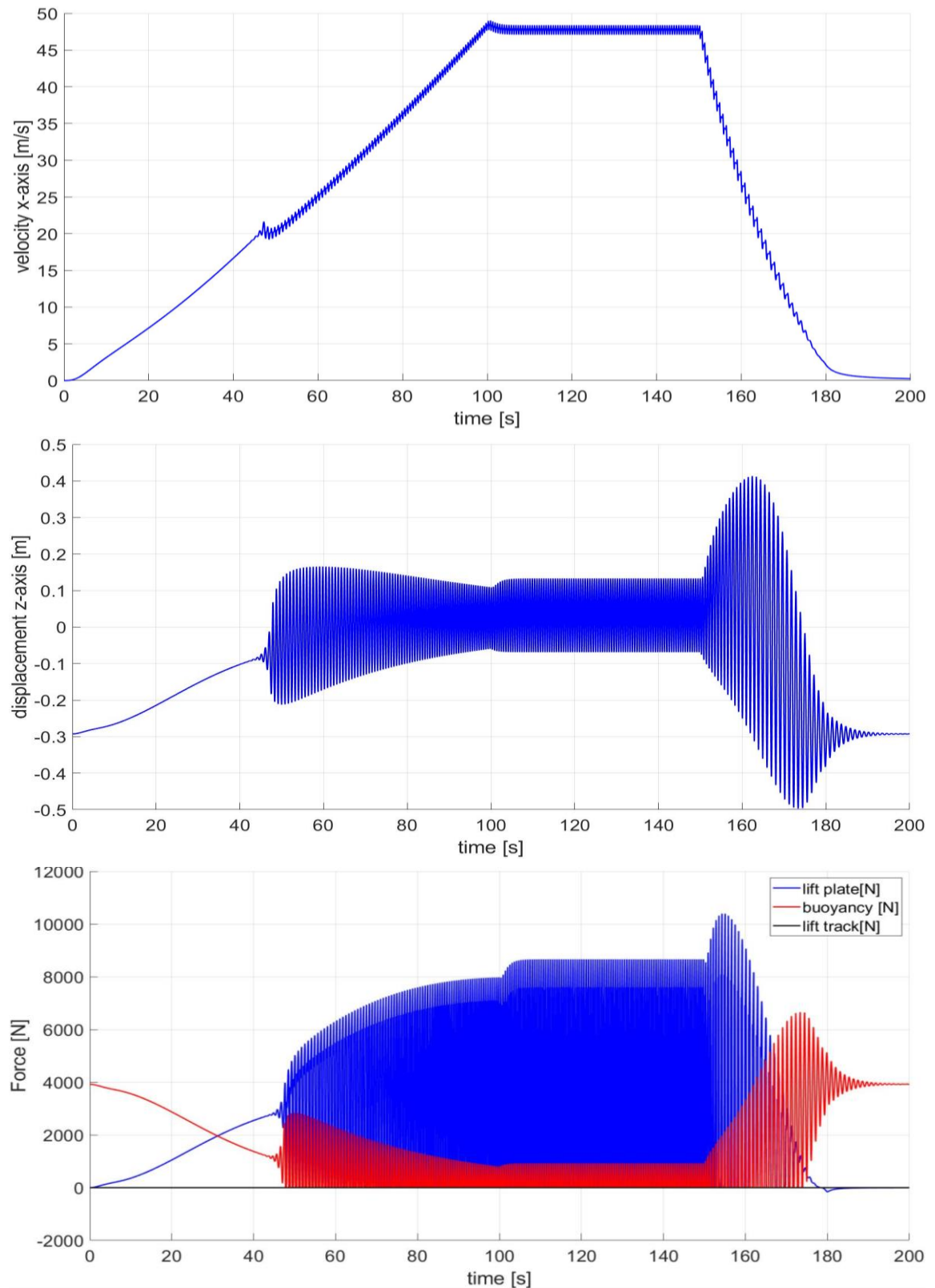


Figure 50 The output of the system when the entire system relies on the force generated by the plates. The first plot represents the translational velocity of the system along the x-axis, the second plot is the vertical displacement of the system and the last one is the forces applied to the system regarding the z-axis

4. Dynamic Analysis

The results of the simulations show that the system can rely on the forces generated by the plates, but it can create fluctuations that lead to unpleasant actions. When the body approaches the water surface, the plates start emerging from the water as well, which makes a loss of the active contact area and consequently the force generated by them decreases. At this moment, due to the reduction of the supporting force, the body descends again. Thus, an oscillation occurs and every time that the propulsion system touches the water, it creates a large drag force, which is not relevant especially at high velocities, as it makes a sudden change of the velocity.

- **The results of the plant (with the force applying to the track)**

Analyzing the forces applied to the gaps among the plates is complex. Due to the presence of plates, the flow starts recirculating behind the plates and not easy to be predicted, moreover, other factors such as the action of the track itself can interfere with the flow. To understand this condition correctly, the body is assumed to be fixed, while the velocity of the flow is the same as the translational velocity of the body. However, the track itself has the same velocity as the plates.

To estimate the force generated by the track (in the gaps among the plates) the lift coefficient of the track is measured regarding various angles.

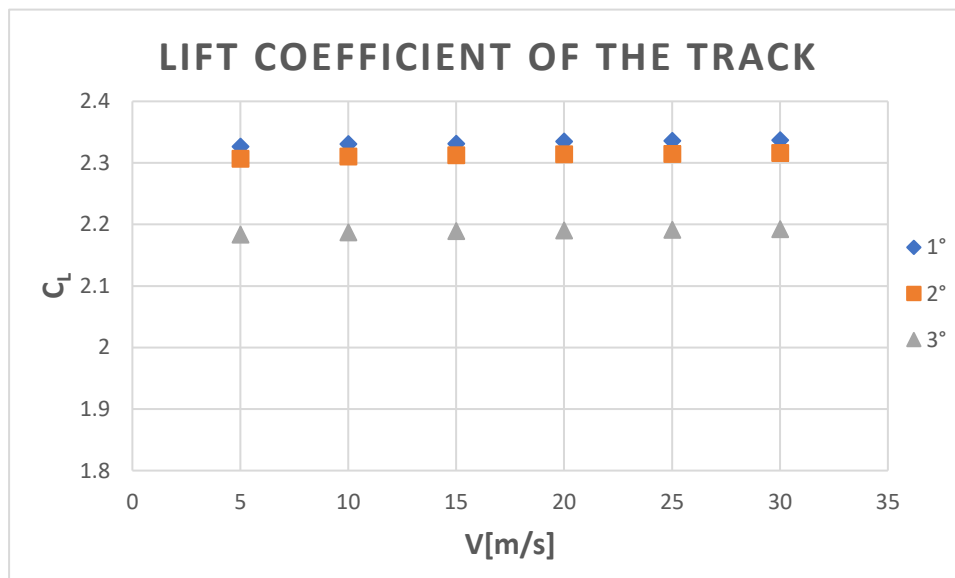


Figure 51 The lift coefficient of the track measured in CFD simulation

4. Dynamic Analysis

Since the variation of the angle is small, the variation of the coefficients evaluated at different angles is not remarkable, thus, an averaged value can be considered for the simulations.

As mentioned earlier, it is assumed that in the simulations the flow facing with the track is not distorted by the plates. So, to consider the effect of the plates on the force created by the track (gaps between the plates), an effective factor is included.

It can be assumed that the velocity of the water facing the track would be affected by the recirculation made by the plates and the thin layer created by the track itself. The factor is set to decrease the effect of the force created by the track by up to 70%. The results show that even such a small percentage of the force generated by the track can improve the performance of the system significantly and can provide better operation of the system by limiting the pitch angle and vibrations.

This effect is added through equations 40 and 41, while the effective factor D is introduced in the equation to make the results more realistic and taking into account the distraction of the flow among the plates. The gain corresponding to the effect of the lift generated by the track is placed in the Simulink model as represented in figure 42.

The following figures indicate the outputs of the system in the case of considering the force applied to the track.

4. Dynamic Analysis

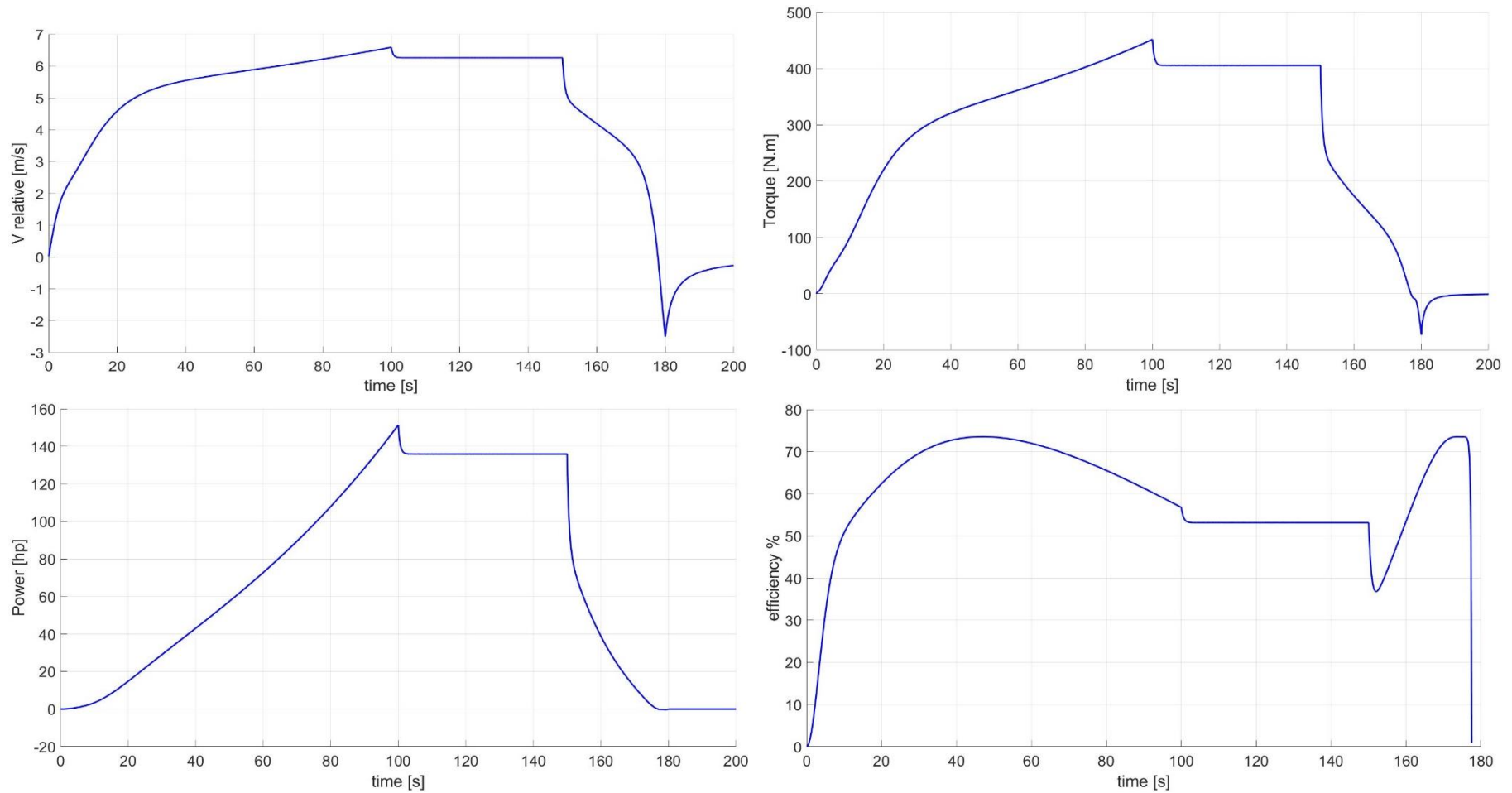


Figure 52 The plot in the top-left represents the relative velocity of the plates through the water and along the x-axis, the top-right plot is the torque of the motor, the plot on the bottom-left is the power required by the system, and the plot on the bottom-right is the efficiency during the energy conversion from mechanical to fluid.

4. Dynamic Analysis

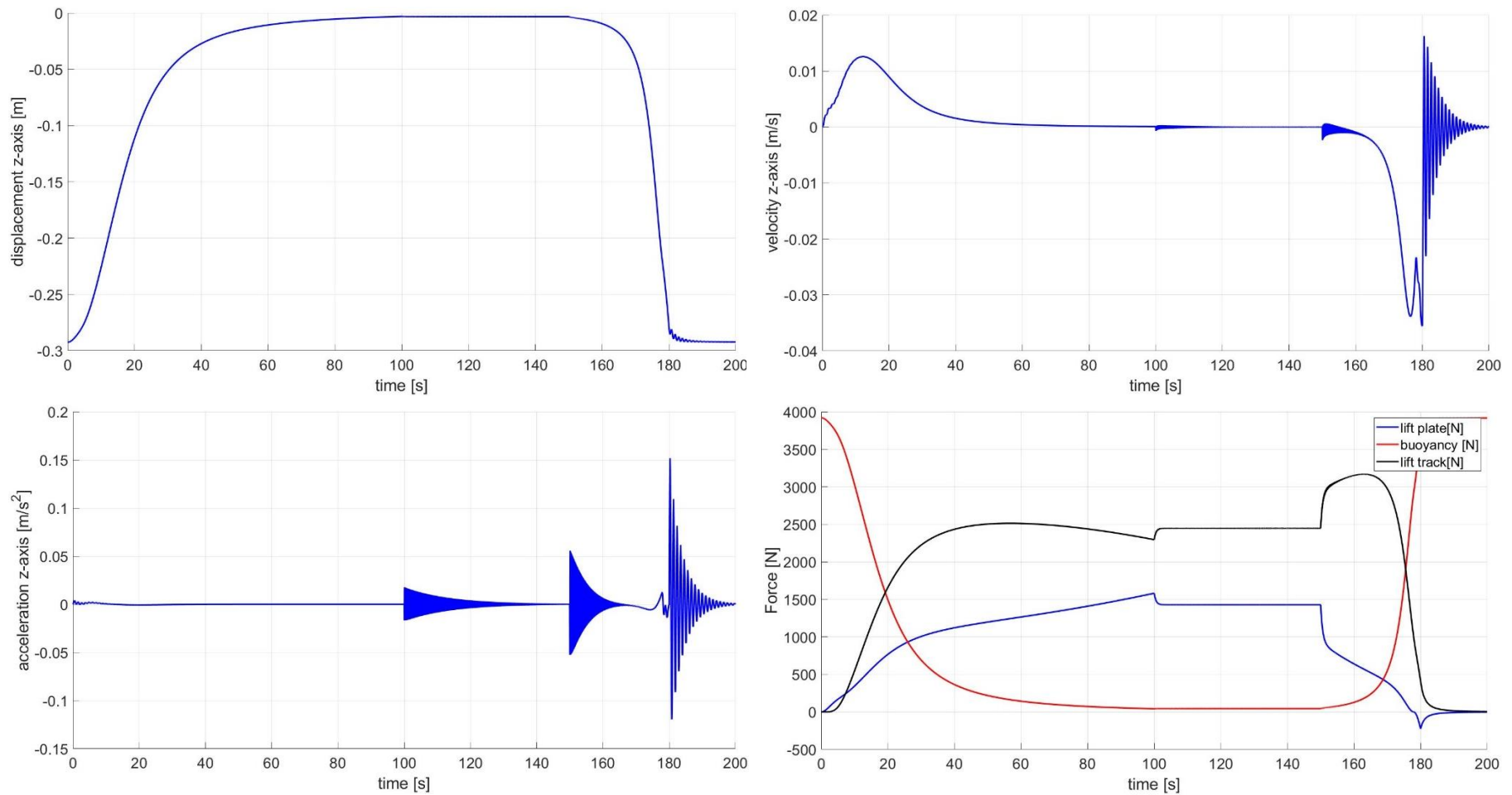


Figure 53 z-axis analysis, The plot in the top-left represents the vertical displacement, the top-right plot is the velocity along the z-axis, the plot on the bottom-left is the acceleration along the z-axis, and the plot on the bottom-right indicates the vertical forces applying to the system.

4. Dynamic Analysis

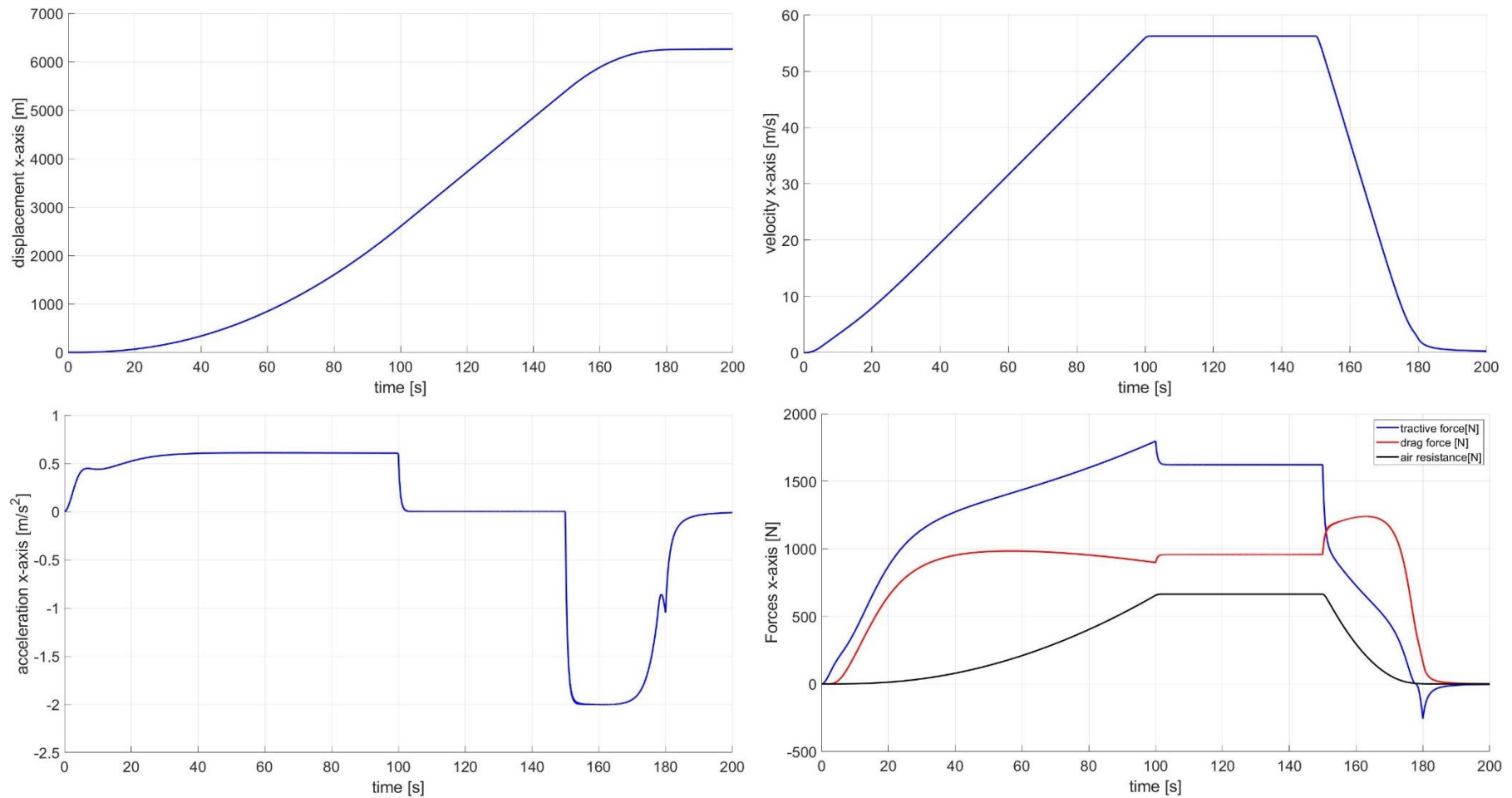


Figure 54 x-axis analysis, The plot in the top-left represents the displacement along the x-axis, the top-right plot is the velocity along the x-axis which is the same as the translational velocity of the entire system, the plot on the bottom-left is the acceleration along the x-axis, and the plot on the bottom-right indicates the forces along the x-axis.

5. Dynamic Analysis

As the results show, contrary to the previous case (where the effect of the force applying to the gaps among the plates was neglected) the system behaves smoothly, and no significant vibrations appear during the operation. As mentioned earlier, in this case, the force generated by the track part limits the fluctuations of the system, and every time the body tends to descend the lift generated by the track pushes the body upward.

The difference between figure 47 and the following plots is due to the force applying to the gap among the plates, which is called the lift of track shown in figure 36. This additional lift improves the vibrations that were present in the previous case, as every time the system wants to emerge through the water, the additional lift of the track pushes the body upward again, so the lift is not only generating by the plates but also takes advantage of the track for each time the system goes through the water. The vibrations still exist, but the amplitude is so small concerning the previous case and seems to be linear.

The input velocity used is the same as the previous case, while the main difference is the force applying to the lower side (in the gaps among the plates). As the results show, there is a delay in the system to follow the command. Since the system starts working from the rest, a minimum velocity is required to generate enough force to propel the system forward and start elevating. The following figure represents the time needed for the system to follow the input.

4. Dynamic Analysis

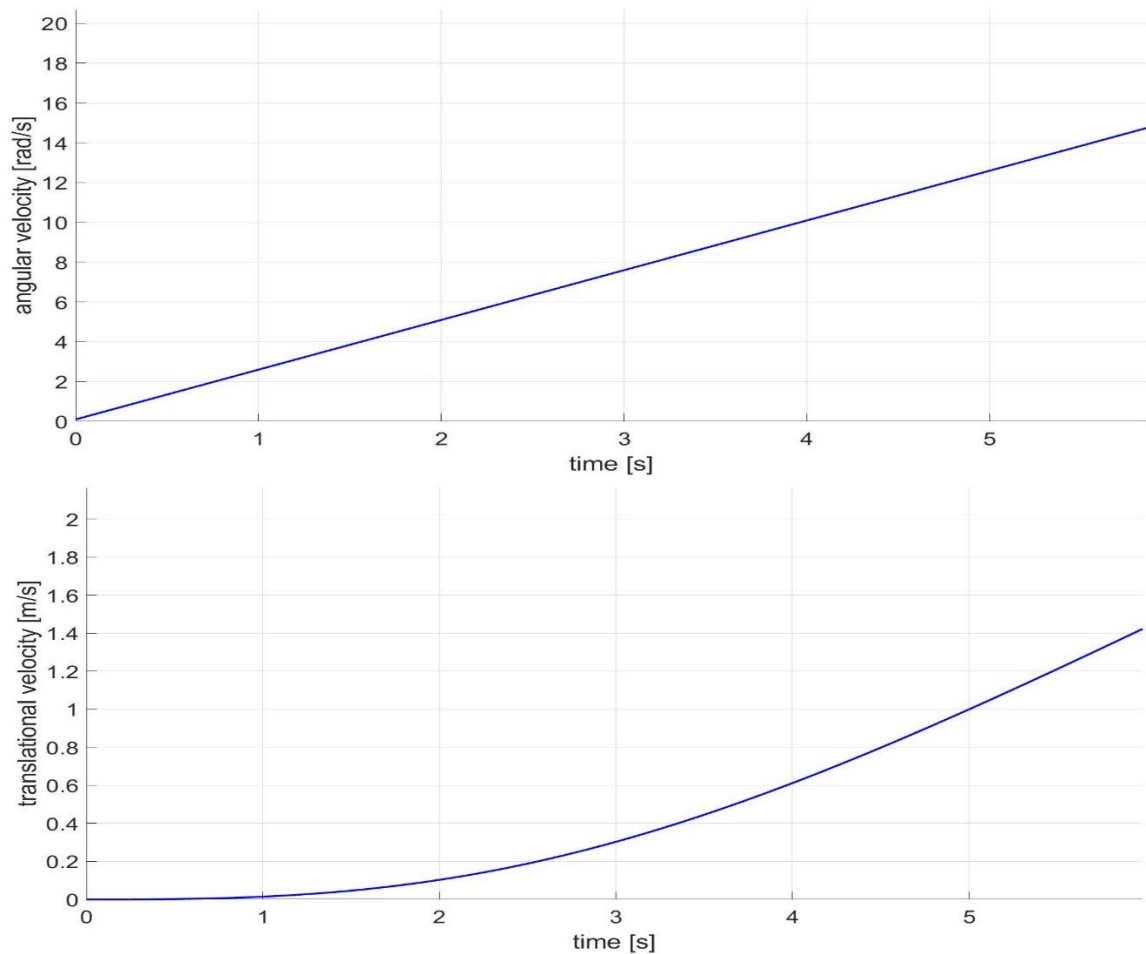


Figure 55 The plot on the top is the input velocity and the plot on the bottom is the translational velocity corresponding to the input, the delay in which the output can follow the input is well evident.

As the results show, in the beginning, the body is immersed through the water. Once the motor starts rotating and pushes the plate through the water, it generates a force that propels the body forward, moreover, as the velocity increases, it also lifts the entire body upward. By elevating the body, the effect of the buoyancy decreases.

Figure 46 represents the presence of oscillations appearing during the transition states, which is due to the buoyancy force applying to the body. As mentioned earlier, the buoyancy force works as a spring, thus, at low velocities, it affects the operation of the system. However, by increasing the velocity and elevating the body, the buoyancy loses its importance and the system will be mainly supported by the hydrodynamic force generated by the plates.

As soon as the velocity increases and the force generated by the system becomes large enough to support the system, it stops fluctuating. It is also well evident that by increasing

4. Dynamic Analysis

the velocity the body starts elevating and the drag force due to the frontal area hitting the water decreases as well. However, by elevating the body, the buoyancy force which is a function of the depth through the water reduces and becomes negligible when the body approaches the water surface.

As the acceleration along the z-axis indicates, the system goes to a steady-state at time $t_{steady}=20$ [s], and the entire body stops vibrating. It keeps accelerating till $t_1=100$ [s], then, the velocity remains constant for a period of 50 [s] and at the end at $t_2=150$ [s], it goes to zero suddenly, which means the plates cannot provide a supporting force to the system, and the body starts decelerating. Once the system starts decelerating and is not capable of supporting the weight of the body, it starts descending and the drag force against it becomes too large immediately until it stops moving and remains steady. The negative acceleration indicated in figure 47 at $t_2=150$ [s] represents a sudden shift of the velocity.

Although the plates stop generating the supporting force and the torque of the motor goes to zero, still a lift force applies to the body, which is due to the contact area of the lower part of the body hit by the water, that generates lift and drag at the same time.

As indicated in figure 45, the system performs a remarkable achievement, as the maximum power during the acceleration is approximately 200 [hp] when it is running at a velocity of 200[km/h] across the water. Referring to table 1 and similar systems, these results are remarkable.

5. Conclusions

The project denotes that the water is not a boundary for high-speed transports anymore and traveling long distances in a fair amount of time and energy is achievable. Presenting much higher efficiency and more reliable operations in terms of stability and safety of the system leads to having a new layout referring to this kind of transportations.

The experimental trials have already proved the feasibility of executing the proposed idea, while the project investigates the performance and the working states of the system by using simulations. It is relevant to highlight the efficiency in the first place, as it is a big concern of fast watercrafts such as jet skis and boats. The analysis revealed exceptional efficiency and a smooth response under several circumstances.

The concept provides more reliable performance than other applications as it can reduce the drag force opposing the body by elevating the body from the water, accordingly, drag which is a function of velocity squared is not a concern.

The water behaves differently at various velocities. The dynamic analysis of the system showed that in a condition when the water level is uniform and no waves exist, the system represents a satisfying behavior in both conditions, transition, and steady states.

Based on the preliminary studies and the outputs of simulations it can be concluded that the concept represents valuable results comparing to other technologies and systems. However, the assumptions used for simulations consider mostly the behavior of the system in steady states and under certain circumstances, such as the pitch moment which is large during the starting of the system. Therefore, it is suggested to include such conditions in later numerical analysis and the stability of the entire system.

There is a lot to learn about the behavior of the system in a real-world condition, moreover, because of the complexity of the system and its dependence on the environment conditions, it is strongly recommended to work on a prototype based on the method proposed in this project for later studies.

6. References

- [1] Alexander Beckley (2013), *Drive Train for an Electric Jet Ski Conversion*. Department of Engineering University of Western Australia.
- [2] Ten of the fastest boats ever made, URL <https://jalopnik.com/ten-of-the-fastest-boats-ever-made-1697883988>.
- [3] Eric Besnard, Adeline Schmitz, George Tzong, Kalle Kaups, Hamid Hefazi, John Hess Hsun Chen, and Tuncer Cebeci (1998), *HYDROFOIL DESIGN & OPTIMIZATION FOR FAST SHIPS*, Aerospace Engineering Department, California State University, Long Beach Long Beach, CA 90840.
- [4] HYDROFOILS - Renewable Energy Research, URL <https://www.bluebird-electric.net/hydrofoils.htm>.
- [5] Surjatin Wiriadidjaja1*, Amzari Zhahir2**, Zahratu Hilall Mohamad2 , Shikin Razali2 , Ahmad Afifi Puaat2 , Mohamed Tarmizi Ahmad3, *Wing-in-ground-effect craft: A case study in aerodynamics* International Journal of Engineering & Technology.
- [6] Glenna T. Clifton1,*, Tyson L. Hedrick2 and Andrew A. Biewener1 (2015), *Western and Clark's grebes use novel strategies for running on water*, Published by The Company of Biologists Ltd | The Journal of Experimental Biology (2015) 218, 1235-1243 doi:10.1242/jeb.118745.
- [7] S. Tonia Hsieh* and George V. Lauder (2004), *Running on water: Three-dimensional force generation by basilisk lizards*, Department of Organismic and Evolutionary Biology, Harvard University, 26 Oxford Street, Cambridge, MA 02138 Edited by David B. Wake, University of California, Berkeley, CA, and approved October 16, 2004 (received for review August 5, 2004).
- [8] Steven Floyd, Terence Keegan, John Palmisano, and Metin Sitti (2006), *A Novel Water Running Robot Inspired by Basilisk Lizards*, NanoRobotics Laboratory, Department of Mechanical Engineering, Carnegie Mellon University, PA 15213, USA.
- [9] Linsen Xu, Kai Cao, Xianming Wei and Yungao Shi (2013), *Dynamics Analysis of Fluid-Structure Interaction for a Biologically-inspired Biped Robot Running on Water*, International Journal of Advanced Robotic Systems.
- [10] Steven Floyd, Serhat Adilak, Steven Ramirez, Raphael Rogman, and Metin Sitti (2008), *Performance of Different Foot Designs for a Water Running Robot*, 2008 IEEE International Conference on Robotics and Automation Pasadena, CA, USA, May 19-23, 2008.
- [11] Hyun Soo Park, Steven Floyd, and Metin Sitti (2008), *Dynamic Modeling of a Basilisk Lizard Inspired Quadruped Robot Running on Water*, NanoRobotics Laboratory, Department of Mechanical Engineering, Carnegie Mellon University, Pittsburgh, PA 15213.
- [12] Hyun Soo Park, Steven Floyd, and Metin Sitti (2009), *Dynamic Modeling and Analysis of Pitch Motion of a Basilisk Lizard Inspired Quadruped Robot Running on Water*, NanoRobotics Laboratory, Department of Mechanical Engineering, Carnegie Mellon University, Pittsburgh, PA 15213.

- [13] Norway man beats snowmobile water record, URL <https://www.thelocal.no/20150924/norway-sets-new-snow-mobile-on-water-world-record>.
- [14] *The secret to riding a motorcycle on water*, URL <https://www.cartoq.com/the-secret-to-riding-a-motorcycle-on-water-we-explain/>.
- [15] Jialun Liu & Robert Hekkenberg (2017), Sixty years of research on ship rudders: *effects of design choices on rudder performance*, Ships and Offshore Structures, 12:4, 495-512, DOI: 10.1080/17445302.2016.1178205.
- [16] John W.M. Bush and David L. Hu, (2006), *Walking on Water: Biocomotion at the Interface*, Department of Mathematics, Massachusetts Institute of Technology, Cambridge, Massachusetts 02139
- [17] YUNUS A. ENGEL, JOHN M. CIMBALA, *Fluid mechanics, fundamentals and applications*, Published by McGraw-Hill, a business unit of The McGraw-Hill Companies, Inc., 1221 Avenue of the Americas, New York, NY 10020. Copyright © 2014 by The McGraw-Hill Companies, Inc.
- [18] DET NORSKE VERITAS (2011), *MODELLING AND ANALYSIS OF MARINE OPERATIONS, RECOMMENDED PRACTICE DET NORSKE VERITAS DNV-RP-H103*.
- [19] Xia Qingfu, Liu Zhiping, a* (2012), *Study on Flow Reattachment Length*, State Key Laboratory of Simulation and Regulation of Water Cycle in River Basin, China Institute of Water Resources and Hydropower Research, Beijing, 100038, China.
- [20] M. Sajben, J.C. Kroutil, and C.P. Chen, “*A High-Speed Schlieren Investigation of Diffuser Flows with Dynamic Distortion*”, AIAA Paper 77-875, 1977.
- [21] T.J. Bogar, M. Sajben, and J.C. Kroutil, “*Characteristic Frequencies of Transonic Diffuser Flow Oscillations*,” AIAA Journal, vol. 21, no. 9, pp. 1232–1240, 1983.
- [22] J. T. Salmon, T.J. Bogar, and M. Sajben, “*Laser Doppler Velocimetry in Unsteady, Separated, Transonic Flow*”, AIAA Journal, vol. 21, no. 12, pp. 1690–1697, 1983.
- [23] T. Hsieh, A.B. Wardlaw Jr., T.J. Bogar, P. Collins, and T. Coakley, “*Numerical Investigation of Unsteady Inlet Flowfields*,” AIAA Journal, vol. 25, no. 1, pp. 75–81, 1987.
- [24] URL <http://www.grc.nasa.gov/WWW/wind/valid/transdif/transdif01/transdif01.html>
- [25] URL <http://www.grc.nasa.gov/WWW/wind/valid/transdif/transdif02/transdif02.html>
- [26] Walter Frei (2017), *Which Turbulence Model Should I Choose for My CFD Application?*, COMSOL Blog, URL <https://www.comsol.com/blogs/which-turbulence-model-should-choose-cfd-application/>
- [27] Ed Fontes, (2018), *Two Methods for Modeling Free Surfaces in COMSOL*, COMSOL Blog, URL <https://www.comsol.com/blogs/two-methods-for-modeling-free-surfaces-in-comsol-multiphysics/>
- [28] Ed Fontes, (2018), *Modeling Free Surfaces in COMSOL Multiphysics® with Moving Mesh*, COMSOL Blog, URL <https://www.comsol.com/blogs/modeling-free-surfaces-in-comsol-multiphysics-with-moving-mesh/>
- [29] Christian Wollblad, (2018), *How to Set Up a Mesh in COMSOL Multiphysics® for CFD Analyses*, COMSOL Blog, URL <https://www.comsol.com/blogs/how-to-set-up-a-mesh-in-comsol-multiphysics-for-cfd-analyses/>

[30] Christian Wollblad, (2018), *Your Guide to Meshing Techniques for Efficient CFD Modeling*, COMSOL Blog, URL <https://www.comsol.com/blogs/your-guide-to-meshing-techniques-for-efficient-cfd-modeling/>

[31] C.L. Ladson, (1988) “*Effects of Independent Variation of Mach and Reynolds Numbers on the Low-Speed Aerodynamic Characteristics of the NACA 0012 Airfoil Section*,” NASA TM 4074.